ASSEMBLY OF MICRO / NANOPARTICLES AND ITS INTEGRATION WITH PROTEIN AND CELL MICROPATTERNING

YAP FUNG LING

(B.Eng.(Hons.), NUS)

A THESIS SUBMITTED FOR THE DEGREE OF DOCTOR OF PHILOSOPHY
NUS GRADUATE SCHOOL FOR INTEGRATIVE SCIENCES AND ENGINEERING
NATIONAL UNIVERSITY OF SINGAPORE
2007

Preface

This thesis is submitted for the degree of Doctorate of Philosophy in NUS Graduate School for Integrative Sciences and Engineering at the National University of Singapore. No part of this thesis has been submitted for any other degree or equivalent to another university or institution. All the work in this thesis is original unless references are made to other works. Parts of this thesis had been published or presented in the following:

International Refereed Journal Publications

1. **Yap FL**, Zhang Y. 2005. Protein micropatterning using surfaces modified by self-assembled polystyrene microspheres. Langmuir 21(12):5233-5236. *(Langmuir 2005 most accessed article, no. 11)*

2. Wang C, **Yap FL**, Zhang Y. 2005. Micropatterning of polystyrene nanoparticles and its bioapplications. Colloids and Surfaces B: Biointerfaces 46(4):255-260.

3. **Yap FL**, Zhang, Y. 2007. Protein and Cell Micropatterning and its Integration with Micro / Nanoparticles Assembly. Biosensors & Bioelectronics 22(6):775-788. *(Biosensors & Bioelectronics January – March 2007 most accessed article, no. 9)*

4. **Yap FL**, Zhang Y. 2007. Assembly of polystyrene microspheres and its application in cell micropatterning. Biomaterials 28(14):2328-2338.

International Conferences Presentations

1. **Yap FL**, Chatterjee DK, Zhang Y. Gene transfection on micropatterned cells. 7th World Biomaterials Congress, 17-21 May 2004, Sydney Convention & Exhibition Centre, Sydney, Australia. Final program book p147. Poster Presentation.

2. **Yap FL**, Zhang Y. Gene transfection analysis on micropatterned cells. 4th Asian International Symposium on Biomaterials and 2nd International Symposium on Fusion of Nano and Bio Technologies, 16-18 November 2004, Tsukuba International Congress Centre, Tsukuba, Japan. Proceedings p190. Poster Presentation.

3. **Yap, FL** and Zhang Y. Micropatterning of proteins via self-assembly of polystyrene microspheres. 15th Interdisciplinary Research Conference on Biomaterials, 18-20 March 2005, Shanghai, China. Oral Presentation.

4. **Yap FL**, Zhang Y. Self-assembled polystyrene microspheres for protein micropatterning. 6th International Symposium on Frontiers in Biomedical Polymers, 16-19 June 2005, Hotel Saray, Granada, Spain. Abstract book pP-26. Poster Presentation.

5. Zhang Y, **FL Yap** and JT Cheng. Novel Method for Micropatterning of albumin proteins. International Conference on Surfaces, Coatings and Nanostructured Materials, 7-9 September 2005, Aveiro, Portugal. Oral Presentation.

Acknowledgements

I would like to express my sincere gratitude to those who had contributed in one way or another towards the completion of my thesis. First and foremost, I am deeply grateful to my supervisor, A/P Zhang Yong. He offered me immense support and guidance to steer me in the right direction when I just begin my research. I greatly appreciate his patience, constructive suggestions and encouragement throughout the entire course of work.

This work would not have been possible without the generous financial support from Agency for Science, Technology and Research and National University of Singapore, in the form of scholarship and research grant.

I like to thank the Technology Centre for Nanofabrication and Materials at Singapore Polytechnic for providing microfabrication facilities. I am also grateful to Mr. Tua Puat Siong for his valuable assistance in fabrication of the fluidic chamber; Mr. Zhang Zaoli and Ms. Loh Wei Wei for help in parylene coating and Dr. Dharmarajan, Ms. Tay Choon Yen, Ms. Lim Mui Keow, Agnes and Ms Tan Phay Shing, Eunice for their assistance in equipment operation.

I am thankful to my lab members in Cellular & Molecular Bioengineering Laboratory for their friendship and support, which made my stay in the lab enjoyable and fulfilling.

Most of all, I would like to thank my family for their immense support and care.

Yap Fung Ling

26th June 2007

Table of Contents

Page

Summary

Protein and cell micropatterning have important applications in the development of biosensors and lab-on-a-chip devices, microarrays, tissue engineering and fundamental cell biology studies. The conventional micropatterning techniques involve patterning over a planar substrate. In this thesis, the introduction of topographical features on the adhesive regions to enhance proteins and cells behaviour is proposed. A textured substrate for proteins and cell adhesion is created by the assembly of micro and nanoparticles into an array of microwells on a silicon substrate. The topography can be controlled by varying the size and density of the particles.

Firstly, a technique of generating spatial arrangement of particles on a non-fouling background is developed. This is achieved by using a bi-functional template which can overcome the conflict between the pre-requisites for particles assembly and micropatterning of biomolecules. A fluidic chamber was designed to control the movement of the particle suspension across the template so as to attain uniform particles pattern over a large area.

After assembling the particle, proteins can be conjugated to the curve surface of the particles. Attachment of biomolecules on surfaces of particles can increase the density of biomolecules and proteins can retain its native structure and function better than on a planar surface. Alternatively, cell micropatterning can be performed and it was shown that the textured surface helped to improve the proliferation and adhesion of cells.

List of Tables

List of Figures

Abbreviations

AFM	atomic force microscopy
Amino-silane	[3-(2-aminoethylamino)propyl]trimethoxysilane
BSA-FITC	bovine serum albumin conjugated to fluoresceinisothiocyanat
CAM	cell-cell adhesion molecules
CD	circular dichroism
DMEM	Dulbecco's modified Eagle's medium
ECM	extra cellular matrix
EDAC	1-ethyl-3-(3-dimethylamino-propyl) carbodiimide
FBS	fetal bovine serum
FTIR	fourier transform infra red
HMDS	hexamethyldisilazane
IFN- γ	recombinant human interferon-gamma
IgG-Cy3	sheep anti-rabbit immunoglobulin G Cy3 conjugate
NHS	N-hydroxy-succinimide
OTS	octadecyltrichlorosilane
PAA	poly(acrylic acid)
PAH	poly(allylamine hydrochloride)
PBS	phosphate buffer saline
PDMS	poly(dimetlylsiloxane)
PEG	poly(ethylene glycol)
PEG-silane	2-[methyoxy(polyethylenoxy)propyl]trimethoxysilane

PMMA	polymethyl methacrylate
PS-COOH	carboxylated polystyrene
PS-NH_2	amino polystyrene
SAM	self assembled monolayer
SEM	scanning electron microscopy

CHAPTER 1

LITERATURE REVIEW & RESEARCH PROJECT

1.1 Introduction

Protein micropatterning refers to the organization of proteins on surfaces with microscale resolution. The history of protein micropatterning can be dated back to 1978 when McAlear and Wehrung first patented their micropatterning technique which originated from the semiconductor industry. Their micropatterns were intended for the integration of protein molecules into bio-electronic microcircuits. Since then, a variety of techniques have been developed for protein and cell micropatterning. Protein and cell micropatterning have numerous applications in the biomedical field. Cellular patterns are used to address fundamental issues in cell biology, like cell-cell, cell-substrate and cell-medium interactions. Patterning of two or more cell types in a co-culture system allows manipulation of cell-cell interaction which has potential in tissue engineering. The accurate positioning of cells and biomolecules is essential for the development of cell and molecular-based biosensors.

In most of the micropatterning techniques, the proteins and cells are immobilized over a planar substrate. It is well documented that the substratum topography will have an influence on protein and cells functionality. Efforts have been made to engineer micro and nano scale features on implants and tissue engineering scaffolds to improve cellular behaviour. Similarly, topographical features can be introduced onto the substrate for patterning to improve protein bioactivity and enhance cellular response. A micro or nanotopograhy can be constructed easily by assembly of micro and nanoparticles.

In this chapter, the techniques that are commonly adopted for protein and cell micropatterning and its biomedical applications are reviewed. Next, the advantages of integrating micro and nanoparticles assembly with protein and cell micropatterning are discussed. The last section will give an overview of the thesis.

1.2 Techniques for Micropatterning

The main requirement for protein micropatterning is the selective attachment of protein at the desired regions and high protein resistivity by other regions on the substrate. Apart from surface coverage, there are two other key aspects for protein immobilization, i.e., protein orientation and protein functionality. Protein orientation is particularly important in the development of immunodiagnostic device as the optimum orientation of an antibody can increase the surface binding ability and therefore enhance the sensitivity of the assay (Alarie et al., 1990; Chen et al., 2003). Retaining the protein functionality is crucial for ensuring that the immobilized protein will serve its designated purpose and provide reliable analysis.

Attachment of proteins falls into two basic categories, i.e. non-covalent and covalent interaction. Protein adsorption by non-covalent interactions can be based on hydrophobic, van der Waals interactions, hydrogen bonding or electrostatic forces. An advantage of these concepts is their ease of application since no chemical modification is required prior to immobilization. The drawback is that proteins may get denatured due to uncontrolled interactions between protein and the surface material. Physical adsorption of

proteins can also lead to problems with protein desorption during the assay, which will result in loss of signal (Sydor and Nock, 2003). A more stable means of protein immobilization is to link a protein to the surface covalently via a chemical bond. An example is the use of bi-functional cross linkers such as silanes, silica-based linkers which attach at one end to silicon wafer or metal surface via a silanol bond while the free end has a variable functional group for binding protein.

When the patterned protein is a cell adhesive protein, e.g. fibronectin, laminin, collagen or vitronectin, the patterned substrate can be used to generate a cell pattern, the areas attached with adhesive protein allow the selective attachment of cells. Apart from physiological biomolecules, other materials like amino terminated self-assembled monolayers (SAM) and Arg-Gly-Asp (RGD) peptide can also mediate the attachment of cells (Folch and Toner, 2000).

Microfabrication and robotic printing techniques are the basic tools for creating protein and cellular micropattern. The next section will describe the basic principles of these techniques with its advantages and drawbacks highlighted.

1.2.1 Photolithography

Photolithography which is used in the semiconductor industry for metal patterning in electronic microcircuits has been applied to protein micropatterning. Photolithography is the process of transferring geometric shapes on a mask to the surface of a wafer or substrate. In photoresist lithography, micropatterns are generated using light, photoresist

(light sensitive organic polymer) and mask as shown in Figure 1.1. A layer of photoresist is applied to the surface of the substrate and is selectively exposed to ultraviolet light through a mask containing the pattern. For positive photoresist, the exposed polymer becomes more soluble in a developer solution than the unexposed polymer, whereas for a negative photoresist, the exposed polymer becomes insoluble in the developer solution. The resulting photoresist pattern can then act as a mask for patterning the material of interest. A common adhesion promoting molecule is amino terminated silane, the silane is applied on the photoresist pattern and bound to the exposed areas. The photoresist is then lifted off by sonication in acetone to expose the remaining areas. Next, the chip is incubated with an adhesion resistant silane, typically a methyl or alkyl terminated silane, resulting in a cell adhesive and cell resistant micropattern. A number of groups had worked on patterning silanes using photoresist lithography to control protein attachment (Britland et al., 1992b; Lom et al., 1993) and cell growth (Britland et al., 1992a; Healy et al., 1996; Kleinfeld et al., 1988). The initial work was pioneered by Kleinfeld and colleagues with the patterning of cerebellar cells from perinatal rats on alternating lines of amino-silane and methyl terminated alkylsilane. The patterned growth of cerebellar cells was maintained up to 12 days in vitro and the cell morphology was indistinguishable from those cultured on conventional poly(D-lysine).

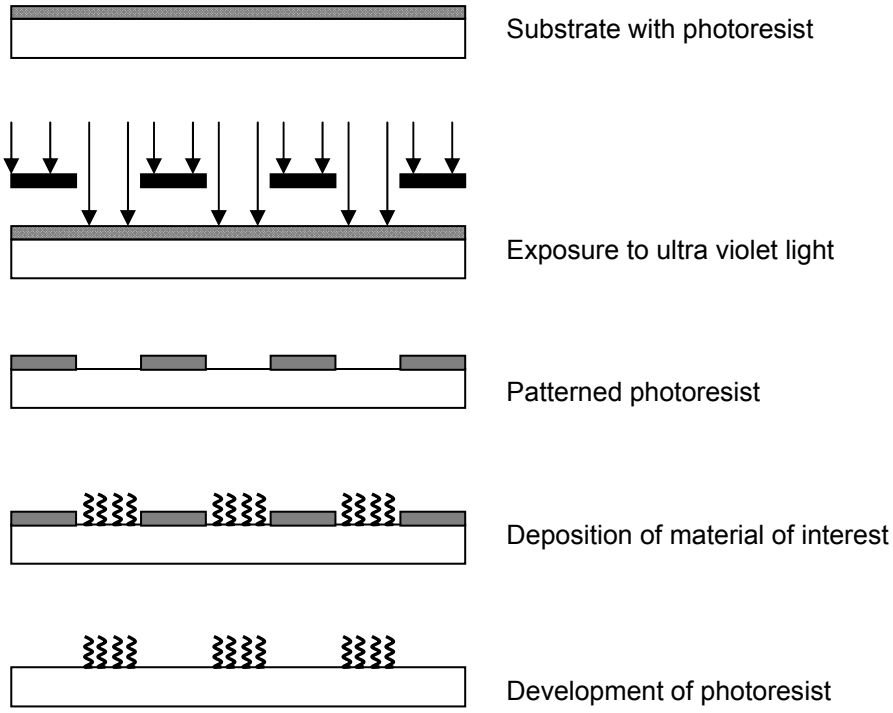

Figure 1.1. Micropatterning using photoresist lithography.

Researchers have made use of photolithography to generate many different chemical micropatterns to assist them in their patterning of biomolecules and cells. For instance, a hydrophobic-hydrophilic micropattern of octadecyltrimethoxysilane on silicon substrate was prepared for the selective assembly of carbohydrates (Miura et al., 2004); a layer-by-layer (LbL) technique was combined with photolithography for the construction of bioactive nanocomposite film (Mohammed et al., 2004), and a high density array of PEG hydrogel microwells was fabricated to control mammalian cell – surface interactions (Revzin et al., 2003).

Photolithography is the dominant technique for patterning solid-state devices; it can produce accurate patterns with submicron resolution. However, photolithography requires clean room facilities and expensive equipment which makes it inconvenient for

biologists. Furthermore, the chemicals used in the process are toxic to cells and they can denature biomolecules. Photolithography is not well suited for introducing specific chemical functionalities and delicate ligands required for bio-specific adsorption (Kane et al., 1999).

1.2.2 Soft Lithography

More recently, Whitesides and colleagues have developed a set of techniques which are more biocompatible for patterning biomolecules. These techniques are collectively known as "soft lithography" because a soft elastomeric stamp with patterned relief structures is used to generate patterns and structures with feature size ranging from 30 nm to 100 μm (Kane et al., 1999; Xia and Whitesides, 1998). Elastomer is the material of choice as they can make conformal contact with non-planar surfaces. The stamp is prepared by casting the liquid prepolymer of poly(dimethylsiloxane) (PDMS) against a master that has patterned relief structures (Figure 2). In soft lithography, photolithography is required only during the fabrication of the masters. As the stamps and masters can be reused indefinitely (Kane et al., 1999), soft lithography is a more convenient, effective and cheaper method compared to photolithography since the use of a clean room environment is minimized. Microcontact printing, microfluidic patterning and stencil patterning are the common soft lithography related techniques that are used for proteins and cells micropatterning.

1.2.2.1 Microcontact Printing

Microcontact printing is based on the transfer of the material of interest from a PDMS stamp onto a surface at the areas contacted by the stamp. The stamp is fabricated by replica moulding using a rigid master. This procedure has been widely used for printing SAMs of alkanethiols on films of gold and silver. The stamp is 'inked' with a solution of an alkanethiol in ethanol and brought into conformal contact with a gold substrate (Kane et al., 1999). The alkanethiols are transferred from the PDMS stamp onto the substrate surface through a conformal contact with the surface. Upon removing the stamp from the surface, a pattern is left behind on the surface (Figure 1.2 A). The bare areas of the surface can be modified with another material by immersing it into a solution of another kind of alkanethiol.

Mrksich et al.(1997) used microcontact printing to pattern hydrophobic, methyl terminated lines separated by SAMs terminated in oligo(ethylene glycol) groups. Fibronectin adsorbed only on the methyl terminated regions while oligo(ethylene glycol) successfully resisted protein adsorption. Bovine capillary endothelial cells attached selectively to the fibronectin coated methyl terminated region. The cells confined to the pattern of underlying SAMs for at least 5 - 7 days.

Microcontact printing is a simple and inexpensive method. It is useful when one needs to patterns only one or two types of molecules. Microcontact printing is not limited to transferring alkanethiols to gold surface, the same principle works for patterning alkylsiloxanes on hydroxylated surfaces of glass and silicon dioxide (Xia et al., 1995);

the direct transfer of dried proteins from the PDMS stamp to various surfaces was demonstrated by Bernard et al.(1998) while Csucs et al.(2003) used the technique to transfer a polycationic graft copolymer, poly-l-lysine-g-poly(ethyleneglycol) to a negatively charged substrate. Microcontact printing is a versatile method for patterning as a variety of substrates and molecules are compatible with the technique.

1.2.2.2 Microfluidic Patterning

This method involves sealing a PDMS mould against a substrate to form a network of microchannels which defines the desired pattern. By injecting fluids into the microchannels, selected areas of the substrate are exposed to the microflow and result in the patterning of the material of interest onto the substrate (Figure 1.2 B). The fluid when placed at the open ends of the channels can be injected spontaneously into the microchannels by capillary force (Kim et al., 1995). However, capillarity driven flow is limited to small areas and channels and it is not suitable for viscous fluid. Toner's group improved on this technique by using pressure assisted flow to pattern proteins (Folch and Toner, 1998) and cells (Folch et al., 1999). Microfluidic patterning is suitable for patterning delicate materials like proteins and cells on a variety of substrate; however, it is limited to interconnecting patterns.

1.2.2.3 Stencil Patterning

A thin sheet of material containing through holes laid on a substrate can be used to perform micropatterning. The substrate is prevented from coming into contact with the material for patterning while the holes are left exposed. PDMS is a suitable material for

stencil (Folch et al., 2000; Ostuni et al., 2000) as it seals spontaneously to most dry surfaces. These PDMS stencils are fabricated in a manner similar to the PDMS stamps used in microcontact printing. For fabrication of a stencil, the PDMS prepolymer should not cover the micropillars on the master so that through holes will be created on a thin film of PDMS (Figure 1.2 C). PDMS stencils were used to pattern 3T3 fibroblast cells (Folch et al., 2000) and fibronectin (Ostuni et al., 2000). The stencil was applied to the substrate before seeding. After the proteins or cells have attached, the stencil was removed and patterns with shapes similar to the holes remained on the substrate. Stencil patterning is a simple method which allows patterning even without chemical modification on the substrate.

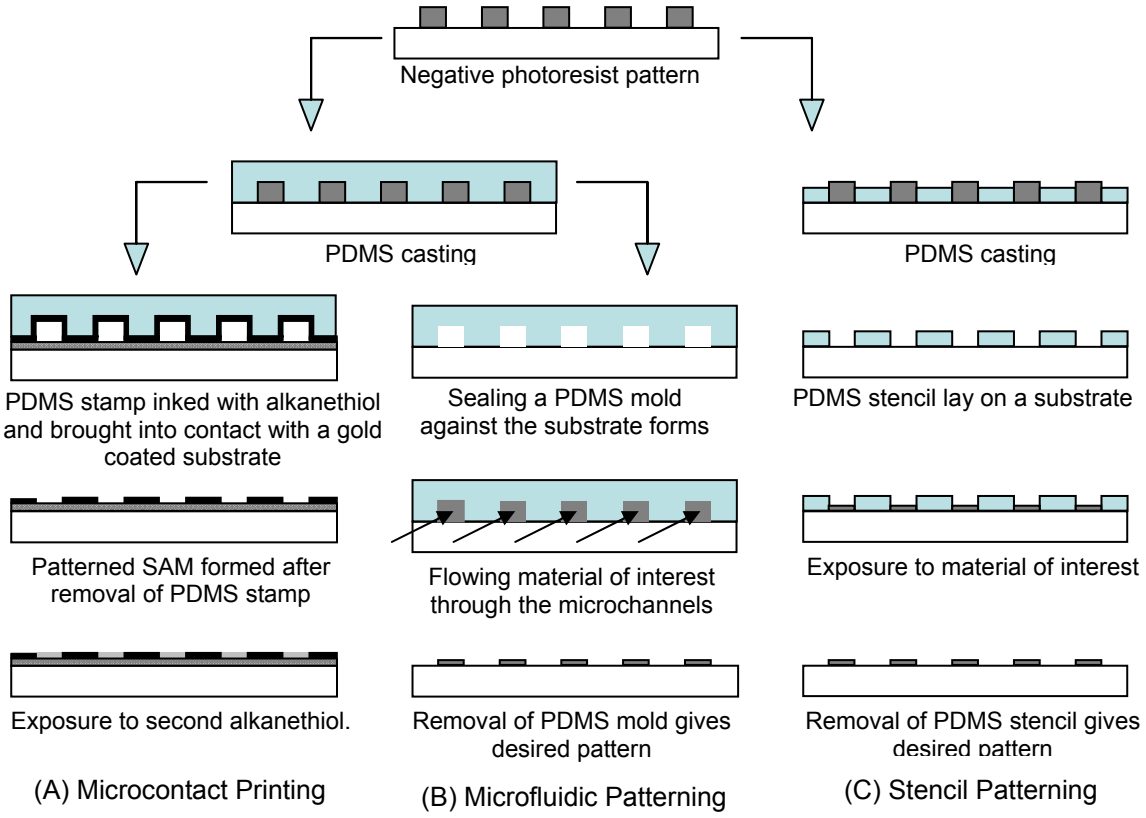

Figure 1.2. Schematic procedure for patterning using soft lithography related techniques. (A) Microcontact Printing, (B) Microfluidic Patterning, (C) Stencil Patterning.

1.2.3 Robotic Printing

Although lithographic techniques can produce patterns with sub-micron features, the number of ligands that can be patterned simultaneously on a substrate is limited. A high precision robotic printer can immobilize a variety of proteins on a solid substrate (MacBeath and Schreiber, 2000). It allows high throughput and rapid deposition of thousands of proteins onto different spots with sizes typically around 100 μm.

There are two types of printing techniques for microarrays, contact and non-contact printing. The contact printing arrayer is capable of delivering sub nano-litre volume directly to the surface using tiny pins. Contact pin printing techniques tend to damage the surface mechanically, causing defects and irregular spots (Wagner and Kim, 2002). Non-contact robotic printers uses ink jet technology; the piezoelectric fittings attached to glass capillaries allow the selective contraction of the capillaries in an electrically controlled manner (Lemieux et al., 1998). The ink jet microarrayer can be slow when spotting many different samples and the shearing force during drop formation may damage some samples (Haab, 2001). However, this technique is not hindered by surface structure since there is no contact between the nozzle and the surface.

Apart from high precision robotic arrayer, researchers also make use of office based ink jet printer to deposit chemical and biomolecular substances. This non-contact technique can deliver a small sample volume onto the printing surface via controlling conventional word processing or graphics editing software. Multifunctional surface can be created easily by using a number of nozzles. Furthermore, mixing of the feed molecules is

possible by simultaneously actuating several nozzles, thus allowing chemical gradients to be created with relative ease (Pardo et al., 2003). Compared to the robotic arrayer, the ink jet printer has the advantage of being inexpensive, flexible, simple and desktop computer controlled. However, the size of the features created is larger than that of the robotic arrayer. Boland's group has performed a series of research on using the ink jet printer to deposit a variety of molecules. They tested the technique by depositing a variety alkanethiols onto gold substrate. Their alkanethiol self-assembled monolayers patterns created by this method are comparable to those obtained by microcontact printing or solution adsorption (Pardo et al., 2003). The technique was also used to print biologically active collagen proteins to control cell attachment; the cellular pattern obtained had a resolution of 350 μm (Roth et al., 2004). The group also fabricated bacterial colony array by directly ejecting Escherichia coli onto agar-coated substrates at a rapid arraying speed of 880 spots per second (Xu et al., 2004). The concentration of bacterial suspensions can be adjusted to allow single colonies of viable bacteria to be obtained.

1.3 Applications of Protein and Cell Patterning

1.3.1 Protein Micropatterning

1.3.1.1 Molecular Biosensors

There is a growing interest in the use of molecular biosensors for environmental, medical, toxicological, and defence applications (Pancrazio et al., 1999). Molecular biosensors utilize biomolecules such as enzymes, antibodies, nucleic acids, receptors etc. The basic feature of the biosensor is the immobilization of biomolecules onto a conductive or semi-

conductive support, and the electronic transduction of the biological functions associated with the biological matrices (Willner and Katz, 2000). The integration of micropattening techniques for biosensor applications requires patterning on substrate of more than one material, especially in an electrode-insulator format. Veiseh et al.(2002) developed a technique for patterning proteins on gold-silicon dioxide substrate using photolithography and chemical selectivity. The gold regions were modified to have a high affinity for proteins while the silicon regions were modified to resist protein adhesion. In this setting, the biomolecules are patterned on electrodes on a substrate that can be integrated with signal processing microdevices.

1.3.1.2 Protein Microarray

Robotic printing method is used to fabricate protein microarray which allows the simultaneous determination of a large variety of parameters from a minute amount of sample within a single experiment. Molecules are immobilized in rows and columns on a solid support and exposed to samples containing the corresponding binding molecules. Protein microarray can be used for identification, quantification and functional analysis of proteins that are of interest for proteomic research in basic and applied biology and for diagnostic application. They are also of interest to the pharmaceutical industry which focuses on the validation of potential target molecules (Stoll et al., 2004). Protein microarray is becoming an indispensable tool for protein profiling; however several challenges have to be overcome before the technique can be used successfully. Protein is a complex molecule. The tertiary structure of proteins are extremely sensitive to environmental and interfacial conditions such that most proteins will require customized

attachment solution to preserve their conformation and activity. This is complicated by diversity of proteins in terms of structure, function, expression level and stability (Wagner and Kim, 2002).

1.3.2 Cell Micropatterning

1.3.2.1 Fundamental Studies in Cell Biology

The ability to position cells on a substrate has facilitated fundamental studies in cells. Micropatterned cell cultures are ideal to address fundamental issues like cell-cell interaction and cell-substrate interaction.

Cell adhesive regions of varying shapes and sizes can be fabricated on a single substrate by using microfabrication techniques. When cells are plated on the substrate, the shape of the cells will match the size and shape of the adhesive patterns closely. In this way, the degrees of cell extension and spreading can be manipulated. Chen et al.(1997) studied the effect of spreading on cell growth and apoptosis for human and bovine capillary endothelial cells. As angiogenesis is the prerequisite for tumour growth, the understanding of how cell shape controls the apoptotic switch in capillary cells will have enormous clinical applications. It was found that when the adhesive island decreases in size, cells are limited from spreading and shifted from growth to apoptosis. Their studies demonstrated that cell shape affects cell growth and cell function. More recently, the issue of whether the form of the tissue can feedback to regulate patterns of proliferation was addressed by Nelson et al.(2005). The group demonstrated that the shape of the cellular island has a prominent effect on the pattern of proliferative foci by using

microfabricated extracellular matrix (ECM) protein islands of different geometric shape to control the organization of bovine endothelial cells. The regions of concentrated growth corresponded to sites with high tractional stress generated within the cell sheet. Their results demonstrated the existence of patterns of mechanical forces that originate from the contraction of cells and resulted in patterns of growth.

Substrate patterning provides a useful tool for studying neuronal behaviour (Corey and Feldman, 2003). ECM proteins and cell-cell adhesion molecules (CAM) (Berry et al., 2004) play important roles in the development and differentiation of neurons. Experiments performed using substrates with ECM and CAM patterns have provided unique insights into the roles of cell-substratum adhesion, cell shape, and ECM composition on important cell functions, including survival, migration, neurite outgrowth, and development of polarity. The behaviour of neurons on patterned substrates may aid in the design of scaffoldings and nerve guides tailored for regeneration and repair of the nervous system.

In addition, micropatterning provides a miniaturized platform that allows parallel and quantitative analysis on cell population. Chin et al. (2004) microfabricated a high density array of microwells to analyze a heterogeneous neural stem cell population. This approach offers the ability to screen a large number of clonal populations and study the response of distinct stem cell subpopulations to micro environmental cues (mitogens, cell–cell interactions, and cell–extracellular matrix interactions) that govern their behaviour.

1.3.2.2 Tissue Engineering

Micropatterned co-culture provides a platform for the study of cell-cell interaction between two or more types of cells in a functional tissue model. Cell-cell interactions are vital for normal physiology of many organ systems including vasculature (smooth muscle cell and endothelium), skeletal muscle (monocyte and peripheral nerve) and liver (hepatocyte and sinusoidal endothelium). Bhatia et al. (1997) first demonstrated co-cultivation of hepatocytes and 3T3 fibroblast. Co-cultivation of hepatocytes and fibroblasts preserved the phenotype of hepatocytes for several weeks. The ability to modulate the function of multicellular systems by manipulation of the spatial relationship between cell populations will facilitate more effective *in vitro* reconstruction of liver, skin, vascular grafts, muscle, and many other tissues (Bhatia et al., 1999).

The spatial organization of cells is vital in engineering tissues that require precisely defined cellular architectures. For example, functional nerve and blood vessels form only when group of cells are organized and aligned in specified geometries (Wang and Ho, 2004). Most efforts in cell micropatterning use microfabrication techniques that are based on silicon or glass substrates which limits applications to tissue engineering. Creating cellular patterns on biocompatible and biodegradable biomaterials is the first step towards engineering functional tissues in vitro. Wang & Ho (2004) developed a technique to pattern human microvascular endothelial cells on chitosan and gelatin films. These two materials were chosen because of their high biocompatibility, low toxicity, and wide use in biomedical applications. In another paper by the same group (Co et al., 2005), fibroblast and human microvascular endothelial cells were patterned on a chitosan

substrate. The co-culture of the two cell types resulted in the structured assembly of capillary tube-like structures.

1.3.2.3 Cell-based Biosensors

Cell-based biosensors are sensors which incorporate cells as a sensing element that convert a change in environment to signals conducive for processing. Cells express an array of potential molecular sensors (such as receptors, channels, and enzymes) that are maintained in a physiological relevant manner by native cellular machinery. A cell-based biosensor has a distinct advantage over molecular sensor; in a cell-based biosensor, the sensing element is maintained in the native state, whereas in a molecular sensor, there is always the problem of protein degradation which will affect the affinity and accuracy of the sensor. Potential applications of cell-based biosensors include high throughput screening of drugs, clinical diagnosis and detection of toxicants, pathogens and other environmental threats (Pancrazio et al., 1999).

Electrically excitable cells such as neurons and cardiomyocytes are particularly useful as the sensing element in cell-based biosensor as the activity of the cells can be monitored by recording the extracellular potentials with a microelectrode (Pancrazio et al., 1999). In neurons, a change in chemical environment will result in changes in action potential patterns, hence they can be used to screen for novel pharmacological substances, toxic agents, and for the detection of certain odorants (Gross et al., 1997). In order to measure electrical signals from cells, the cells must ‘sit’ on a microelectrode. In early works, cells were seeded on the substrate at a relatively high density with the hope of having good

coverage of cells on the electrodes (Connolly et al., 1990). More recently, chemical patterning on microelectrode array are used to guide the organization of the cells on the device. James et al. (2004) used microcontact printing and a photoresist lift off method to selectively localize poly-L-lysine on the surface of the array of microelectrode. Haptotaxis led to the organization of neurons into network localized adjacent to the microelectrodes.

1.4 Integration of Micro / Nanoparticles with Protein and Cell Micropatterning

Due to a strong interest in the various applications for protein and cell micropatterning, tremendous efforts have been put in by many research groups to develop techniques that are compatible for patterning biomolecules as reviewed in section 1.1. Most of these conventional micropatterning methods involve attachment of biomolecules and cells over a planar substrate. In this project, a new technique of micropatterning that involves integration of a micro or nanostructured region for biomolecule and cell attachment is proposed. Topographical features can be fabricated by various techniques. Electron beam lithography and photolithography are well established methods that can create organized and highly reproducible features such as grooves, columns and pits (Dalby et al., 2004; Teixeira et al., 2003; Whitehead et al., 2005). Electrochemical techniques like acid etching, anodic dissolution and electropolishing are used to fabricate micro and nano-structures on metals (Landolt et al., 2003). Polymer demixing, for example blends of hydrophobic polystyrene and hydrophilic poly(4-bromostyrene) undergo phase separation

during spin casting and form various topography depending on the blend composition (Affrossman et al., 1996).

In this work, colloidal particles are utilized to modify the topography of the adhesive regions. By systemically varying the density and the size of particles, the surface roughness can be fine tuned and surfaces with micro or nano-topography can be produced without the need for state-of-the-art equipments or undergoing chemical processes. Biomolecules or cells are then selectively attached to the particles while the background regions are rendered protein resistant. The schematic diagram for the proposed technique is depicted in Figure 1.3.

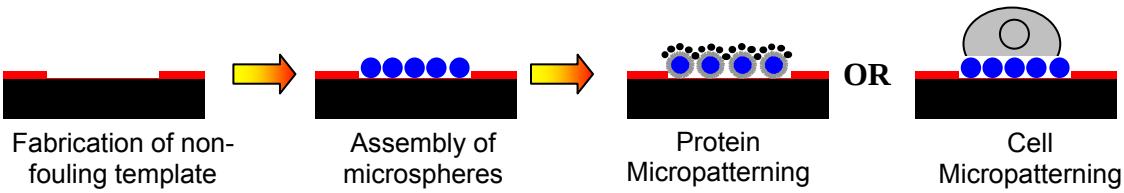

Figure 1.3. Procedure for proposed cell and protein micropatterning technique via assembly of particles.

The rationale for utilizing micro and nanoparticles is easily understandable. The technology for synthesizing many types of inorganic (e.g. silica, gold, iron oxide) and organic (e.g. polystyrene, poly(methyl methacrylate)) particles is well established; particles of varying sizes ranging from nano to micro scale can be synthesized. With an array of particles available for selection, the surface properties of the patterned substrate can be tailored by choosing the particles having the desired characteristics (for e.g. hydrophobicity / hydrophilicity, surface potential and functional groups on particles for

subsequent conjugation to biomolecules). The roughness of the topography can be fine-tuned by using particles of different sizes. Furthermore, the unique properties of some types of particles can be utilized to serve as an additional functional role. For example, gold nanoparticles can be assembled to give rise to an electrode-insulator format which provides a pathway for measurement of electrical signal in biosensors; while an array of magnetic particles may be used for separation or purification purposes in microfluidic devices.

Micro and nanoparticles functionalized with biomolecules already have numerous applications in the biomedical field, for example, drug and gene delivery, biosensors, immunoassay etc. The idea of patterning micro and nanometer scale particles into ordered arrays has generated much interest due to its unique potential for application in photonic (Wijnhoven and Vos, 1998; Yang et al., 2002) and optoelectronic devices (Veinot et al., 2002; Yamasaki and Tsutsui, 1998). The existing knowledge on particle functionalization and assembly gained from other fields can be integrated with protein and cell micropatterning.

There are several advantages of introducing a nonplanar topography with protein and cell micropatterning. Firstly, the curve surfaces of the particles increase the surface area for immobilization of biomolecules. Although it is possible to achieve a high molecular density on a planar substrate, for example, via thiols-based self assembled monolayers on a gold substrate (Smith et al., 2004), the density can be further improved by using a nonplanar micro / nanostructure to enhance the surface available for attachment of

biomoleules. The amount of increase in the surface area can be calculated by considering that each closely packed particle occupies a hexagonal area on the surface (Figure 1.4).

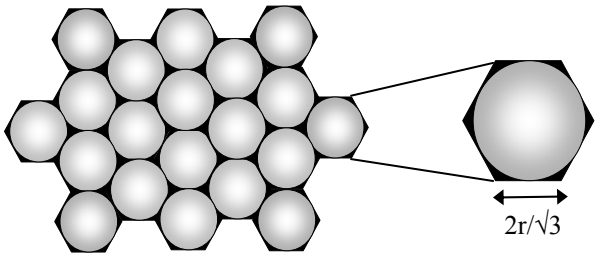

Figure 1.4. Each closely packed particle occupies a hexagonal area on the planar substrate.

$$\textit{area of planar hexagonal area} = 6r^2/\sqrt{3} \qquad (1.1)$$

$$\textit{curve surface area on microspheres} = 2\pi r^2 \qquad (1.2)$$

$$\textit{ratio of curve surface area to planar area} = 1.81 \qquad (1.3)$$

$$\textit{where } r \textit{ is the radius of the particle}$$

As derived above, the curve surface area created by closely packed particles is approximately 1.81 times higher than a planar surface, regardless of the size of the particles. The increment in the surface area will subsequently increase the density of biomolecules that can be immobilized and the sensitivity for detection. As the demand for sensitive biosensors continues (Mehrvar and Abdi, 2004), this technique may be used as an immobilization strategy in biosensor devices to enhance the signal for detection. More recently, patterning of biomolecules with nano-resolution has been made possible with the support of techniques such as dip pen lithography (Piner et al., 1999) and e-beam patterning (Eck et al., 2000). As the size of the pattern becomes smaller, it is crucial that sensitivity is not compromised due to a reduction in surface area. This strategy of using particles for patterning may resolve the conflict between feature size and sensitivity.

With the improvement in microfabrication techniques for patterning over the last couple of years, achieving a good spatial arrangement of protein is no longer a daunting task. On the other hand, the structure and functionality of the proteins after immobilization warrants further studies. It is well-documented that immobilization of protein on surfaces typically affects its conformation (Nakanishi et al., 2001); furthermore, the procedure for patterning may induce structural changes in the protein. A good protein micropatterning technique is one which does not damage the protein functionality in the process of patterning. By designating the attachment of proteins as the last step in the procedure will help to minimize the deleterious effect on protein. Furthermore, when protein is attached on surface assembled with nanoparticles, the protein is immobilized on the curve surfaces of the particles instead of the planar surface. As the surface is highly curved, there is a smaller area for interaction between the protein and the substrate and this will promote the retention of the protein native structure (Lundqvist et al., 2004; Vertegel et al., 2004).

The topographical properties of a substrate affect the cellular behaviour of anchorage-dependent cells in terms of adhesion, spreading, proliferation, differentiation, apoptosis and gene expression (Curtis and Wilkinson, 1997; Dalby et al., 2003; Singhvi et al., 1994). Topographical features created by assembly of particles at designated regions for cell attachment may be systematically varied to study its effect on cellular response and optimized to enhance cell adhesion and preserve cell phenotype.

1.5 Thesis Overview

Performing protein and cell micropatterning on surfaces assembled with particles brings many advantages which cannot be realized via patterning a planar substrate. The objective of this thesis is to develop a novel protein and cell micropatterning technique that can integrate with colloidal assembly. Each of the following four chapters will focus on a specific step in the developmental process.

Step 1: Fabrication of a template (Chapter 2)

The design of a bi-functional template that is compatible for colloidal assembly and protein and cell micropatterning is necessary. A hydrophilic-hydrophobic template that satisfies the pre-requisites of these two processes was fabricated.

Step 2: Assembly of particles on the template (Chapter 3)

Particles were assembled on the template by selective wetting of the hydrophilic regions. The assembly of a variety of particles, with various sizes and packing density was demonstrated.

Step 3: Protein Micropatterning (Chapter 4)

Protein micropatterning was performed on the colloidal assembled substrate. The protein density on the microsphere structured surface and a planar film was compared. The bioactivity of the patterned protein was also characterized.

Step 4: Cell Micropatterning (Chapter 5)

Cell micropatterning was integrated with colloidal assembly. The adhesion, proliferation and morphology of the cells adhered onto the microstructured surface was characterized.

CHAPTER 2

MICROFABRICATION OF A TEMPLATE COMPATIBLE FOR COLLOIDAL ASSEMBLY & PROTEIN AND CELL MICROPATTERNING

2.1 Introduction

The ability to pattern colloids, proteins and cells in a bioinert environment play an important role for the development of biosensors and lab-on-chip devices (Willner and Katz, 2000) for use in diagnostic, therapeutic and basic science applications. The fabrication of a template is the first and foremost step towards micropatterning; therefore, it is crucial that the design and surface properties of the template are compatible with the requirements for colloidal assembly and proteins and cells micropatterning.

Site selective assembly of particles can be achieved by using template with patterned surfaces having distinct differences in charge and / or wettability. Templates with relief structures can also be used for patterning particles by physical confinement. (The various techniques for colloidal patterning will be discussed further in Chapter 3.) On the other hand, protein and cell micropatterning is based on the patterning of substrate into regions that promote or resist adhesion of biomolecules. There are many surfaces that allow proteins and cells to adhere, but few that can prevent adhesion. The common repellent surface modifications include poly(ethylene glycol) (PEG) and poly(ethylene oxide) (Folch and Toner, 2000). Other materials that have been explored as viable bioinert alternatives include PEG-based hydrogels (Tziampazis et al., 2000), agarose (Folch and Toner, 1998), dextran (Massia et al., 2000), phosphorylcholine (Tegoulia et al., 2001), polyelectrolyte multilayers (Mendelsohn et al., 2003) and immobilization of albumin or other proteins that do not contain any known integrin binding domains (Folch and Toner, 2000). As the background modifications required for bio-patterning is limited to the

above polymers, this may conflict with the requirements for colloidal assembly which commonly involve modification with hydrophobic and charged polymers on the background. Some template designs that can integrate patterning of colloids with proteins and cells are reviewed in the following paragraphs.

Gleason et al.(2003) used a combination of gravimetric settling and electric field driven assembly to organize protein functionalized colloids onto gold coated substrates. Patterning of the colloids was guided by a separate piece of indium tin oxide coated glass template that served as an electrode. The areas that are not covered by particles were made non-adhesive to other proteins and cells by incubating with bovine serum albumin. In another paper, a simultaneous process for patterning of particles and passivation of template was developed by Pregibon et al.(2006) using photopolymerization of beads containing hydrogels precursors. In short, the process involved treatment of a glass substrate, conformal contact bonding of a PDMS microchannel on the substrate, filling of the channel with beads and prepolymer solution, and UV-initiated photopolymerization of a mask-defined pattern using a typical inverted microscope. This technique resulted in stable colloidal patterns which were covalently linked to the substrate. Both of these methods are fast and inexpensive; however, they involve the assembly of protein coated colloids which may become denatured in the process of assembly.

Zheng et al.(2004) developed a polyelectrolyte multilayer template that involved assembly of pre-functionalized colloids. The template consisted of a polyamine surface patterned onto a poly(acrylic acid)/poly(allylamine hydrochloride) (PAA/PAH) using

PDMS stamping. The alternate deposition of PAA and PAH formed a polyelectrolyte multilayer platform that exhibited long term cell resistant properties (Mendelsohn et al., 2003). The patterned polyamine surface (PAH) was used to direct the deposition of net negatively charged carboxyl amine functionalized polystyrene particles. The selectivity of particle deposition was controlled by manipulating the pH of the template environment. However, it was difficult to achieve closely packed monolayer of particles which is necessary for generating uniform protein spots.

In view of the limitations of these techniques, the fabrication of a bi-functional template that is compatible with both colloidal assembly and protein and cell micropatterning is developed in this chapter. The template consisted of hydrophilic amine-terminated microwells surrounded by a parylene hydrophobic matrix which can facilitate patterning of colloids. After colloidal assembly; the parylene layer can be peeled off to expose a bioinert background, rendering the template useful for biological applications.

2.2 Materials and Methods

2.2.1 Materials

AZ 4620 and AZ 400K Developer were purchased from Clariant (Singapore). Negative photoresist SU 8-50 and SU-8 Developer were purchased from MicroChem (MA, US). Poly(dimethylysiloxane) (PDMS) and curing agent (Sylgard 184 kit) were purchased from Dow Corning (Singapore). 2-[methyoxy(polyethylenoxy)propyl]trimethoxysilane

(MW460-590, PEG-silane) was purchased from Gelest, Inc. 4 inch (1 0 0) p-doped prime grade silicon wafers with 1-20 ohm/cm reisitivity was purchased from MOS Group Pte. Ltd. (Singapore). Sulphuric acid (98%), [3-(2-Aminoethylamino)propyl]trimethoxysilane (amino-silane), hydrogen peroxide, sulphuric acid, hydrochloric acid, Dulbecco's Modified Eagle's Medium (DMEM), phosphate buffer solution (PBS) and trypan blue were purchased from Sigma-Aldrich. Fetal bovine serum was bought from PAA Laboratories (Austria), while penicillin-streptomycin was purchased from Invitrogen (Singapore). HT-29 human adenocarcinoma cell line was obtained from American Type Culture Collection (Manassas, VA). All reagents and materials were used as received.

2.2.2 Surface Modification

Grafting of PEG. The silicon wafer was modified with PEG-silane to create a non-fouling surface according to the method reported previously (Papra et al., 2001). The wafer was rinsed with deionized water prior to use. Oxidation of wafer was carried out by treatment with hot piranha solution (30 % hydrogen peroxide with 98 % sulphuric acid in ratio 1:4 v/v) at 100°C for 10 min. The mixture should be used with extreme caution due to its high oxidizing power and risk of explosion. The wafer was then rinsed with copious amount of deionized water and dried. Grafting was done by a solution of 3 mM PEG-silane in toluene (with 0.8 mL of concentrated HCl /L) for 18 h at room temperature. The PEG treated wafer was rinsed with toluene and ethanol, followed by sonication in deionized water for 2 min to remove the loosely bound molecules.

Grafting of amino-silane. The designated adhesive regions were modified with amino-silane according to similar methods reported previously (Petri et al., 1999). The chips were immersed in 2% amino-silane in deionized water for 4 min at room temperature, followed by rinsing with deionized water and baking for 10 min at 120°C.

2.2.3 Microfabrication

Positive photoresist lithography. The PEG grafted silicon wafer was spin coated with a positive photoresist AZ 4620 at 2000 rpm for 30 s. The resist was soft baked at 95°C for 1 min. The mask for photolithography containing a positive image of the design was created using AutoCAD (Autodesk, Inc., CA) and printed on a transparency with a high resolution printer. The transparency mask was adhered to a blank photomask and placed in contact with the resist under a mercury lamp (EVG EV620 Mask Aligner). The photoresist was exposed for 60 s at 10 mW/cm^2. The resist was developed with AZ 400K Developer : deionized water 1: 4 for 2 min and rinsed with deionized water. This was followed by a post exposure bake at 95°C for 10 s.

Fabrication of master. A master containing an array of cylindrical posts was fabricated with negative photoresist lithography. A piece of 4 inch silicon wafer is cleaned by rinsing in isopropyl alcohol, followed by deionized water. The wafer was subjected to a piranha clean (30% hydrogen peroxide with 98% sulfuric acid in a ratio of 1:4 v/v) at 100 °C for 10 min. The wafer was then rinsed with copious amount of deionized water, dried with nitrogen stream and dehydrated at 200 °C for 5 min on a hotplate. Negative photoresist SU 8-50 was spin coated at 1500 rpm for 30 s. The wafer was then pre-baked

at 65°C for 8 min, followed by soft-bake at 95 °C for 25 min on a hotplate to evaporate the solvent and densify the film. Next, the wafer was exposed to collimated ultra violet light through a high resolution transparency mask pressed against the photoresist layer. Following exposure, the wafer was subjected to a two step post exposure bake at 65°C for 1 min and 95°C for 8 min to selectively cross-link the exposed portion of the film. The pattern was developed by immersion in SU-8 Developer for 8 min. The substrate was rinsed briefly with isopropyl alcohol and dried with a stream of nitrogen. Finally, the resist was hard baked at 150 °C for 5 min on a hotplate to further cross-link the material.

Fabrication of PDMS stencil. The PDMS stencils were fabricated using the procedure described by Jackman et al.(1999) PDMS prepolymer was prepared as a mixture of two components. The base and catalyst were mixed at 10:1 ratio by weight. The mixture was degassed to eliminate bubbles created during mixing by placing it in a desiccator at low vacuum. The PDMS prepolymer was spin cast onto the master at 2000 rpm for 60 s, followed by curing at 60°C for 2 h. The stencils were then peeled off from the master with a tweezer.

Parylene template. Prior to the standard positive photolithography process, parylene was deposited onto the PEG grafted silicon wafer by chemical vapour deposition. Parylene C dimmer (di-para-xylylene) was used to deposit a pin-hole free conformal layer of parylene film of approximately 1 μm thick using the PDS-2010 Labcoater 2 Parylene deposition system (Specialty Coating Systems, Indianapolis, IN). Next, hexamethyldisilazane (HMDS) was spun at 3000 rpm for 30 s to improve the adhesion

between parylene and the photoresist. The standard process for positive photolithography was performed according to the procedure described earlier.

Reactive ion etching. The exposed region on the wafer was subjected to reactive ion etching (SAMCO RIE-10NR). The exposed parylene film was etched by exposure to oxygen plasma (100 W, oxygen at 100 sccm) for 6 cycles of 1 min, with an interval of 1 min between each cycle to allow the photoresist to cool down. PEG film was removed by exposing to oxygen plasma (100 W, oxygen at 100 sccm) for 1 min. The unit was then operated under a mixture of CF_4 and oxygen gas (300W, CF_4 at 30 sccm and oxygen at 5 sccm) for 30 s to etch the silicon so as to give an outline of the microwell on the wafer.

2.2.4 Cell Experiments

Cell culture. HT-29 human adenocarcinoma cell line was cultured in a humidified atmosphere of 5% CO_2 in 25 cm^2 flask and fed with fresh medium every 2-3 days. The growth medium consisted of DMEM supplemented with 10 % fetal bovine serum, 100 units/mL penicillin, and 100 μg/mL streptomycin. Subconfluent cells were passaged by trypsinization in 1 mL of Trypsin-EDTA (50 μg/mL trypsin, 20 μg/mL EDTA in PBS) for 30 s. After removal of trypsin, the cells were incubated at 37°C for 5 min. Fresh medium was then added to inhibit the effect of trypsin and the cells were dispersed by pipetting. The cells were washed by centrifugation and resuspended in complete medium. The cell viability was determined by staining with Trypan Blue and the cell density was estimated by using a 0.9 mm^3 hemocytometer.

Cell seeding. The substrates were immersed in 70% ethanol in deionized water for 30 min to minimize the risk of bacterial and fungal contamination. It was then rinsed with copious amount of PBS to remove ethanol remnants. Cells were seeded on the substrates placed in 24-well culture plate at a density of 5 x 10^4 cells per well. The cells were allowed to adhere for 24 h under standard culture conditions. The substrates were rinsed vigorously with PBS to remove the non-adherent cells.

2.3 Results & Discussion

2.3.1 Template Design and Prerequisites

The template contains an array of 50 x 50 microwells which form the designated adhesive regions. The diameter of each microwell is 35 μm with a centre to centre spacing of 100 μm. The size of the microwell is sufficient to accommodate attachment of a few HT-29 cells. The mask for photolithography was created using AutoCAD and printed on a transparency with a high resolution printer (Duffy et al., 1998). This method of mask printing is more efficient and economical than a chrome mask which is generated with electron beam lithography. The drawback of a transparency mask is that the edge resolution is less than 5 μm for linear features; however, this is not a constraint for cell micropatterning as the required feature size are typically more than 30 μm.

As the template will be used for colloidal assembly and integrated with protein and cell micropatterning subsequently, it is important that the pre-requisites for the two processes

do not conflict with each other. The major requirement for biomolecules micropatterning is an inert background surface which is resistant to protein and cell adhesion. Poly(ethylene glycol) (PEG) is a non-toxic, non-immunogenic and non-antigenic polymer that can provide protein repellent surface on various kinds of substrates (Alcantar et al., 2000; Massia and Stark, 2001; Zhang et al., 1998b). PEG is known to decrease the attractive forces between solid surfaces and proteins because of its highly hydrated polymer chains, steric stabilization forces, as well as chain mobility. PEG-silane was grafted onto the silicon wafer via covalent bonding to the hydroxyl groups onto silicon surfaces using a one step reaction method (Papra et al., 2001).

The grafting of PEG onto the silicon wafer is the first step of the patterning procedure; therefore, it risks being damaged by the succeeding fabrication steps. Three microfabrication processes were designed to pattern PEG and its functionality was evaluated at the end of the process. In the first and second technique, PEG was patterned using conventional photoresist lithography and a PDMS stencil to act as a mask respectively. Both of these techniques induced deleterious effects on the PEG as evident by its inability to withstand cell adhesion. The third method makes use of photoresist lithography but an additional layer of parylene film was deposited between the PEG grafted surface and the photoresist, which successfully protected the PEG. The details of these fabrication procedures are described below.

2.3.2 Photoresist Lithography on PEG

In the first attempt, conventional photoresist lithography was used to generate a PEG pattern. Firstly, PEG was grafted onto the silicon wafer and photolithography was performed on it. The positive photoresist was spin coated on the PEG film, followed by exposure to UV and developing. The schematic diagram for the procedure is depicted in Figure 2.1 A. Figure 2.1 B shows the SEM image of the photoresist pattern, the view was tilted by 45° in Figure 2.1 C to illustrate the depth of the photoresist wells. The profile of the microwells was characterized with an optical profiler (Wyko NT3300, Veeco, New York); the depth of the wells was approximately 12 μm (Figure 2.1 D). The photoresist pattern acts as a mask for reactive ion etching. The exposed regions on the wafer were subjected to oxygen plasma to remove the PEG film, while those regions below the photoresist were protected from oxygen plasma. The exact thickness of the photoresist layer is not critical but it must be sufficient to act as a protective layer during etching. The microwells were then modified with amino-silane to generate a hydrophilic domain; this is to facilitate assembly of colloids in the later stage. Finally, the photoresist was stripped by rinsing in acetone and deionized water.

The silicon wafer was then used as a substrate for HT-29 cell culture to test the functionality of PEG after performing photolithography on it. The substrate was observed 24 h after cell seeding. The results show that the substrate which was grafted with PEG was not efficient in resisting cell adhesion (Figure 2.1 E). On the other hand, the control substrate, which was grafted with PEG but not subjected to further processing, was able to resist cell adhesion (result not shown) This suggests that PEG grafting was performed

successfully but the direct contact of photoresist with the PEG film and the use of acetone to strip the photoresist may have affected the functionality of PEG. This result is not unforeseen as it is known that some classes of materials, for example, biological materials, gels, some polymers, and organic and organometallic species are often incompatible with the chemicals used in photolithography (Kane et al., 1999) and PEG is proved to be one of them.

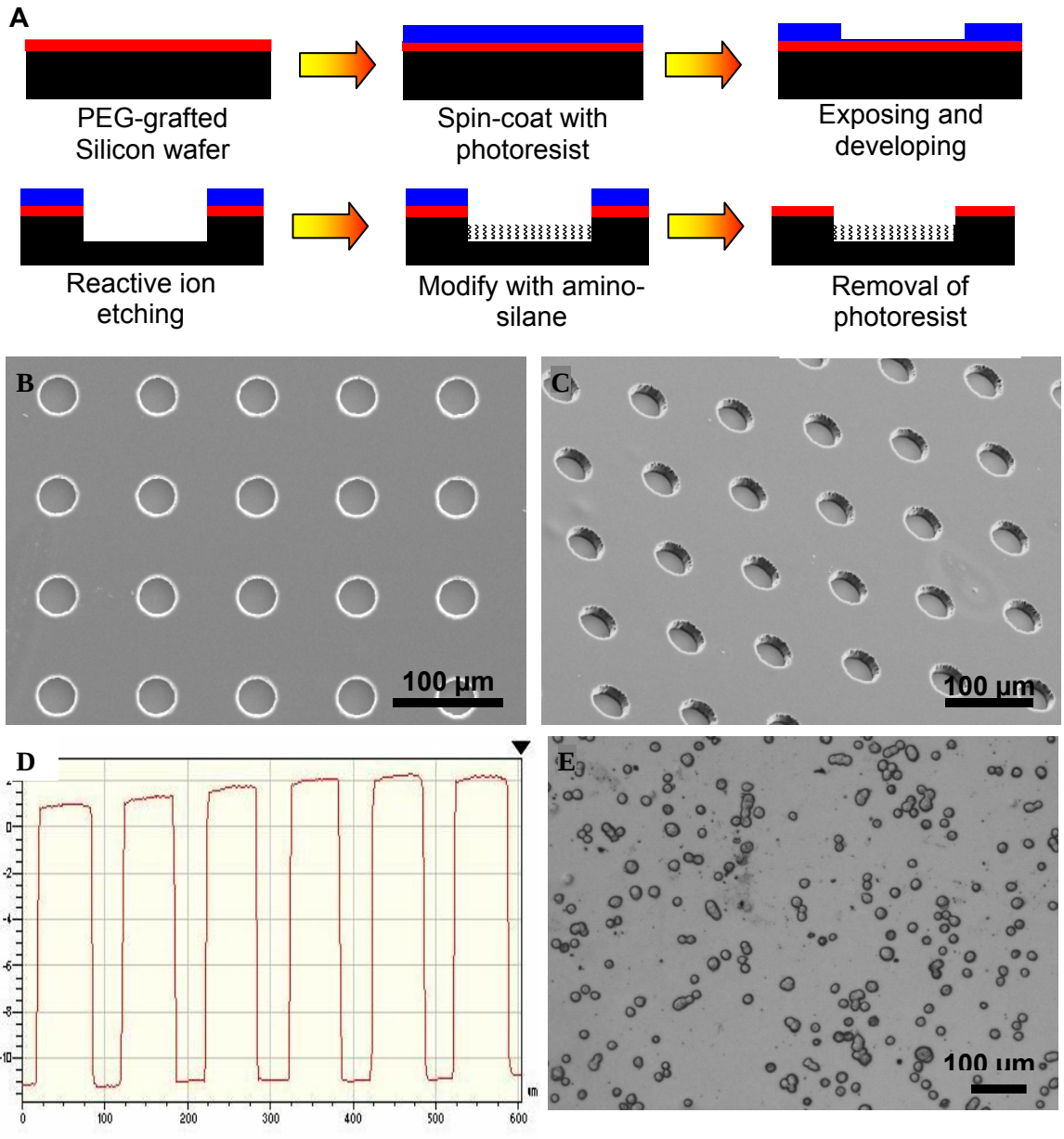

Figure 2.1. Patterning of PEG with photoresist lithography. (A) Schematic diagram of the patterning process. SEM images of photoresist pattern (B) Top view; (C) Tilted at 45°. (D) Cross-sectional profile of photoresist pattern. (E) Optical image showing cells adhered on the PEG grafted silicon substrate. (A non-patterned region on the silicon wafer was used)

2.3.3 PDMS Master

Due to the incompatibility of the PEG film with photoresist, it is necessary to modify the procedure. The use of the patterned photoresist as a mask can be replaced with a elastomeric PDMS stencil (Folch et al., 2000; Ostuni et al., 2000). The stencil can conform to and seal reversibly to most substrate, hence, it can serve as a mask for patterning. It is a "dry" mask as no solvents are involved when applying the patterned mask onto the substrate or removing it from the surface.

The elastomeric stencil was fabricated by replica moulding of PDMS against a master consisting raised structures on a silicon wafer. A master containing of raised features was fabricated using negative photoresist lithography. The SEM images of the master containing micropillars are illustrated in Figure 2.2 B and C. The height of the micropillars is approximately 60 μm as characterized by the optical profiler (Figure 2.2 D). In order to create stencil with through holes, the thickness of the PDMS prepolymer cast on the master must be smaller than the height of the micropillars. PDMS was spin cast onto the master and the thickness of the polymer can be controlled by varying the spinning speed. Stencils with through holes were obtained by spin casting PDMS at 2000 rpm for 60 s on the master. Figure 2.2 E shows the SEM image of the PDMS stencil. The thickness was approximately 50 μm (Figure 2.2 F); which is less than the height of the micropillars.

After fabrication of the stencil, it was laid in conformal contact with PEG-grafted wafer. The exposed regions were subjected to oxygen plasma to remove the PEG, followed by

modification with amino-silane. The PDMS stencil was then peeled off with a tweezer. The schematic procedure for patterning is depicted in Figure 2.2 A.

HT-29 cells were seeded on the PEG grafted substrate to check for PEG functionality after the application and removal of a PDMS film. It was observed that there were several patches on substrate that were cell adhesive as shown in Figure 2.2 G. This may be attributed to the presence of unreacted highly mobile oligomers on the surface of the PDMS stencil which resulted in a strong adhesion between the surface of the stencil and the PEG film (Yao et al., 2004). The PEG molecules adhered to the stencil and were removed from the silicon wafer upon peeling of the stencil. Although there was some improvement in PEG preservation, the results was unsatisfactory for generating a high selectivity substrate for cell micropatterning.

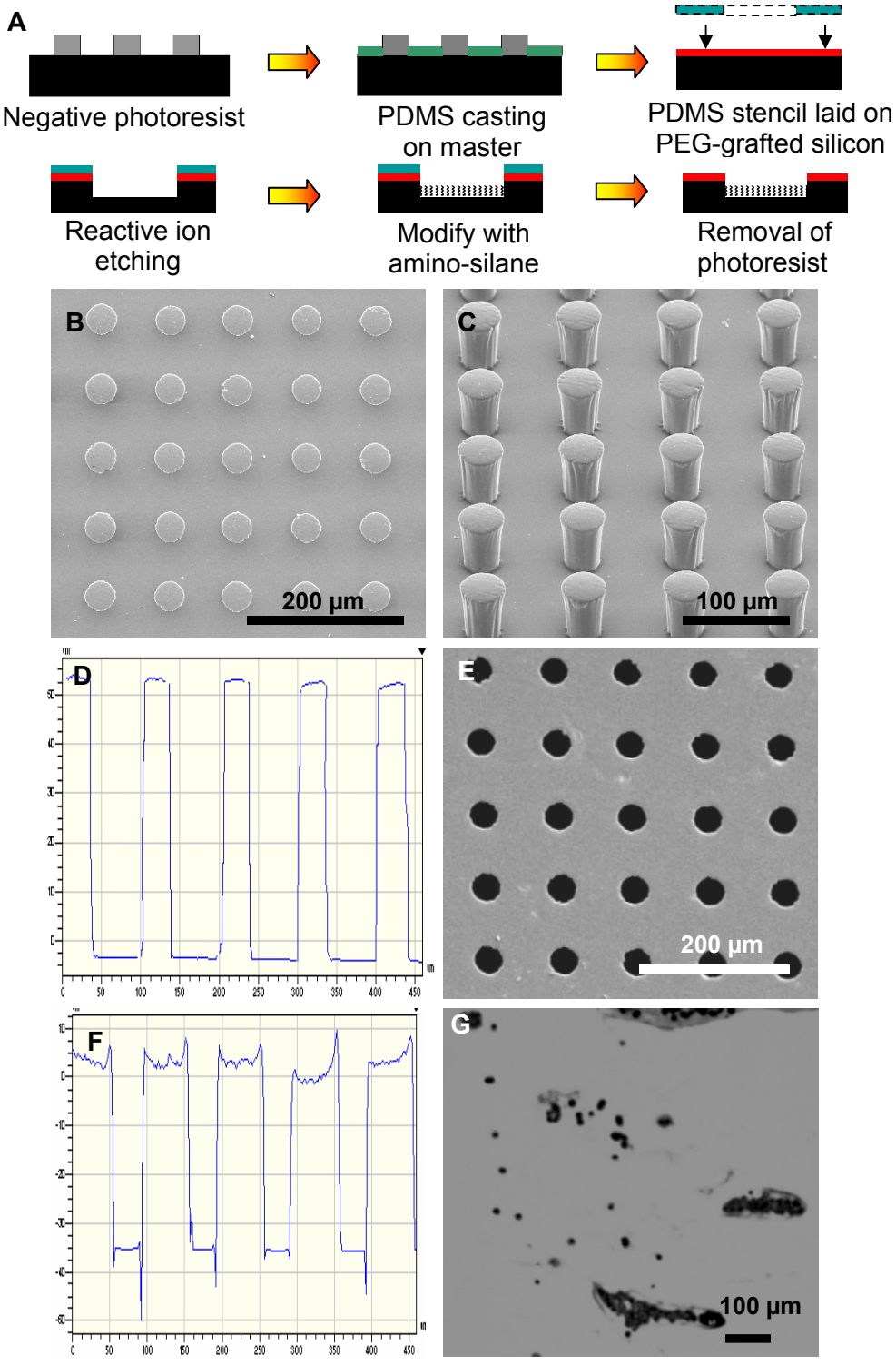

Figure 2.2. Patterning of PEG with PDMS stencil. (A) Schematic diagram of the patterning process. SEM images of the negative photoresist master, (B) Top view; (C) tilted at 45°. (D) Cross sectional profile of master. (E) SEM image of PDMS stencil. (F) Cross sectional profile of PDMS stencil. (G) Optical image of the PEG grafted silicon substrate after subjected to cell culture.

2.3.4 Parylene Template

The third approach made use of conventional photoresist lithography but with some modifications. Firstly, the silicon wafer was grafted with PEG; this was followed by chemical vapour deposition of a thin polymeric parylene film (Ilic and Craighead, 2000). The parylene film formed a conformal and pin-hole free inert polymer layer on the PEG grafted silicon wafer upon deposition. It acted as a barrier between the PEG and the photoresist, hence protecting the PEG from the deleterious effect of photoresist. It has been demonstrated previously that parylene is able to maintain the activity of PEG brushes as characterized by water contact measurement, fluorescently labelled proteins and cell adhesion experiments (Andruzzi et al., 2005).

The thickness of the parylene film on a 4 inch silicon wafer was measured using a spectral reflectance system (F50 Automated Thin Film Mapping System, Filmetrics, Inc., San Diego). The average thickness of the film is 1.0614 ± 0.0255 μm, obtained from 41 points spread over the wafer, the deviation is small and gives a uniformity of ± 4.8 %. It is crucial that the parylene film has consistent thickness so that the depth of the microwells created will be uniform across the entire wafer.

Photoresist lithography was performed atop the parylene film to pattern it. After development, the wafer was exposed to oxygen plasma to etch the parylene film and the underlying PEG; this was followed by modification with amino-silane. After the photoresist was stripped off, a hydrophobic parylene template surrounding hydrophilic wells was left on the wafer. A schematic diagram of this process is shown in Figure 2.3

A. Figure 2.3 B and C depict the SEM images of the parylene template. The template was tilted at 45° in Figure C to show the thickness of the parylene film with respect to the diameter of the microwell. The depth of the features are uniform and approximately 1 μm (Figure 2.3 D), corresponding to the thickness of the parylene film characterized earlier.

The parylene film was peeled off from the substrate by initiating the peeling at the edge with a piece of scotch tape and pulling it away from the substrate. HT-29 cells were seeded on the substrate to check for PEG activity. The substrate was successful in resisting cell adhesion, suggesting that the parylene film is effective in protecting the PEG from the negative effects of photoresist (Figure 2.3 E). The PEG film remained efficient even when it was tested 6 months after parylene deposition.

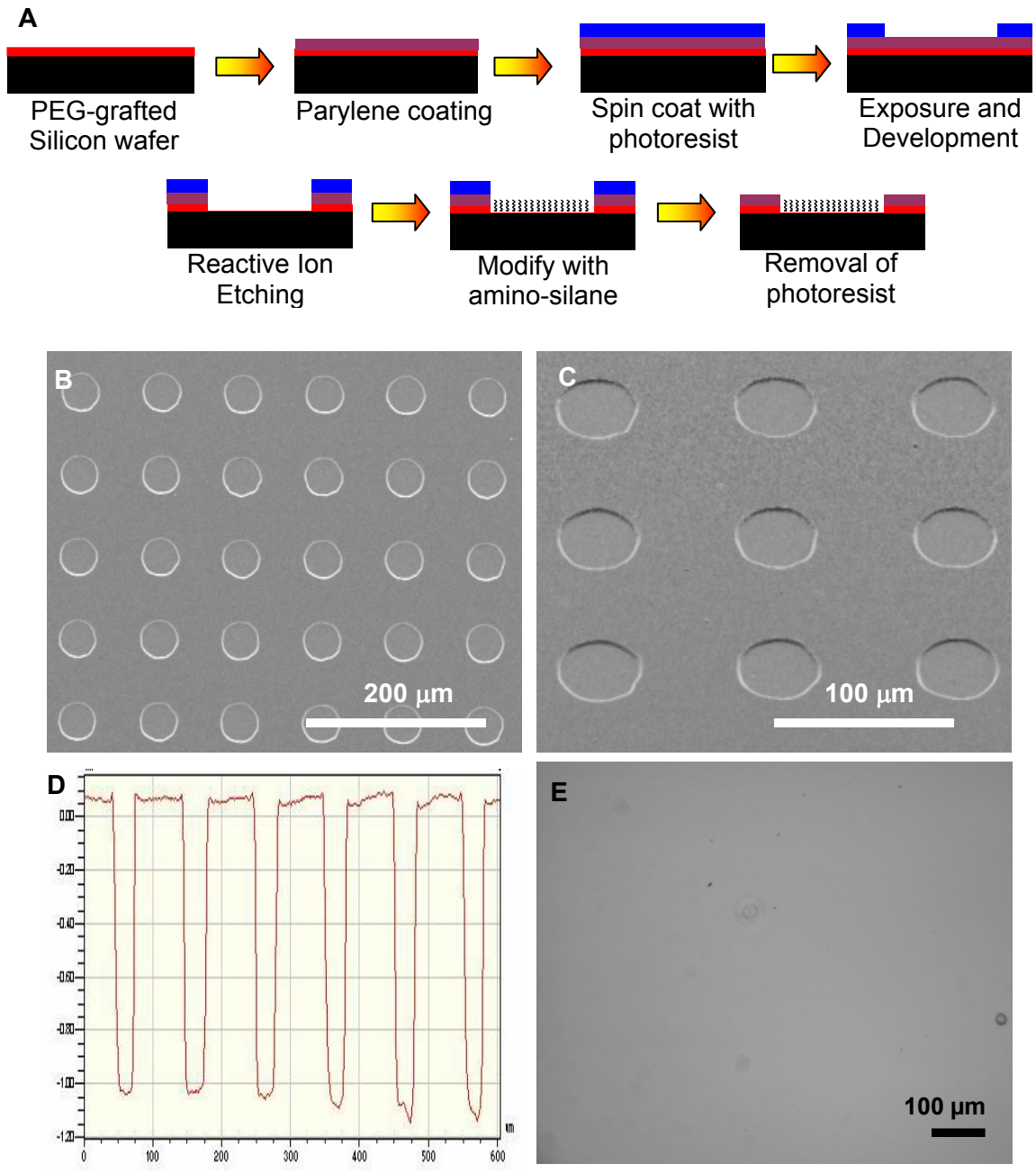

Figure 2.3. Fabrication of parylene template. (A) Schematic diagram of the patterning process. SEM image of an array of parylene microwells, (B) Top view, (C) 45° tilted view. (D) Cross sectional profile of the template. (E) Optical image of the PEG grafted silicon substrate after subjected to cell culture.

Apart from protecting the PEG modified surface, the hydrophobic parylene film plays an important role in facilitating colloidal assembly by selective wetting. The surface wettability determines the strength and direction of the capillary force acting on the particles and hence controls the deposition of the particles. The wettability of substrates was evaluated by measuring the static water contact angle on the non-patterned substrates. A small contact angle indicates that the surface is more wettable or hydrophilic, whereas a large contact angle suggests a hydrophobic surface. The contact angles for the oxidized, PEG-silane grafted, amino terminated and parylene coated silicon wafer were measured and summarized in Table 2.1.

Table 2.1. Water contact angle on surface modified silicon substrates.

Modification	**θ °**
Oxidized	< 5
PEG	38.1 ± 0.63
NH_2	40.7 ± 3.74
Parylene	100.8 ± 0.63

The template containing an array of hydrophilic amine-terminated wells is surrounded by a hydrophobic parylene matrix. A hydrophobic-hydrophilic template is suitable for patterning of colloidal particles via selective wetting in the hydrophilic regions (the mechanism for particles assembly will be discussed in chapter 3). The static contact angle of parylene film and the amine terminated silicon microwells is 100.8° ± 0.63° and 40.7° ± 3.7° respectively. A contrast in surface wettability is a prerequisite for assembly of particles, but this prerequisite may conflict with the requirements for protein and cell

micropatterning as non-fouling surfaces are not necessarily hydrophobic. The parylene film helps to overcome the incompatibility by acting as a sacrificial layer; after assembly of particles, the parylene can be peeled away. In this way, the base layer (PEG film, contact angle 38.1°) which is essential for device functionality does not have to be hydrophobic. Furthermore, any unspecific deposition of the particles on the parylene film can be removed by dry lift-off, giving a spotless background.

2.4 Conclusion

The PEG grafted surfaces hold delicate molecules which are incompatible with the chemicals used in photolithography. The conformal contact of PDMS stencil on the PEG modified surface also caused some regions on substrate to lose its cell resistant property. Nevertheless, PEG functionality can be preserved by deposition of a parylene film on the substrate prior to subjecting it to photoresist lithography. The parylene film acts as a barrier to protect the PEG film from the deleterious effects of the solvents and materials used in microfabrication. At the same time, the parylene matrix provides a hydrophobic background to facilitate particles assembly by selective wetting. The parylene template is bi-functional and is instrumental in providing a platform to integrate colloidal assembly with protein and cell micropatterning.

CHAPTER 3

ASSEMBLY OF MICRO / NANOPARTICLES INTO TWO DIMENSIONAL ARRAYS

3.1 Introduction

Patterning micro and nanometer scale particles into ordered arrays has generated much interest due to its unique potential for application in photonic (Wijnhoven and Vos, 1998; Yang et al., 2002), optoelectronic devices (Veinot et al., 2002; Yamasaki and Tsutsui, 1998), biochips (Stevens et al., 2003) and fabrication of porous structures (Velev and Kaler, 2000) and microlens array (Yabu and Shimomura, 2006). This promise cannot be fulfilled unless methods of accurate positioning the particles can be developed. Advances in top-down lithography techniques have enabled the precise and reproducible fabrication of features. A synergistic combination with bottom-up self assembly of colloidal particles into patterns is foreseen to generate new devices. Colloids such as metal nanocrystals (Cui et al., 2004), semiconductor quantum dots (Jun et al., 2006; Lu et al., 2004) and magnetic particles (Lyles et al., 2004; Pregibon et al., 2006) are promising building units as they can serve a specialized function when integrated into the device.

The potential applications of these colloids ensemble have aroused interest in exploring methods for their assembly onto patterned substrate. A variety of methods have been explored for patterning of particles into well ordered array, this include electrostatic template (Aizenberg et al., 2000; Chen et al., 2000), confinement in physical templates (Maury et al., 2005; Xia et al., 2004; Xia et al., 2003), assembly on a hydrophilic hydrophobic pattern (Fan and Stebe, 2004; Fustin et al., 2004; Masuda et al., 2005), dielectrophoretics (Docoslis and Alexandridis, 2002; Suzuki et al., 2004), microcontact

printing (Yan et al., 2004) and ink-jet printing (Park and Moon, 2006). Some of these techniques are reviewed below.

3.1.1 Electrostatic Template

In a demonstration of using electrostatic forces for assembly of particles, Aizenberg et al.(2000) chemically micropatterned the substrate with anionic and cationic regions to control the deposition of charged polystyrene particles. The patterned substrate was immersed in a suspension of particles and the excess suspension was rinsed from the surface. The charged particles preferentially attached to oppositely charged regions on the substrate with little unspecific interactions. This method offers a simple and convenient way to direct the assembly of particles into ordered array.

Hammond's group performed extensive studies on patterning of particles based on electrostatic forces (Hammond, 2004). They used microcontact printed polyelectrolyte multilayer patterns to serve as an electrostatic template for particles deposition. The success of this technique depends on the interaction between the colloid and the polyelectrolyte surface and the background region. Chen et al.(2000) demonstrated control over particles density and selectivity of adsorption by using three mechanism: (1) pH of the colloidal suspension can determine the charge density of the polyelectrolyte and the colloids; (2) ionic strength of the colloidal suspension affects the degree of charge screening on the particles and the polyelectrolyte surface; and (3) addition of surfactant shield charges on the particles while increasing hydrophobic interaction between the surfactant and polyelectrolyte. The group also demonstrated an approach to assemble

two different types of polystyrene microspheres by manipulating the adsorption conditions of the substrate (Zheng et al., 2002). The sorting of particles on the substrate requires careful manipulation of interactions that can prevent deposition, such as steric or hydration forces or electrostatic repulsion, and those that promote it.

3.1.2 Hydrophobic-Hydrophilic Template

A template consisting of a hydrophobic background surrounding hydrophilic domains is suitable for colloidal assembly. A colloidal suspension with the fluid contact line sweeping across the surface will result in the selective wetting of the hydrophilic regions and deposition at these regions. Fan & Stebe(2004) fabricated a substrate with 50 μm hydrophilic carboxylic-terminated features on a continuous hydrophobic methyl-terminated background. Polystyrene microspheres were self-assembled into the hydrophilic regions by placing a drop of the suspension on the template and allowing it to evaporate. Evaporation of the droplet resulted in a moving fluid contact line on the substrate and particles were spontaneously assembled into the hydrophilic regions.

Masuda et al.(2005) developed a novel two-solution self assembly method for micropatterning of silica particles. Silica particles dispersed in methanol was dispensed on a patterned hydrophobic octadecyltrichlorosilane (OTS) self assembled monolayer (SAM). The hydrophobic regions lightly repelled the particles suspension and it existed mainly on the hydrophilic silanol regions. The assembly was then immersed in hexane, and this drove the methanol to exist selectively on the hydrophilic regions. As the methanol slowly dissolved into hexane, the concentration of the particles increased and

close-packed structures was formed due to capillary force. This method of self-assembly is able to create colloidal crystal patterns with high edge acuity and regularity.

3.1.3 Physical Confinement

Xia et al.(2004) assembled silica nanoparticles into nanometer scale grooves and cylindrical holes by spin-coating. A combination of gravity-driven sedimentation, evaporation induced capillary forces, centripetal forces, and blocking forces from physical confinement at the edges of the pattern resulted in the assembly of the silica particles into the confined spaces. By varying the spin speed, pH value of the nanoparticle suspension, particle size, and the geometry of the grooves and cylindrical holes on the substrate, the group achieved linear, zizag and two columns of silica nanoparticles in narrow grooves. Two dimensional arrays of silica nanoparticle including colloidal clusters of monomers, dimmers, trimers and quatramers on patterned samples was achieved by tuning the ratio between diameters of the holes and particles.

Xia and colleagues(2003) self-assembled polystyrene beads into holes patterned in a thin film of photoresist based on physical confinement and capillary force. The photoresist substrate was enclosed between two glass substrate with micrometer gap between them. A suspension of the beads was added into this cell and the front of this thin film of liquid was allowed to move slowly along the patterned substrate. When the front of the liquid crossed the hole, the beads were dragged into the hole by capillary force. The diameter and height of the hole will determine the number of beads that can be retained in it. By

varying the size of the holes, a range of uniform, polygonal cluster of beads was formed in the wells.

Kim et al.(1996) formed well-ordered arrays of hexagonally packed polystyrene microspheres by microfluidic patterning. The poly(dimethylslioxane) (PDMS) channels sealed against the substrate confined a suspension of microspheres and water was allowed to evaporate through the opening of the channels. Crystalline arrays of microspheres remained on the substrate after removal of the PDMS master. Formation of this closely packed structure involves two steps, i.e. nucleation and growth. The attractive lateral capillary force among the microspheres causes the microspheres to aggregate into nucleation site while the growth of the array is attributed to fluid influx to the nucleation site so as to compensate water loss due to evaporation.

3.1.4 Dielectrophoretics

Dielectrophoresis is the phenomenon in which polarisable objects are manipulated due to their interaction with a non-uniform electric field, created by one or more pairs of oppositely charged electrodes. The movement of particles towards the strong electric field region is known as positive dielectrophoresis while movement towards the weak electric field region is called negative dielectrophoresis (Pohl, 1978). Dielectrophoresis was first investigated a few decades ago but interest in this phenomenon was recently revived due to its potential application for organization of particles. Docoslis and Alexandridis(2002) demonstrated the organization of one-, two- or three-dimensional colloids by using dielectrophoresis. Non-uniform electric fields were generated by sets of

gold electrode patterned on the glass substrate. By controlling parameters such as electrode configuration, voltage, AC frequency and particle concentration, particles were organized into the required pattern. To maintain the arrangement of the particles after the removal of the AC voltage, the particles were covalently linked to the substrate using cross-linking reagents.

Instead of fabricating the electrodes on the patterning substrate, the electrode can be created on a separate substrate and place above the sample substrate. Suzuki et al.(2004) created patterns of microparticles using a dielectrophoretic cell composed of an electrode template and a substrate facing the template with a spacer. The frequency of the AC electric field was adjusted to obtain repulsive negative dielectrophoresis force that arranged the particles into pattern similar to the template electrode.

3.1.5 Microcontact Printing

Microcontact printing developed originally for patterning of biomolecules and organic chemicals can also be used to pattern microspheres. Yao et al.(2004) reported on a lift-up soft lithography technique to fabricate ordered colloidal crystals on a substrate. In brief, monodisperse silica microspheres were assembled into colloidal crystal on silicon wafer by evaporation. A PDMS stamp with relief features was then brought into contact with the crystal film. Upon peeling off the PDMS stamp, a layer of closely packed microspheres adhered to the stamp and the corresponding pattern was formed in the crystal film on the silicon surface. Yan et al.(2004) continued to demonstrate how the microspheres on the PDMS stamp can be printed onto polymer-coated solid substrate.

The printed patterns consisted of highly ordered silica microspheres packed in a hexagonal arrangement, indicating that there was perfect transfer of the ordered array of microspheres from the crystal film to the PDMS stamp and to the substrate. The success of this method depends on manipulating the interaction among the microspheres, PDMS stamp and the substrate for patterning. Due to the flexibility of the PDMS stamp, this technique can be used to pattern colloidal crystal on a nonplanar surface.

A myriad of mechanism is capable of assembling colloids into pattern; however each technique has its limitation. Patterning of particles via electrostatic attraction allows one to control the packing density, however, even at a high density; the particles are not arranged in a closely-packed manner. This may be due to the strong adhesion between the particles and the oppositely charged substrate which inhibits the rearrangement and close packing of particles during the drying process (Zheng et al., 2002). On the other hand, when capillary force is involved in driving the assembly of particles, close packed array of particles will be produced. Patterning of particles by physical confinement is effective only when the dimension of the hole is comparable to the size of the particle.

The assembly of colloidal particles is an important first step towards its integration with protein and cell micropatterning. In this work, the micro and nanoparticles will be assembled into designated regions to form the protein and cell adhesive areas. The micro or nanotopography created by the particles is expected to have several advantages over conventional micropatterning that are performed on a planar substrate (discussed in Chapter 4 and 5). To achieve this, micro and nanoparticles will be assembled into regions

that are several times larger than the diameter of the particle. The density of particles in these regions can vary between sparsely packed to closely pack ordered structures. A close packed ordered structure has the advantage of increasing the surface area for biomolecules conjugation to the maximal and creates uniform protein and cell adhesive regions. Furthermore, varying the density of particles deposited in the designated regions allows fine-tuning of the surface roughness and this can be used as a platform for studying the effect of roughness on cell adhesion.

Although significant progress has been made to assemble particles into patterns, most of the methods are not compatible with protein and cell micropatterning. For example, in some techniques, particles are assembled into recessions that are comparable in size to the diameter of the particle (Cui et al., 2004; Xia et al., 2003) which is too small for cell adhesion. In other methods that involved assembly of particles into sufficiently large regions (Fan and Stebe, 2004), the particles failed to assemble into a monolayer of order structures. In addition, the background regions are usually hydrophobic (Fan and Stebe, 2004; Masuda et al., 2005) or charged (Aizenberg et al., 2000; Xia et al., 2004) to prevent unspecific deposition of particles in the background but theses surface cannot resist adhesion of proteins and cells. In view of the restrictions inherent in these reported techniques, a new method of colloidal assembly has to be developed so that it can be incorporated with protein and cell micropatterning.

The development of a bi-functional template which is compatible for colloidal assembly and cell micropatterning was described in Chapter 2. In this chapter, a technique of

generating spatial arrangement of microspheres on the bi-functional template is developed. As the template has hydrophilic microwells surrounded by hydrophobic parylene film on the background, particles were assembled by selective wetting of the hydrophobic-hydrophilic template. A fluidic chamber was designed to control the movement of the particle suspension across the template so as to attain uniform particles deposition over a large area. The topography of the adhesive regions was controlled by varying the size and the density of particles deposited onto it. After deposition of particles, the parylene film can be lift-off, revealing a protein resistant PEG background which is compatible with protein and cell micropatterning.

3.2 Materials and Methods

3.2.1 Materials

0.454 μm (solid content 2.59 %), 0.984 μm (2.62 %) and 2.022 μm (2.65 %) carboxylated polystyrene (PS-COOH) microspheres, 0.913 μm (2.62 %) amino polystyrene (PS-NH_2) microspheres and 0.3 μm silica microspheres were purchased from Polysciences, Inc. 50 nm gold nanoparticles was purchased from British Biocell International Ltd. All reagents and materials were used as received.

3.2.2 Fabrication and Operation of Fluidic Chamber

The chamber consisted of a polystyrene sheet with a channel cut on it and two pieces of PMMA (polymethyl methacrylate). The dimension of the PMMA is 6.5 x 3.0 x 0.4 cm.

The patterned substrate was sandwiched between the polystyrene sheet and the PMMA. The assembly was held together by four binder clips. A through hole of approximately 1.5 mm in diameter was created on the top PMMA using a diamond driller. A hollow metallic tube (outer diameter 1.5 mm; inner diameter 1.0 mm) was fitted snugly into the hole and held firmly by applying epoxy adhesive. The polystyrene sheet containing the channel was adhered to the top PMMA using double sided adhesive. The other face of the polystyrene sheet was laminated with a layer of cellulose transparent tape. The device consisted of a single channel originating at the inlet with a 30° angle expansion to give a 5 mm wide channel which runs for a length of 2.5 cm before it was subjected to a 30° angle contraction to form a 0.15 cm wide channel. The depth of the channel is approximately 630 μm, which is equivalent to the total thickness of the polystyrene sheet, a layer of double sided adhesive and cellulose adhesive tape.

A suspension of monodispersed particles was injected into the channel with a syringe pump at a flow rate of 5 mL/h via a silicone tubing fitted to the metallic tube on the fluidic chamber. The assembly was kept in an upright position during injection so that the channel can be filled to the brink. The volume of the channel is approximate 150 μL. After the channel was filled, the fluidic chamber was laid horizontally and the syringe pump continued to inject air into the channel which resulted in a pressure driven fluid front moving along the channel. The density of particles in the microwells was controlled by varying the air flow rate between 5 - 50 μL/h, corresponding to a fluid front movement of 1.6 – 16 mm/h, while the concentration of the microsphere suspension injected ranged from 1.5 – 7.5% w/w.

3.2.3 Equipments

Microscopy. The samples were visualized and images were captured using an upright optical microscope (Zeiss Axiostar Plus) equipped with a CCD camera (Media Cybernetics, Evolution^{TM} MP) with a pixel size of 3.4 x 3.4 μm.. The samples were sputter coated with gold (JEOL JFC-1600 Auto Fine Coater) for 50 s at 30 mA before examination with Hitachi field emission scanning electron microscopy (SEM), at an accelerating voltage of 15 keV.

Image Analysis. Images of microspheres deposited microwells were analyzed using ImageJ, a public domain image processing program by the U.S. National Institutes of Health (http://rsb.info.nih.gov/ij/ accessed in August 2006).

3.3 Results & Discussion

3.3.1 Mechanism for Assembly of Polystyrene Microspheres

The fabricated template contains an array of hydrophilic microwells grafted with amino-silane, surrounded by hydrophobic parylene film. To assemble particles on a hydrophobic hydrophilic template, a colloidal suspension with the fluid contact line sweeping across the surface will result in the selective wetting of the hydrophilic domains and deposition at these regions. Some of the techniques used to create a moving contact line include evaporation of a droplet (Fan and Stebe, 2004) and lifting of the patterned substrate vertically out of a colloidal suspension (Fustin et al., 2004). In this section, two methods

were used to generate a moving fluid front. Due to the ease of the application, the first method tested was evaporation of a suspension droplet. However, the deposition of the particles was not uniform and a new technique was introduced to drive the fluid front along a channel in a fluidic chamber. The mechanisms involved for assembly of particles involved in these two techniques are discussed.

3.3.1.1 Evaporation of a Droplet

A 30 μL droplet containing suspended PS-COOH microspheres, at pH 4.3 was dispensed on the patterned substrate (Figure 3.1 A). The droplet was exposed to normal atmospheric condition of 25°C and relative humidity of 75% to evaporate over time. The droplet spread to a certain diameter, covering many microwells, with a contact angle of 98°. In the initial stages of evaporation, the contact line of the droplet remained unchanged while the contact angle decreased. During this period, there was a continuous radial outward flow of solvent from the centre of the droplet to the boundary to compensate for the volume lost by evaporation so that the diameter of the drop will not shrink (Deegan et al., 1997). This convective flow carried suspended particles to the edge, resulting in a much higher concentration of particles at the contact line.

After sometime, the contact line begin to recede, the microspheres were pushed inwards by capillary force. Figure 3.1 B depicts the process for the self assembly of PS-COOH microspheres into the mcirowells. When the contact line passes over the hydrophilic microwells, it becomes pinned at leading edge of the hydrophobic-hydrophilic substrate junction but pulled back from the hydrophobic regions. These local dynamics caused

solvent to flow out of the hydrophobic and into the hydrophilic region (Fan and Stebe, 2004) resulting in a corrugated edge on the patterned surface (Figure 3.1 C). When the contact line is pinned at the microwells, particles are deposited due to the electrostatic attraction between the particles and the amino terminated surface. At pH 4.3, the $-NH_2$ groups on the surface of the microwells and the -COOH group on the polystyrene microspheres are ionized into $-NH_3^+$ and $-COO^-$, respectively (Saito et al., 2004).

As the fluid in the microwells evaporated, the contact line de-pinned and receded from the domain, necking and tearing off to form a discrete fluid element in the microwell. When fluid between the microspheres in this element evaporated, the particles are tightly packed into ordered structures by the contraction of capillary bridges connecting them (Kralchevsky and Nagayama, 1994). When the contact line jumped from one hydrophilic microwell to the other, it moved across the hydrophobic parylene surface very quickly, capillary force pushed the particles inwards, hence no particles is deposited on the hydrophobic surface. When the contact line encountered another hydrophilic microwell, the process of particles deposition began again.

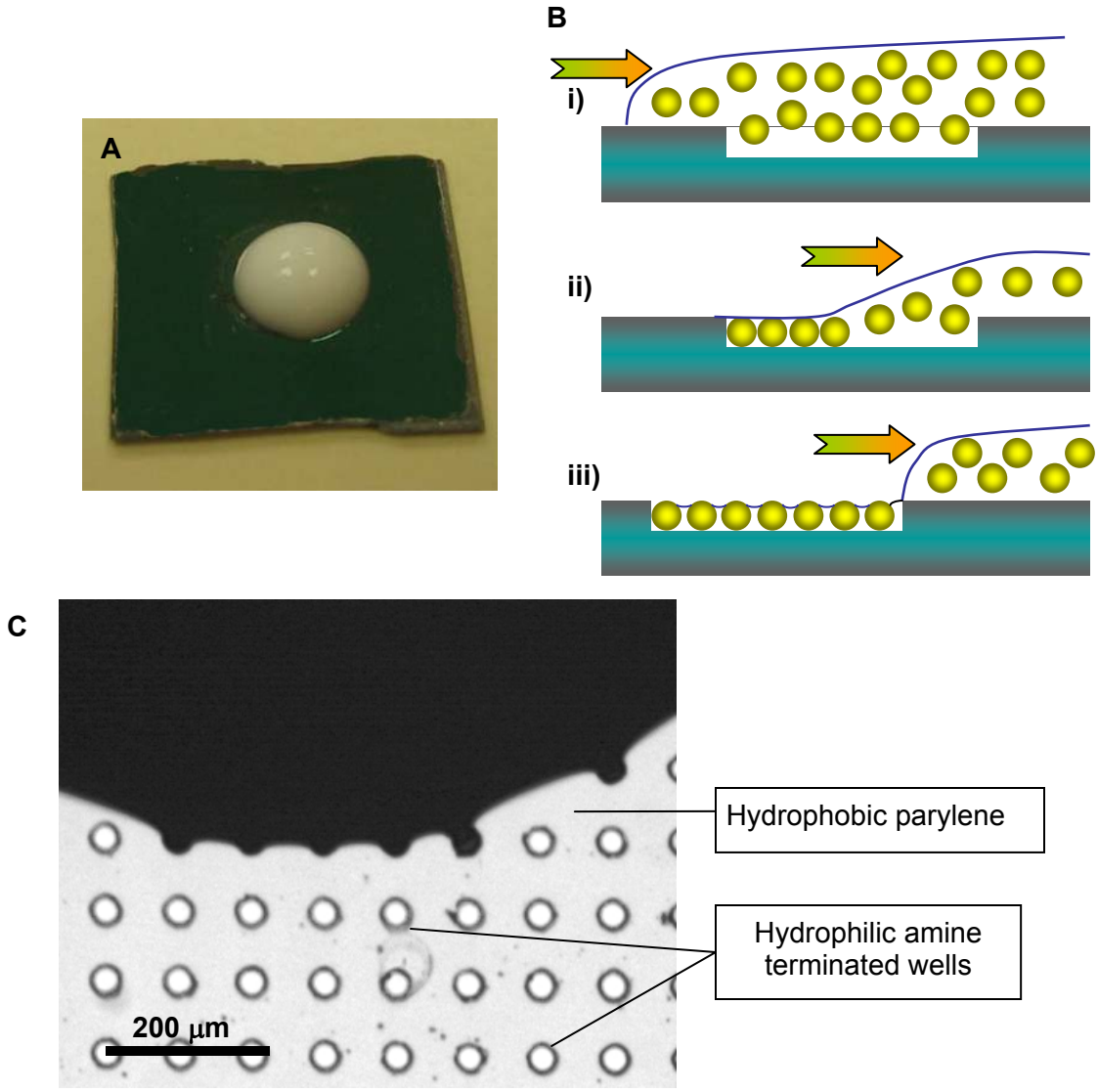

Figure 3.1. Evaporation driven assembly of particles on a hydrophilic-hydrophobic template. (A) Image of a droplet of microsphere suspension cast on the patterned substrate exposed to atmospheric conditions. (B) Schematic diagram for assembly of PS-COOH microspheres. (i) When the contact line of the PS-COOH suspension meets the hydrophobic parylene surface, capillary forces pushes the microspheres inwards. (ii) As the contact line meets the hydrophilic microwells, it becomes pinned and microspheres flow into the microwell. (iii) The contact line recedes and microspheres are deposited in the microwell. As fluid in the microwell evaporates, the microspheres are packed into ordered structures. (C) Optical image of the contact line of a droplet of negatively charged PS-COOH (dark region) at pH 4.3 on 35 µm amine modified microwells with a hydrophobic parylene background. The irregular edge of the droplet is due to flow of particles into the hydrophilic wells.

The amount of particles deposited in the microwells is determined mainly by two factors. (1) The concentration of particles in the suspension. A higher concentration of particles at the contact line will result in a higher density of particles deposited in the microwells. (2) The rate of movement of the contact line. The slower the movement, the higher the amount of particles deposited.

In order to obtain uniform deposition, the concentration of the colloidal suspension and the rate of movement of the contact line over the patterned substrate must remain consistent. It is difficult to achieve uniform deposition by using the evaporation technique as the rate of movement of the contact line and the concentration of particles at the contact boundary vary significantly during the course of evaporation. In the initial stages of evaporation, the contact line is pinned while there is continuous radial outward flow of solvent, carrying with it suspended particles from the centre of the contact area to the edge (Deegan et al., 1997). An increase in concentration of particles coupled with a pinned contact line resulted in a high density of particles deposited at the boundary, producing the "coffee ring" effect, while the centre regions are depleted of particles. This effect is evident in Figure 3.2 A, where a 30 μL droplet of 0.1% w/w 1 μm PS-COOH microspheres was dispensed on the substrate and allowed to evaporate until dry. A thick ring of microspheres assembled near the boundary of the droplet. The microwells at the centre regions are sparsely filled (Figure 3.2 B) while those at boundary has multilayer of microspheres (Figure 3.2 C).

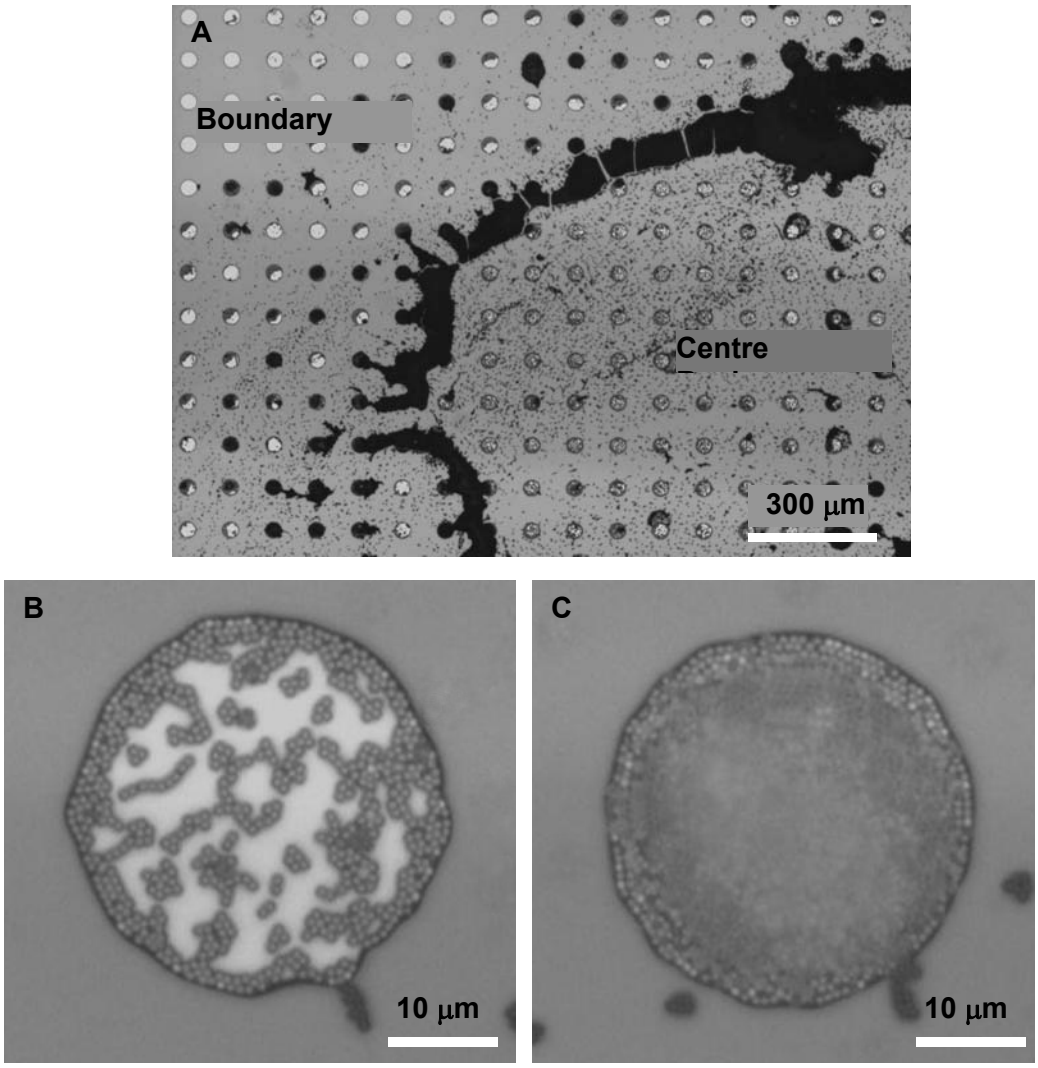

Figure 3.2. PS-COOH microspheres assembled by evaporation. (A)"Coffee ring" effect observed by evaporation of a droplet of microsphere suspension on the patterned substrate. Microwells are sparsely filled with microspheres at the centre region of the droplet while those at the boundary are densely packed. The respective regions are indicated on the figure. Magnified images of (B) a sparsely packed microwell at the centre region and (C) a densely packed microwell at the boundary.

3.3.1.2 Fluidic Chamber

To achieve uniform particle distribution across the substrate, it is predominant that the water contact line shift at a constant rate while the concentration of the particles at the fluid front remains constant. This may be achieved by withdrawing the substrate out of a

colloidal suspension vertically (Fustin et al., 2004). For this technique, the concentration of particles in the reservoir does not vary significantly and by adopting a fixed withdrawing speed, the movement rate of the contact line can be keep constant. However, the drawback is that a large amount of particles (typically a few millilitres) is required so that substrate can be immersed in the suspension. In this section, an alternate method which involves a fluidic chamber consisting of a channel was developed to control the flow of microsphere suspension over the patterned substrate.

The fluidic chamber consists of a polystyrene sheet with a channel cut on it and two pieces of PMMA, sandwiching a strip of the patterned substrate (Figure 3.3 A). The depth of the channel is 630 μm and the shape was designed such that the flow across the channel is uniform (Figure 3.3 B). The schematic representation of the fluidic chamber ensemble is illustrated in Figure 3.3 C.

The fluidic chamber was fabricated using PMMA instead of PDMS, which is commonly used for rapid fabrication of microfluidic systems (Duffy et al., 1998). Although PDMS has many desirable characteristic such as ease of moulding, surface modification, and conformal contact with many surfaces (Ng et al., 2002), the use of PDMS for this fluidic chamber is not suitable. As the microwells are fabricated on the silicon chip as a separate entity, the fluidic chamber should be demountable from the chip but at the same time the seal should be water-tight. PDMS can make reversible sealing to smooth surfaces, however, the seal is not sufficiently strong to withstand a pressure driven flow. Securing the PDMS slabs with mechanical force is not a viable option as it will deform the

channels due to the elastic nature of PDMS. Furthermore, PDMS tends to adhere to the parylene film on the template and peeled it off when the PDMS is demounted. Hence, the rigid PMMA was used to overcome these problems. The patterned substrate was sandwiched between the two pieces of PMMA using binder clips. In addition, PMMA has good optical property which allows observation with the microscope.

As the dimensions of the required channel are larger than micron scale, it is not necessary to use micromachining to fabricate the channels. Instead, the channel was cut manually on a polystyrene sheet and adhered to the PMMA slab using double sided adhesive. The other face of the plastic sheet is laminated with a layer of cellulose adhesive tape to provide a soft finish to the otherwise rigid PMMA. The soft finish is essential for giving conformal contact between the substrate and the polystyrene sheet so as to prevent leakage of the colloidal suspension and minimize evaporation.

After the chip was mounted in the fluidic chamber, a suspension of monodispersed particles was injected into the channel with a syringe pump to fill the channel completely. This was followed by injection of air into the channel to push the particle suspension into the outlet, which resulted in a pressure driven moving fluid front along the channel. By operating the syringe pump at a constant rate, the fluid front moved with a uniform velocity along the channel.

The mechanism for selective deposition of microspheres is similar to that reported by Yin et al. (2001). In their work, they reported the fabrication of a fluidic cell for assembly

of colloids into template by movement of the colloidal suspension induced by evaporation. Capillary force coupled with the confining effect of the template assembled the particles into the holes. In their work, the dimension of their microwell is comparable to the size of the particles; which is about 1 to 3 times larger than the diameter of the particles, allowing it to hold up to 8 particles. However, in this work, the microwell is about 35 times (considering 1 μm particles) larger than the diameter of the particles, which requires more than a thousand particles to fill up a microwell completely. Due to the sheer size of the microwell, it cannot rely on physical confinement exerted by its wall to trap the particles.

In the present work, the patterned hydrophobicity and surface charge of the template affects the forces acting on the microspheres. The forces acting on the microsphere at the fluid interface include capillary force (F_C), electrostatic interaction (F_E) and gravitational force (F_G). Figures 3.3 D and E show the longitudinal section of the channel. The forces acting on the microsphere when the fluid front meets the hydrophilic well and the hydrophobic parylene regions are indicated in the respective diagram. The shape of the fluid front depends on the wettability of the walls of the channel (Huang et al., 2006). The channel roof (PMMA) is slightly hydrophilic with a contact angle of approximately 71°. When the fluid front meets the hydrophilic well, a concave meniscus is attained. Electrostatic attraction is present between the negatively charged PS-COOH microspheres and the positively charged amine-terminated microwell at pH 4.3. The capillary and electrostatic forces acting on the microsphere are in the direction that is favourable for the deposition of the microsphere into the microwell (Figure 3.3 D). When

the fluid front intersects with the hydrophobic background regions, a convex meniscus is formed; the capillary force pushes the microsphere away from the background regions. There is no electrostatic attraction between the microsphere and the parylene surface (Figure 3.3 E). The microspheres are not deposited on the background regions and this resulted in the selective deposition of microspheres in the microwells.

Figure 3.3 F shows the SEM images of the microspheres assembled microwells obtained by this technique at different magnifications. The assembly of PS-COOH microspheres into the hydrophilic microwells was highly selective, with little unspecific deposition on the hydrophobic background. The distribution of particles in the microwells across the substrate is uniform.

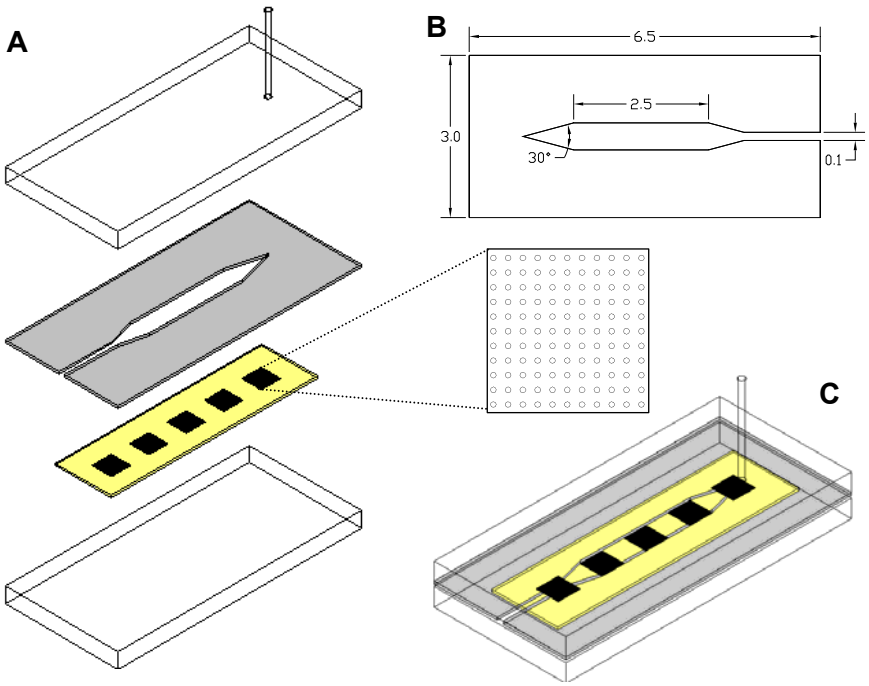

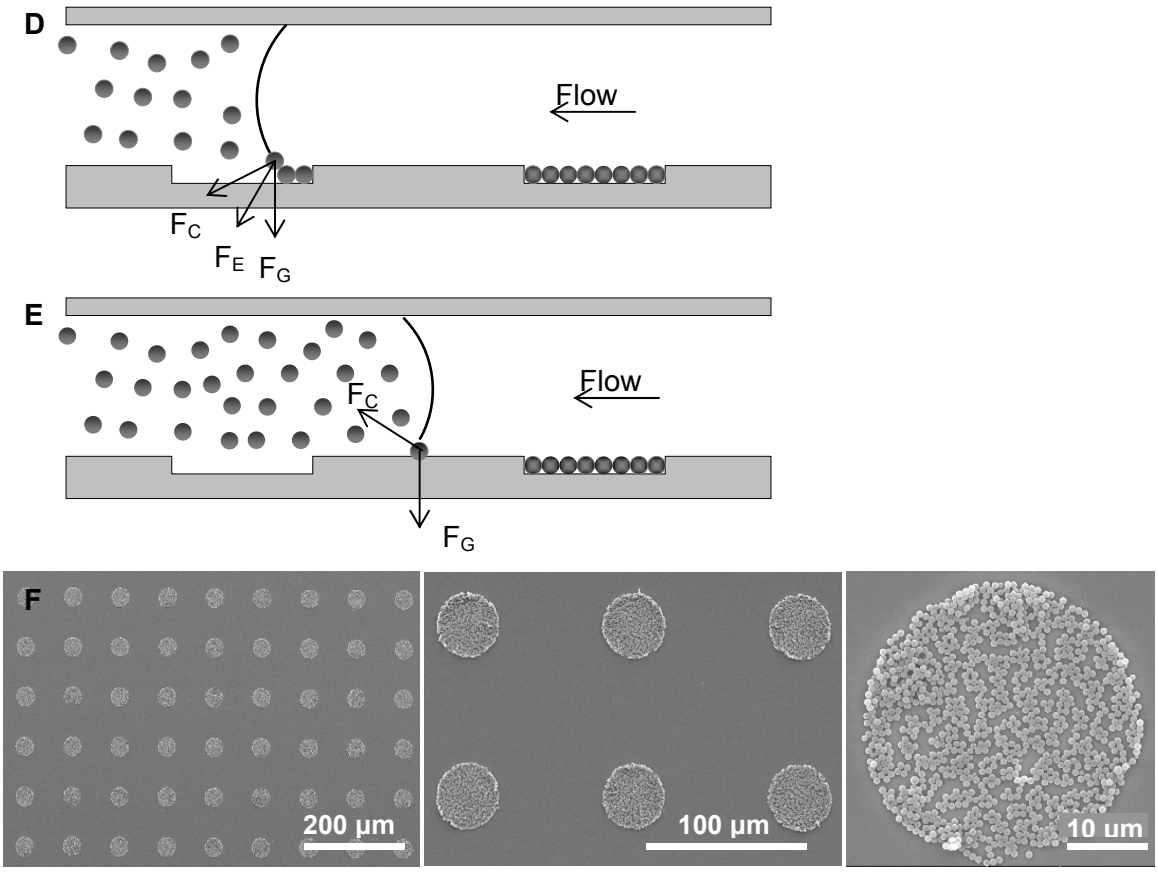

Figure 3.3. Assembly of particles on a hydrophilic-hydrophobic template using a fluidic chamber. (A) Components of the fluidic chamber, which includes a top PMMA slab, a polystyrene sheet with the channel cut on it, the template and a bottom PMMA slab. (B) Illustration of the channel profile with the dimension given in centimetres. (C) Schematic representation of the fluidic chamber with the components assembled together. (D, E) Longitudinal view of the fluidic channel. The possible forces acting on the microspheres when the fluid front meets the (D) hydrophilic amine terminated microwells, and (E) hydrophobic parylene are indicated. Capillary force (F_C), Electrostatic force (F_E), Gravitational force (F_G). The direction of the flow is shown with an arrow. Diagrams are not drawn to scale. (F) SEM images of 1 µm PS-COOH microspheres assembled in microwells at various magnifications.

3.3.2 Controlling the Assembly of Particles

The fluidic chamber offers a more controllable method for assembly of particles compared to the evaporation technique. The fluidic chamber was employed to control the packing density of particles deposited in the microwells. The patterning of PS-COOH of various sizes and different types of particles are also demonstrated.

3.3.2.1 Packing Density

The amount of PS-COOH microspheres deposited in the microwells can be controlled by varying the concentration of the particles and the rate of movement of the fluid front. The amount of particles inside the microwells was quantified by acquiring the SEM images and the number of particles in the microwell was counted using the Cell Counter plug-in in ImageJ. The maximum number of particles that can be packed into a monolayer in the microwell, N_{max} was estimated by dividing the area of the microwell with the hexagonal area occupied by a 1 μm particle. The Packing Density is expressed as:

$$\text{Packing Density (\%)} = \text{No. of particles in microwell} \times 100 / N_{max}$$

To study the effect of suspension concentration on Packing Density, the concentration of the colloidal suspension was varied between 1.5 – 7.5% w/w while the fluid front was pushed at a constant rate of 10 μL/h, which is equivalent to 3.2 mm/h. The SEM images showing the typical amount of microspheres assembled in the microwells for different suspension concentration are shown in Figure 3.4 A-D. The Packing Density was quantified and summarised in Figure 3.4 E. Five- fold increase in the suspension concentration from 1.5 % w/w to 7.5 % w/w resulted in a 25% increase in Packing Density from 62% to 87%, When a higher concentration of particles was used, more particles are present at the fluid front and a larger amount of particles become deposited as the contact line shifted. With an increase in the suspension concentration, the occurrence of non-specific deposition on the background region becomes more prominent, this nevertheless can be removed when the parylene is peeled off.

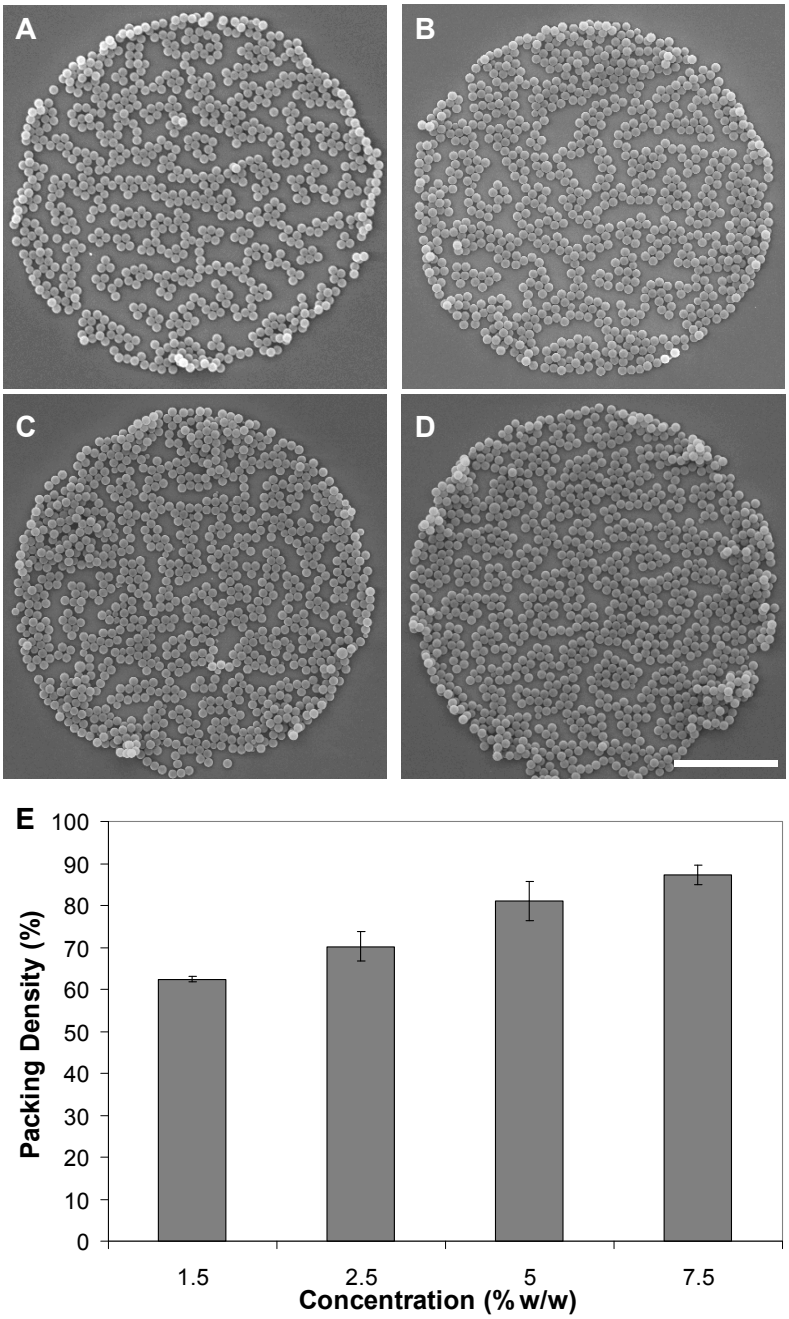

Figure 3.4. Controlling the Packing Density of PS-COOH microspheres by varying the suspension concentration. (A-D) SEM images of microwells packed with different amount of 1µm PS-COOH microspheres. The fluid front was pushed at 10 µL/h while the concentration of the microsphere suspension injected into the channel was (A) 1.5, (B) 2.5, (C) 5.0 and (D) 7.5% w/w. The scale bar represents 10 µm. (E) Graph of Packing Density in microwells as a function of micosphere suspension concentration. Results are mean values and standard deviations are indicated with error bars (n = 15; 3 microwells each from 5 arrays).

Next, the effect of rate of fluid front movement on Packing Density of particles was investigated by varying the flow rate between 5 – 50 μL/h (1.6 – 16 mm/h) while the concentration of the microsphere suspension was maintained at 2.5% w/w. The SEM images of the microwells having the typical Packing Density are shown in Figure 3.5 A-D. As the fluid front movement becomes slower, more time is allowed for the deposition of particles into the hydrophilic domains, resulting in a higher Packing Density. When the Packing Density in the microwell is low (Figure 3.5 A), the edge of the microwell is more closely packed compared to the centre regions. At a flow rate of 5 μL/h, a monolayer of hexagonal closely packed microspheres was assembled in the microwells (Figure 3.5 D). In previous studies which involved colloidal deposition by withdrawing the patterned substrate from a suspension (Fustin et al., 2004), a monolayer of closely particles in the hydrophilic domains was not achieved. Instead, multilayer of colloids was deposited with the number of layers increasing steadily from the edges of the hydrophilic domains to the centre. This may be attributed to the non-uniform height of fluid over the hydrophilic domain which arises when the microsphere suspension is not confined. In this work, the fluid conforms to the walls of the channel and hence the fluid thickness is consistent and equivalent to the height of the channel. The graph of Packing Density in microwells as a function of flow rate is plotted in Figure 3.5 E.

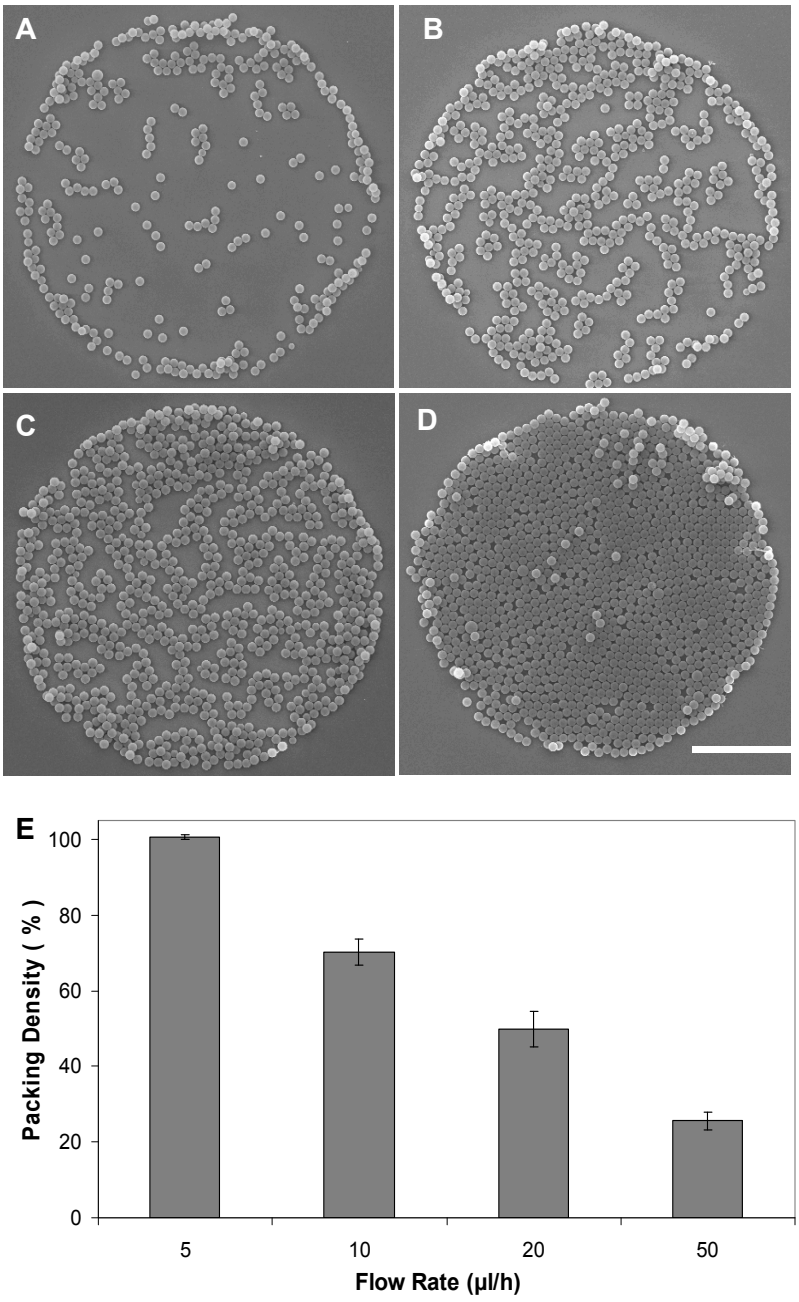

Figure 3.5. Controlling the Packing Density of PS-COOH microspheres by varying the rate of fluid front movement. (A-D) SEM images of microwells packed with different amount of 1µm PS-COOH microspheres. The concentration of the microsphere suspension injected into the channel was 2.5% w/w and the fluid front was pushed at different air flow rate, (A) 50, (B) 20, (C) 10 and (D) 5 µl/h. The scale bar represents 10 µm. (E) Graph of Packing Density in microwells as a function of flow rate. Results are mean values and standard deviation are indicated with error bars (n = 15; 3 microwells each from 5 arrays).

The uniformity in the Packing Density on an array of 2500 microwells over an area of 500 x 500 μm was assessed. Using a constant microsphere suspension of 2.5% w/w and a flow rate of 50, 20, 10 and 5 μL/h, the average Packing Density obtained was 25, 50, 70 and 100% respectively (Figure 3.5). Three arrays were analyzed for each of these conditions. The number of microwells having the expected Packing Density (± 5%) was counted and expressed as percentage probability (Figure 3.6). Generally, the uniformity in the Packing Density in the microwells decreases as the Packing Density increases. At 25% Packing Density, the uniformity was high, with more than 90% of the microwells possessing the expected density. However, the consistency for microwells with higher Packing Density decreases. For samples expecting 100% Packing Density, the percentage of microwells containing the expected amount of microspheres was around 70%. The repeatability was also lower as evident by a larger standard deviation. Nevertheless, the uniformity obtained with the fluidic chamber is significantly better than that achieved using the evaporation technique.

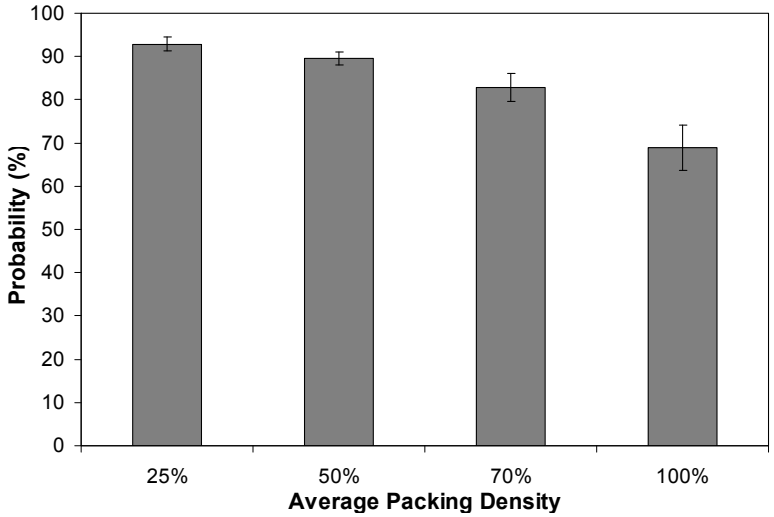

Figure 3.6. Uniformity in Packing Density on an array of 2500 microwells. Graph of probability of microwells with the expected Packing Density as a function of average Packing Density. Results are mean values and standard deviation are indicated with error bars (n = 3; 2500 microwells from 3 arrays).

3.3.2.2 Particle Size

Particles of different sizes ranging from nano to micron scale when assembled on the substrate create surfaces of varying roughness which may influence both protein and cell behaviour. In this section, PS-COOH microspheres of three sizes, 0.5, 1 and 2 μm are assembled into the microwells.

The depth of the microwell affects the size of the microspheres that can be deposited. When microwells of 1 μm depth were used for assembling 2 μm microspheres, few microspheres were retained in the microwell. This may be attributed to the height of the fluid element, which is equivalent to the depth of the microwell as it receded over the microwells. Particles that is larger than the height of the fluid element is not deposited but carried away as the fluid front shifted. When 2 μm deep microwells were used instead, closely packed monolayer of 2 μm particles was obtained (Figure 3.7 C). On the other hand, when the microspheres are smaller than the depth of the microwell, they can be accommodated in the fluid element and become deposited as the fluid receded. A monolayer of closely packed 0.5 μm PS-COOH microspheres was deposited in 1 μm deep microwells (Figure 3.7 A).

The concentration of the microsphere suspension and the flow rate were optimized such that monolayers of closely packed microspheres of various sizes were assembled in the microwells. The SEM images for 0.5, 1 and 2 um PS-COOH microspheres assembled in a close packed arrangement in the microwells are depicted in Figure 3.3.7 and the

optimized conditions are summarized in Table 3.1. The effect of size of microsphere on surface properties and cell behaviour will be investigated in Chapter 4 and 5.

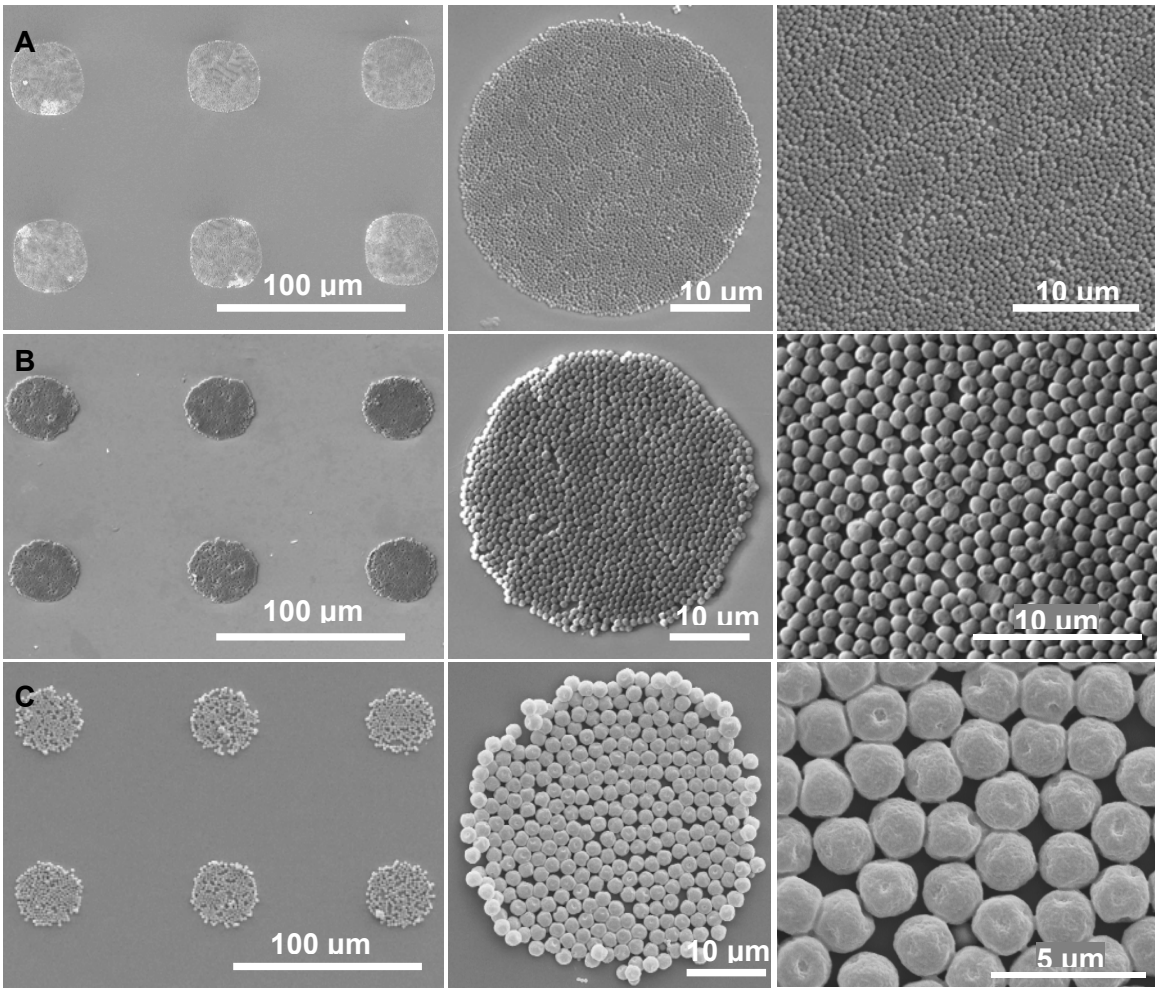

Figure 3.7. Microwells assembled with a monolayer of closely packed PS-COOH microspheres of various sizes. SEM images with different magnifications. (A) 0.5 µm, (B) 1 µm, (C) 2 µm.

Table 3.1 Optimized conditions for assembly of a monolayer of closely packed PS-COOH microspheres of various sizes in the microwells

Size of Microsphere (µm)	Depth of Microwell (µm)	Suspension concentration (% w/w)	Flow rate (µl/h)
0.5	1	2.5	5
1	1	2.5	5
2	2	5	5

3.3.2.3 Different Types of Particles

The particles assembled regions form the protein and cell adhesive regions when integrated with protein and cell micropatterning. By assembling different types of particles, surface with different properties in terms of surface charge, wettability and functional groups can be tailored. The bioactivity of protein and cell functionality can be better preserved by using particles with the appropriate properties. Furthermore, the unique properties of some types of particles can be integrated into the device to serve a functional role. For example, gold nanoparticles can be assembled to give rise to an electrode-insulator format which provides a pathway for measurement of electrical signal in biosensors; while an array of magnetic particles may be used for separation or purification purposes in microfluidic devices.

The assembly of different types of particles, namely 1 μm PS-NH_2, 50 nm gold colloids and 0.3 μm silica microspheres was demonstrated (Figure 3.8). Microwells of 1 μm depth were used for the three types of particles. The surfaces of the microwells were modified such that they present functional groups that can facilitate the assembly of particles by electrostatic attraction or polar interaction.

For assembly of PS-NH_2 microspheres, the microwells were exposed to oxygen plasma before removal of photoresist to generate a layer of silanol (-Si-OH) groups. The silanol groups ionize to give a negatively charged surface at pH > 7 (Xia et al., 2004) while the primary amines on the polystyrene microspheres ionizes at pH < 9 to give a positively

charged interface. At pH 7.6, the amino groups ionize to NH_3^+ and become deposited due to electrostatic attraction with the negatively charged OH^- groups on the microwells.

Negatively charged 50 nm gold nanoparticles were assembled on microwells modified with amine-terminated silanes. The gold nanoparticles are negatively charged due to adsorption of citrate and other anions during the synthesis process. When the amine-terminated microwells were immersed into a suspension of gold nanoparticles, the amino groups were protonated since the pKa (7.4) (Zhang et al., 1998a) of amino groups of the amine-silane monolayers is larger than the pH (6.5) of the suspension. Hence, negatively charged gold nanoparticles can be assembled on the microwells with positively charged amino groups by electrostatic interaction.

Similar to gold nanoparticle, the 0.3 μm silica microspheres were assembled onto microwells modified with amine-terminated silanes. The surface of the particles is terminated with silanol group which ionizes to give negatively charged interface at pH > 7 (Xia et al., 2004). At the pH (7.3) of the silica suspension, both the silanol groups on the silica particles and the amino groups (pKa 7.4) on the microwells are weakly dissociated; therefore the deposition of particles into the microwells is driven mainly by polar interactions, such as hydrogen bonding, with electrostatic attraction playing a minor role. The assembly conditions used for the various types of particles is summarized in Table 3.2.

These experiments demonstrated that the fluidic chamber is applicable to assembling particles of both nano and micro scale. Particles with various functional groups can be assembled by presenting the appropriate functional groups on the microwells.

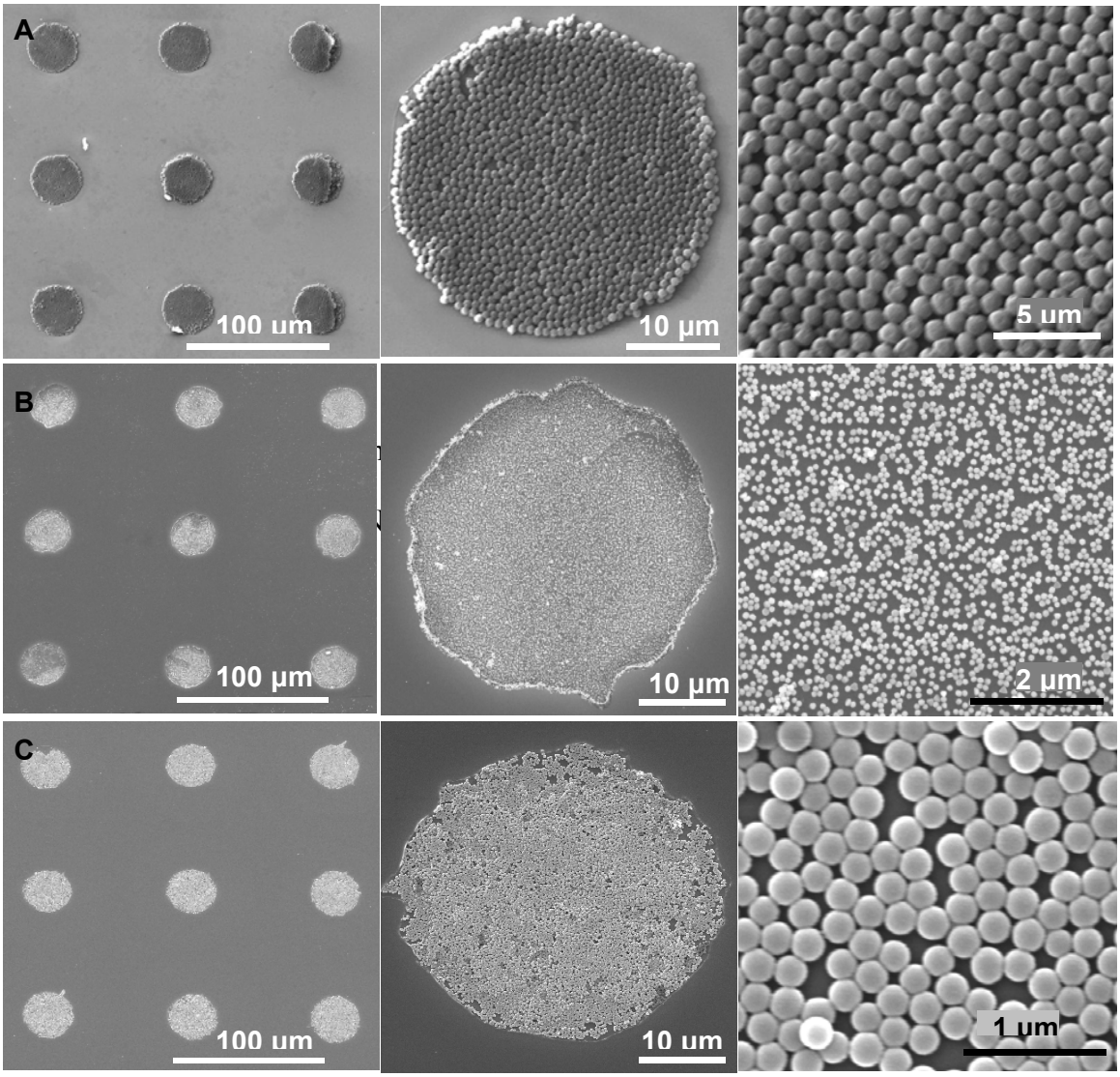

Figure 3.8. Microwells assembled with various types of particles. SEM images at different magnification. (A) 1 µm PS-NH_2 microspheres, (B) 50 nm gold nanoparticles, (C) 0.3 µm silica microspheres.

Table 3.2. Assembly conditions for different type of particles

Type and size of colloid	Modification on microwell	Suspension concentration (% w/w)	Flow rate (μl/h)
1 μm PS-NH_2	Hydroxyl	2.5	5
50 nm Gold	Amine	0.1	5
0.3 μm Silica	Amine	2.5	10

3.4 Conclusion

Particles were assembled onto the hydrophobic-hydrophilic bi-functional template by selective wetting. Two methods were used to generate a moving fluid front over the template, namely, evaporation of a suspension droplet and driving the fluid front along a channel in a fluidic chamber. It is difficult to achieve uniform deposition by using the evaporation technique as the movement rate of the contact line and the concentration of particles at the contact boundary varies significantly during the course of evaporation. On the other hand, the fluidic chamber was able to maintain a constant fluid front velocity and suspension concentration, resulting in consistent packing density in the microwells over a wide region.

With the fluidic chamber, different amount of PS-COOH microspheres, ranging from a sparsely distributed to a closely packed monolayer of particles was deposited in the hydrophilic domains by controlling the concentration of the microsphere suspension and the speed of the fluid front movement. The assembly of PS-COOH microspheres of various sizes and different types of particles was also demonstrated. This assembly

technique allows the integration of colloids at desired regions without compromising the functionality of the device, making it suitable for the fabrication of colloidal based devices.

CHAPTER 4

PROTEIN MICROPATTERNING ON TWO DIMENSIONAL ARRAYS OF PARTICLES

4.1 Introduction

Protein micropatterning refers to the organization of proteins on surfaces with micro scale resolution. Protein micropatterning plays an important role in the development of biosensors and lab-on-chip devices (Willner and Katz, 2000). A good protein micropattern is one that has high protein density at designated regions so as to enhance the sensitivity for detection in biosensors. It is also essential that proteins retain their functionality after immobilization. Nevertheless, it is unavoidable for protein to experience some conformational change upon immobilization to the surface (Nakanishi et al., 2001), therefore the micropatterning technique should minimize any further deleterious effect on the protein functionality.

The conventional protein micropatterning technique involves conjugation of proteins to a planar substrate. In this chapter, a new protein micropatterning technique will be developed, whereby proteins selectively attach to regions that are assembled with colloids. The surfaces assembled with colloids create a micro or nanotopography for protein adhesion. The topography can be micro or nano scale, depending on the size of the particles. By using particles of varying sizes, surfaces with different roughness will be created.

There are two main advantages of integrating colloidal assembly with protein micropatterning. Firstly, the curve surfaces of the particles increase the surface area for immobilization of biomolecules, therefore increases the density of the immobilized

protein. Secondly, it is known that substrates with nanotopography can affect the structure of the attached protein (Denis et al., 2002; Galli et al., 2001; Han et al., 2003; Sutherland et al., 2001). Topographies with feature size similar or smaller than the protein may be sensed by the protein and this may affect its structure, adsorption kinetics and amount adsorbed. On the other hand, a substrate with structures larger than the size of the protein may appear smooth to the protein and have minimal effect on it. Hence, it is possible to preserve the functionality of immobilized protein by adopting the appropriate topography. Improving the protein density and functionality are crucial towards the development of biosensors and lab-on-a-chip devices.

Although it is known that the topographical cues can modulate the properties of the protein attached onto it, there is not much work on integrating topographical features with protein micropatterning. The use of colloids introduces a topography that is more controllable and significant than intrinsic roughness arising from microfabrication process, e.g. etching (Ding et al., 2004), grafting of marcomolecules like silanes, thiols and ionic layer by layer assembly (Mohammed et al., 2004).

In this chapter, the integration of protein micropatterning with colloidal assembly was demonstrated with PS-COOH microspheres. The surface properties of the topography created by PS-COOH microspheres of various sizes were investigated so as to understand its influence on protein attached onto it. The density and bioactivity of the immobilized protein was characterized. The conformation of protein conjugated to nanoparticles was investigated using Circular Dichroism.

4.2 Materials and Methods

Materials. N-hydroxy-succinimide (NHS), 1-ethyl-3-(3-dimethylamino-propyl) carbodiimide (EDAC) hydrochloride, bovine serum albumin conjugated to fluoresceinisothiocyanat (BSA-FITC), sheep anti-rabbit immunoglobulin G conjugated to Cy3 (IgG-Cy3) and FITC (IgG-FITC), human fibronectin, polyclonal anti human fibronectin developed in rabbit and phosphate buffered saline (PBS) solution were purchased from Sigma-Aldrich (Singapore). Recombinant human interferon-gamma (IFN-γ) and its monoclonal anti-mouse antibody conjugated to FITC (IFN-γ-FITC) were purchased from R&D Systems, Inc (Minneapolis, USA). BCA assay kit was purchased from Pierce Biotechnology, Inc. (Rockford, IL).

Conjugation of proteins to PS-COOH microspheres. The substrates assembled with microspheres were immersed in aqueous solution of 150 mM EDAC and 30 mM NHS for 30 min to attach the NHS group to the –COOH terminus on the microspheres (Veiseh et al., 2002). The substrates were rinsed extensively with PBS to remove the excess reactant and immersed in a 0.1 mg/mL protein solution in PBS (0.01 M, pH 7.4) at room temperature for 1 h. The proteins were bound covalently to the microspheres by replacing their NHS groups with the N-termini of protein. The samples were rinsed extensively with PBS and deionized water and air-dried before observing under a fluorescence microscope.

Preparation of PS-COOH film. Polystyrene films were prepared according to Qian et al.,(2000) but with some modifications. PS-COOH solution was prepared by dissolving 0.905 μm PS-COOH microspheres. The microspheres suspension was washed with ethanol twice and allowed to dry. The microsphere powder was then dissolved in toluene at a concentration of 10 μg/mL. 1 cm x 1 cm silicon wafer were cleaned in piranha solution. After cleaning, the silicon wafers were immediately spin coated with PS-COOH solution at 3000 rpm for 30 s. Each piece of wafer was then spun to complete dryness for another 60 s. To fabricate an array of polystyrene film island, the polystyrene solution was spin coated onto photoresist pattern instead. After the film was dried, the photoresist was removed by rinsing in ethanol (acetone is not used as it dissolves the polystyrene film). Removal of the photoresist resulted in an array of polystyrene film island.

Fluorescence microscopy. Fluorescent images of patterned protein were acquired by an upright fluorescent microscope (Zeiss Axiostar Plus) equipped with a CCD camera (Media Cybernetics, Evolution^{TM} MP) with a pixel size of 3.4 x 3.4 μm. The filters (Chroma Technologies) used to excite the FITC and Cy 3 probe were 450 – 490 nm and 546/12 nm respectively.

Contact angle. Contact angles were measured by the static drop technique using a video contact angle system (VCA Optima, AST Products Inc., MA, USA). A 1 μL drop of distilled water was applied to the substrate and the angle was measured within 30 s of contact. Five tests were conducted for each sample with the average and standard deviation reported.

AFM imaging. The Digital Instruments Dimension 3100 Scanning Probe Microscope was used. The images were acquired in tapping mode with 256 x 256 data acquisitions at a scan speed of 0.8 Hz at room temperature in air. Silicon tips with integrated cantilevers with a force constant of 42 N/m were used (Nano World, Switzerland). AFM was used to analyze the topographies of surfaces assembled with a monolayer of polystyrene particles of various sizes. The image surface area and roughness parameters such as the mean roughness (R_a) and the root means square roughness (R_q) are used to characterize the surface. R_a is defined as the mean value of the surface profile relative to the calculated centre plane where the volumes enclosed by the image above and below the plane are the same. It is calculated as:

$$R_a = \frac{1}{L_x L_y} \int_0^{L_x} \int_0^{L_y} \left| f(x, y) \right| dxdy$$

where $f(x, y)$ is the surface profile relative to the centre plane, and L_x and L_y are boundaries of the specific measured area in x and y dimensions, respectively. R_q (the RMS of the Z value) is the standard deviation of Z values within the specific area and is calculated as

$$R_q = \frac{\sqrt{\sum (Z_i - Z_{avg})^2}}{N_p}$$

where Z_i is the current Z value, and Z_{avg} and N_p are the average of the Z values and the number of points within the given area respectively.

Immunoassay. The patterned microspheres were conjugated with human fibronectin or recombinant human interferon gamma (IFN-γ) using NHS-EDC as described above. The substrate was immersed in PBS containing 1% BSA for 30 min to block the empty sites.

The patterned surface was then covered with polyclonal anti-fibronectin developed in rabbit (10 μg/mL) or monoclonal anti-IFN-γ-FITC (10 μg/mL) developed in mouse for 30 min at room temperature. Specific antibody binding for fibronectin was revealed by incubation with a FITC conjugated anti-rabbit IgG (10 μg/mL) for 30 min at room temperature. The substrate was rinsed with PBS to remove the loosely bounded molecules after each step. The control samples were subjected to the same protocol except that the microspheres were not conjugated to the antigen. The samples were then examined using a fluorescence microscope.

Protein adsorption on gold nanoparticles. 3 mL of gold nanoparticles (0.01 wt %) was incubated in 0.1 mg/mL of BSA at room temperature for 2 h on a rotator. The gold particles were then centrifuged and the supernatant was carefully removed. The gold nanoparticles were washed thrice to remove the free proteins and suspended in PBS.

BCA assay. The BSA concentration in the supernatant was measured with five test samples. The assay was carried out according to the manufacturer's protocol for the microplate procedure. The absorbance was measured with a spectrophotometric plate reader (FLUOstar OPTIMA, BMG Lab Technologies, Germany) at 562 nm and correlated to a standard BSA protein curve to obtain the protein concentration. The amount of adsorbed protein was calculated from the difference between the initial and the equilibrated concentrations.

Circular dichroism spectroscopy. The far-UV CD spectra of BSA adsorbed on gold nanoparticles were recorded on a JASCO (J-810 UV-Vis, Japan) CD instrument. Each spectrum was recorded at 1 nm interval from 260 – 190 nm, using cylindrical quartz cuvettes of 1 cm path length with an integration time of 1 s. The CD spectra of free proteins, in the absence of gold nanoparticles were also recorded. All CD measurements were taken within 3 – 4 h of BSA adsorption onto gold nanoparticles to ensure adsorption equilibrium in the absence of particle aggregation. The protein spectra were corrected by subtracting the spectrum of a reference solution lacking the protein but otherwise identical. The spectra were averaged using a 13-point FFT algorithm. The α-helix content was calculated on the basis of the mean residue ellipticity at 222 nm, $[\theta]_{222}$ (Equation 4.1) (Berova et al., 2000).

$$[\theta]_{222} = \frac{100[\theta]M_W}{c\,l\,N_a} \tag{4.1}$$

where $[\theta]$ is the measured ellipticity in degrees, c is the protein concentration in g/L, l is the path length in cm, M_w is the molecular weight of the protein (66 000 for BSA), and N_a is the number of amino acid residues (583 for BSA). The measured helicity was computed as $[\theta]_{222}$ /(-39 500), with a value of -39 500° cm^2dmol^{-1} on the basis of both experimental and theoretical estimates of the value of $[\theta]_{222}$ for a polypeptide of 100% helicity (Foresta et al., 2002). The concentration of protein conjugated to the particles was evaluated by BCA assay. The CD spectrum for free BSA was conducted at 10 μg/mL.

4.3 Results & Discussion

4.3.1 Protein Micropatterning on Surfaces Modified by PS-COOH Microspheres

In this work, a new protein micropatterning technique is developed, whereby proteins selectively attach to regions that are assembled with colloids. The assembly of PS-COOH microspheres into an array of microwells was discussed in Chapter 3. The templates with microwells assembled with a monolayer of closely packed PS-COOH microspheres were used for protein micropatterning so as to achieve uniform and high density protein spots. After patterning of PS-COOH microspheres, the parylene was peeled off (Figure 4.1 A). There were two surfaces on the silicon wafer; the background was grafted with PEG while the adhesive regions have carboxylic groups (on the microspheres). Proteins were attached to the microspheres through conjugation with carboxyl groups. Micropatterning of biomolecules was demonstrated with BSA-FITC and IgG-Cy3. It was observed that immersion of the chip in the protein solution did not result in observable disturbance to the microsphere pattern. The fluorescence images for patterning of BSA-FITC and IgG-Cy3 are depicted in Figure 4.1 B and C respectively. Both images confirmed that protein molecules were selectively adsorbed onto the PS-COOH microspheres. The PEG modified regions between the microwells had resisted protein adsorption, resulting in precise deposition of protein on a non-planar surface created by the microspheres. Figure 4.1 D and E shows the surface and line profile of the fluorescent intensity. These two diagrams show that the signal to noise ratio is very high and the peak intensity is uniform, suggesting that the amount of PS-COOH microsphere in the microwells are consistent.

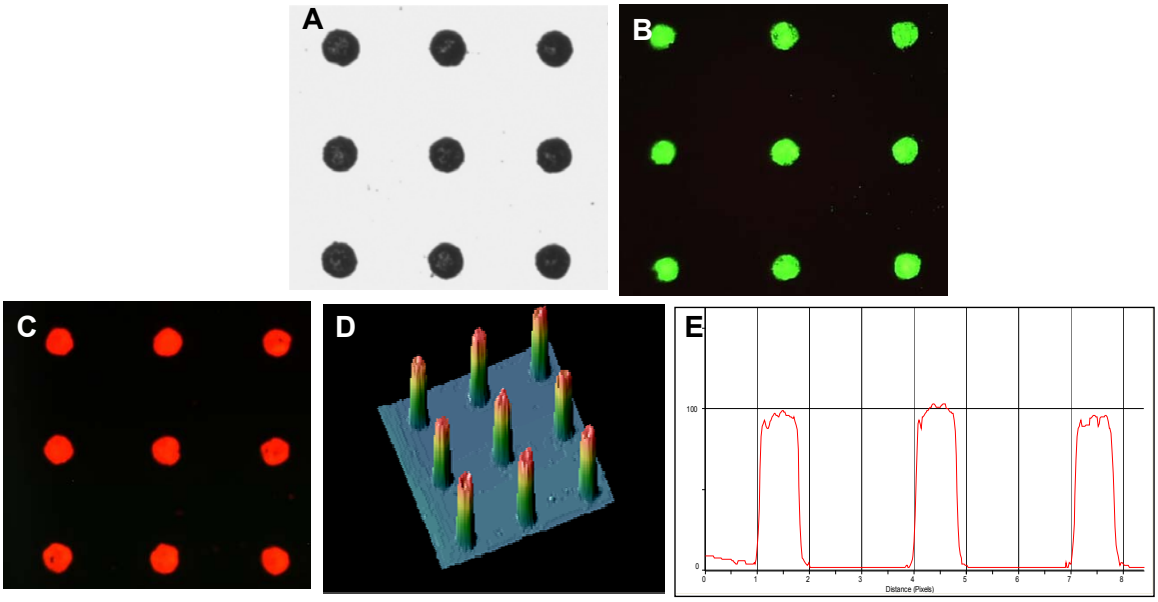

Figure 4.1. Integration of protein micropatterning with colloidal assembly. (A) 1 um PS-COOH microspheres assembled in microwells. Fluorescent images of PS-COOH conjugated with (B) BSA-FITC and (C) IgG-Cy3. (D) Surface plot and (E) line profile of the fluorescent intensity of IgG-Cy3.

In this method, protein immobilization is the last step in the micropatterning process. Hence protein is prevented from being exposed to the harmful physical (Biasco et al., 2005) or chemical effects (Jackson and Groves, 2007) that may be induced during the process. In this way, the protein native conformation can be better preserved after they are attached to the substrate. Although this micropatterning method is demonstrated using proteins, this technique can be easily applied to patterning other biomolecules by ensuring that the microspheres and the background substrate have the relevant functional groups for adhesion and resistivity respectively.

Apart from PS-COOH microspheres, protein micropatterning on other types of assembled particles, namely, 0.3 μm silica nanoparticles and 50 nm gold nanoparticles was also demonstrated. BSA-FITC was attached to the particles by physical adsorption. BSA

binds spontaneously to the negatively charged surface of silica and citrate coated gold nanoparticles by electrostatic interaction (Brewer et al., 2005). This is despite that BSA has an isoelectric point at 4.6 which makes it negatively charged at pH 7. Figure 4.2 A & B depict the fluorescent image of BSA-FITC micropattern on arrays assembled with silica and gold nanoparticles respectively. The silica and gold nanoparticles were not disturbed when immersed in the protein solution, the background remained free of nanoparticles and resulted in a distinct protein pattern.

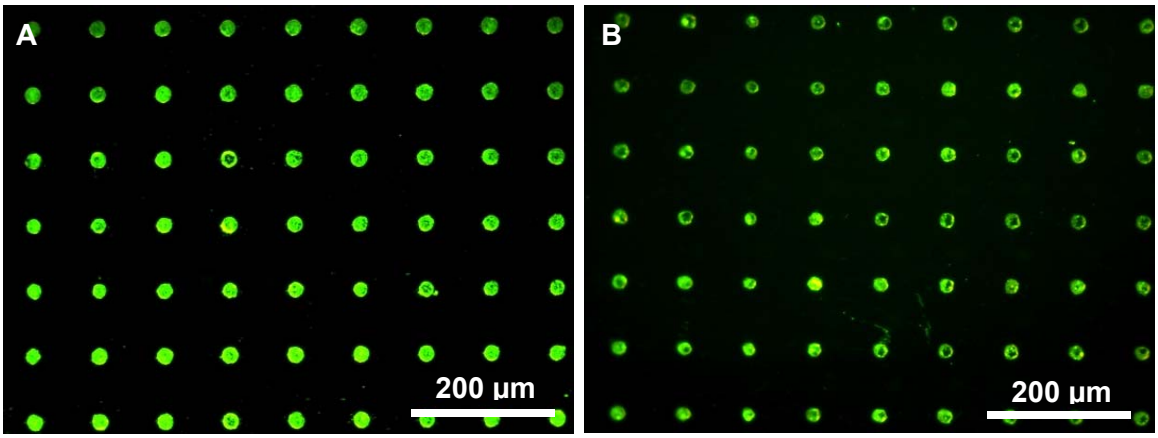

Figure 4.2. Protein micropatterning on microwells assembled with different types of particles. Fluorescent images of BSA-FITC conjugated to (A) 0.3 µm silica nanoparticles and (B) 50 nm gold nanoparticles.

4.3.2 Surface Properties of Closely Packed Microspheres Assembled Surface

In order to understand the behaviour of protein and cell adhesion (Chapter 5) on various microspheres modified surface, the surface properties of these substrates must be examined. In this section, the surface properties of a monolayer of closely packed PS-COOH microsphere of various sizes (0.5 µm, 1 µm and 2 µm) and PS-COOH film is characterized and compared in terms of surface area, roughness and wettability. The film was prepared by dissolving the microspheres and the solution was spin cast onto the

substrate. The PS-COOH microspheres are synthesized by using a co-polymer to provide the carboxyl functionality; hence the carboxyl groups are presented uniformly throughout the microsphere (personal communication with Polysicences, Inc.). The film formed by dissolution of the microspheres will have the same chemical composition as the microspheres and it can serve as a valid control for studying the topographical effects induced by the microspheres. The morphology for closely packed PS-COOH microsphere of various sizes is illustrated in Figure 4.3 with a set of representative images consisting of the SEM, AFM height and AFM surface plot. The AFM images were acquired in a tapping mode with a scan area of 10 x 10 μm to record the surface area and roughness of the topographies.

The curve surfaces of the microspheres assembled on a planar surface increase the surface area of the substrate. Theoretically, the increment in surface area is 1.81 times for hexagonally packed microspheres and this is independent of the size of the particles (discussed in Chapter 1). Base on AFM analysis, the increment was about 1.50, 1.57 and 1.71 times for 0.5 μm, 1 μm and 2 μm microspheres respectively. This is lower than the theoretical increment due to the presence of voids and lines defects and deviation from the ideal hexagonal arrangement. The increment in surface area is slightly higher for the 2 μm microspheres assembled surface, this may be attributed to the coarser surface on the microspheres, as observed with SEM and the section profile from AFM.

The surface roughness of the PS-COOH microspheres assembled surfaces are compared with the PS-COOH thin film. The surface roughness was evaluated by two parameters,

mean roughness (R_a) and root mean square roughness (R_q). The results show that the polystyrene film was very smooth with a R_a of only 4 Å over an area of 100 μm^2. The roughness for the microspheres assembled surfaces varies proportionally with the size of the microspheres. When the size of the microspheres doubles, the roughness increases by approximately two times. The results are summarized in Table 4.1.

The wettability of the surface is affected by its topography. For hydrophobic surfaces (contact angle > 90 °), roughness will magnify its contact angle, while the contact angle of a hydrophilic surface (contact angle < 90 °) is diminished by roughness (Quere, 2002). Contact angle analysis was performed on monolayer of closely packed microspheres and thin film on a non-patterned substrate. The film is hydrophobic with a contact angle of 102°. The 0.5 μm microsphere assembled surface has a larger contact angle 119° due to its increased roughness. Although the 1 μm and 2 μm microspheres assembled surface are rougher than the 0.5 μm, their contact angles are not larger; instead, the surfaces are hydrophilic and the contact angles are 33° and 29° respectively. This may be attributed to water infiltrating the interstices of the microspheres assembly. As a result, the water droplet is deposited on a patch work of solid and liquid, which increases the wettability of the surface (Quere, 2002). The larger interstices between the 1 μm and 2 μm microspheres is able to drive water into its texture while the smaller interstices for the 0.5 μm microspheres prevented it and result in a pearl drop on its surface (Figure 4.4).

The surface properties of the substrates are summarized in Table 4.1.

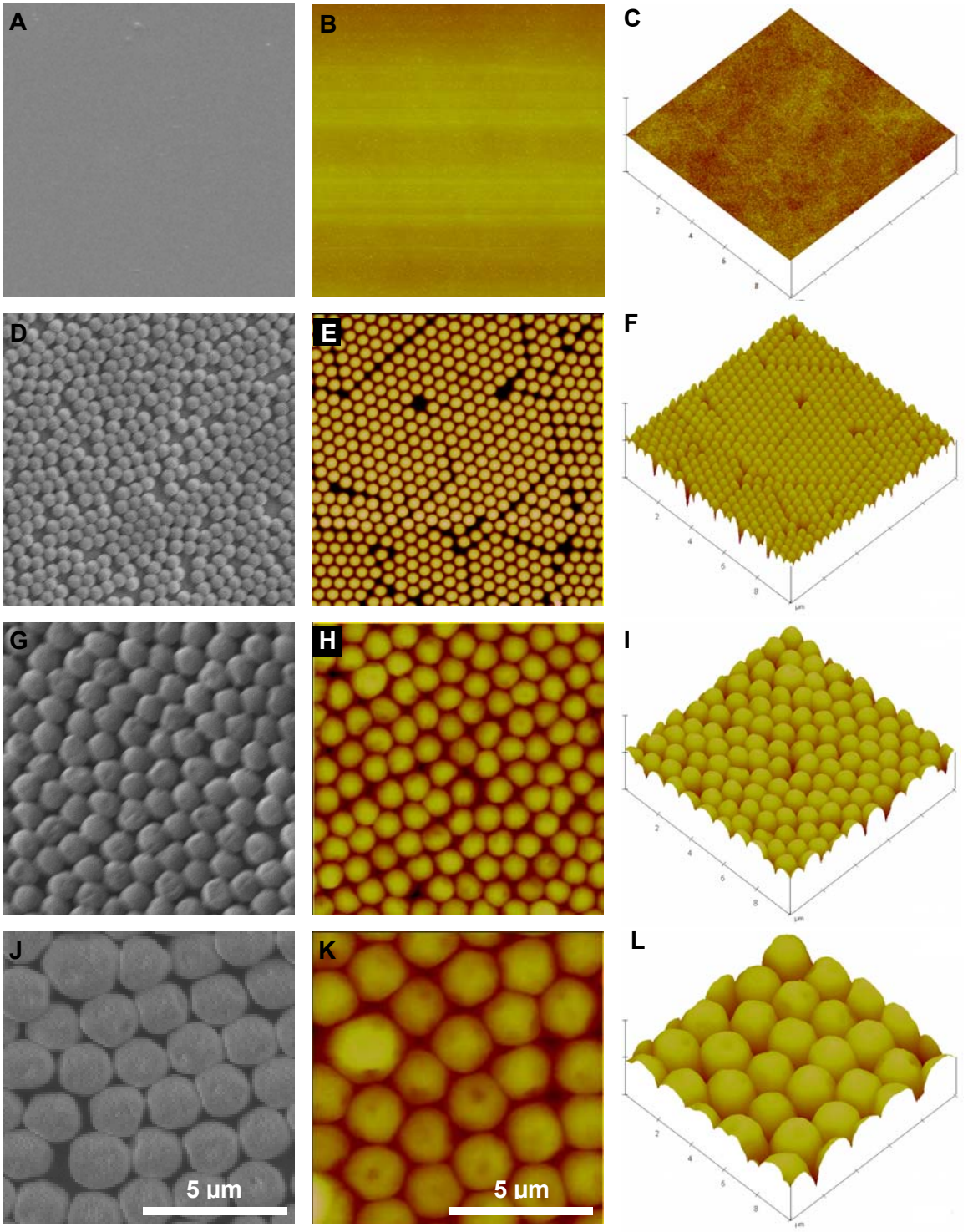

Figure 4.3. Morphology of PS-COOH assembled substrates. Corresponding SEM, AFM height and AFM surface plot of (A-C) PS-COOH film and monolayer of closely packed PS-COOH microspheres of various sizes; (D-F) 0.5 µm, (G-I) 1 µm and (J-L) 2 µm.

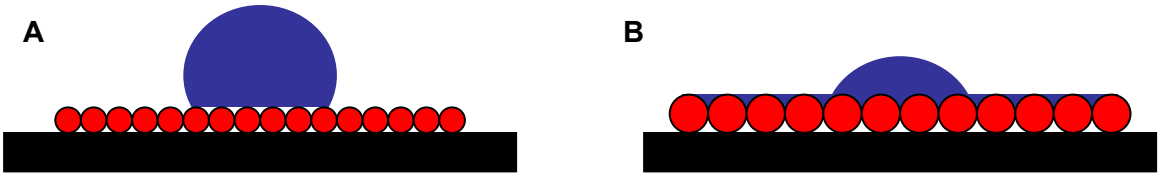

Figure 4.4. Contact angles on a monolayer of closely packed PS-COOH microspheres. Schematic diagram illustrating (A) a pearl drop on 0.5 µm PS-COOH microspheres and (B) an infiltrating droplet on 1 µm and 2 µm microspheres.

Table 4.1. Surface properties of closely packed PS-COOH microspheres and thin film. Results are mean values with standard deviation (n = 3).

Surfaces	Increment in surface area	R_a (nm)	R_q (nm)	Contact Angle (°)
PS-COOH film	1.00 ± 0.00	0.384 ± 0.010	0.545 ± 0.021	102 ± 1.39
0.5 µm PS-COOH	1.51 ± 0.033	54.6 ± 2.21	74.8 ± 3.93	119 ± 2.26
1 µm PS-COOH	1.57 ± 0.074	115 ± 7.71	145.3 ± 10.3	33.0 ± 1.27
2 µm PS-COOH	1.71 ± 0.085	252 ± 19.3	315 ± 24.6	28.9 ± 1.65

4.3.3 Proteins Conjugated on Microspheres Modified Substrates

4.3.3.1 Protein Density

Attachment of protein to the surface is affected by the surface properties such as wettability, electrostatic forces and its topography. Characterization of a monolayer of closely packed microspheres by AFM had shown that there is an increment in surface area compare to the planar substrate. This translates to increase in area for protein immobilization and therefore, an increase in protein density. Before measuring the protein density on microspheres assembled substrate, the confocal image of 3 µm PS-COOH microspheres conjugated to BSA-FITC was acquired (Figure 4.5 A and B). The images show that the fluorescence concentrated on the surface of the particles. This

suggests that the microspheres are not porous; hence the density of surface immobilized protein is dependent on the surface area (not volume) of the microspheres.

The protein density of BSA-FITC conjugated to the monolayer of PS-COOH microspheres of 0.5 μm, 1 μm and 2 μm and PS-COOH film were compared by measuring the fluorescent intensity. The BSA-FITC conjugated substrates were imaged using a fluorescence microscope at 100 times magnification with the same exposure period (Figure 4.5 C-F). The fluorescent intensity was measured using Array Pro, for each image, 30 circular spots, with diameter of 10 μm were randomly selected to measure its intensity. The averaged results and standard deviation are presented in Figure 4.5 G. The increment in intensity for the microspheres assembled substrates was expressed relative to the film. The increment in intensity was around 2.5 – 2.6 times for the microspheres assembled surface of 0.5 μm, 1 μm and 2 μm. The insignificant difference in protein density between the three substrates may be attributed to their similar surface area. The significant differences in wettability between the substrates did not affect the amount of protein conjugated. This may be due to the fact that the contact angle test was conducted over a bed of assembled microspheres (macro wettability) instead of on a single microsphere (micro wettability). As the size of protein is in nano scale, the micro wettability affects the conjugation of protein molecules. While all the substrates have different topography, they have the same chemical properties and are likely to have similar micro wettability. This may explain the similarity in protein density on various sizes of PS-COOH microsphere assembled substrate.

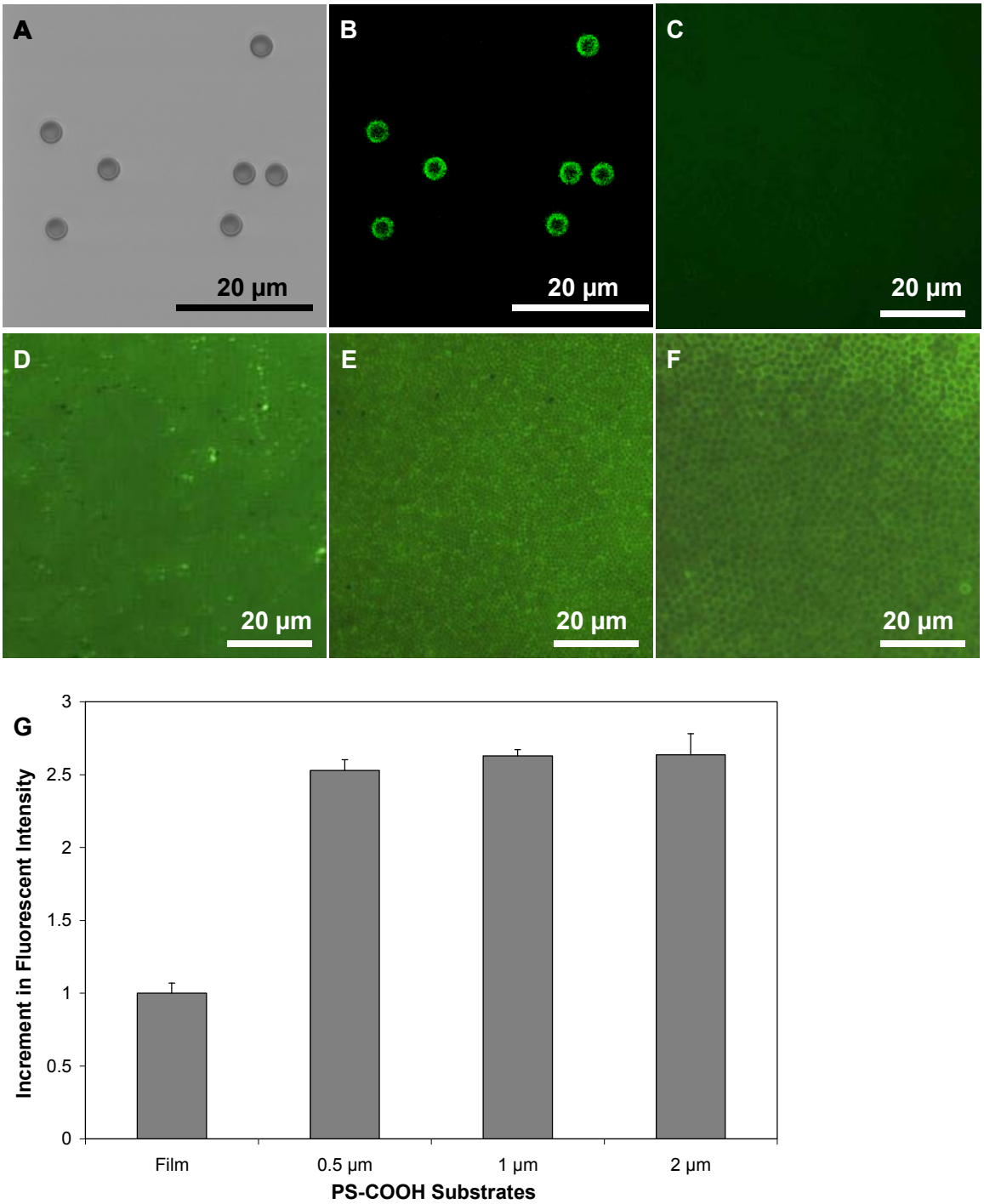

Figure 4.5. Fluorescent intensity of protein conjugated on PS-COOH substrates. (A) Phase contrast and (B) confocal image of 3 µm PS-COOH microspheres conjugated to BSA-FITC. Fluorescent images of BSA-FITC conjugated to (C) PS-COOH film and monolayer of closely packed microspheres of various sizes, (D) 0.5 µm, (E) 1 µm, (F) 2 µm. (G) Graph of increment in fluorescence intensity for various PS-COOH substrates.

4.3.3.2 Bioactivity of Micropatterned Proteins Characterized Using Immunoassay

Protein attachment to solid surfaces typically affects its structure and functionality. The bioactivity of the immobilized protein is a key factor in the development of biosensing microdevices. The bioactivity of the proteins was verified using two antigen-antibody immunoassay. Figure 4.6 A shows the image of an array of 1 μm PS-COOH microspheres after conjugation to IFN and exposed to a solution of FITC conjugated monoclonal antibody. The presence of fluorescence suggests that the specific binding domain on IFN corresponding to the monoclonal antibody was not denatured after conjugation to the microspheres. The recognition of the fluorescent anti-IFN was specified as verified by a control experiment where the microspheres were blocked with BSA solution and no fluorescence was detected on the array (Figure 4.6 B). This experiment was repeated using the human fibronectin and its polyclonal antibody. The result was positive, with specific binding of the FITC secondary antibody detected on the array (Figure 4.6 C & D). As a polyclonal antibody was used, this suggests that several binding domains on fibronectin remained functional after conjugation to microspheres. It is important to note that positive results from the antigen-antibody (monoclonal or polyclonal) immunoassay can only prove that the structure of a protein is preserved partially as it is possible for a partially denatured protein to exhibit affinity binding with its antibody. Therefore it is critical that the protein conformation is evaluated by different methods to substantiate the results.

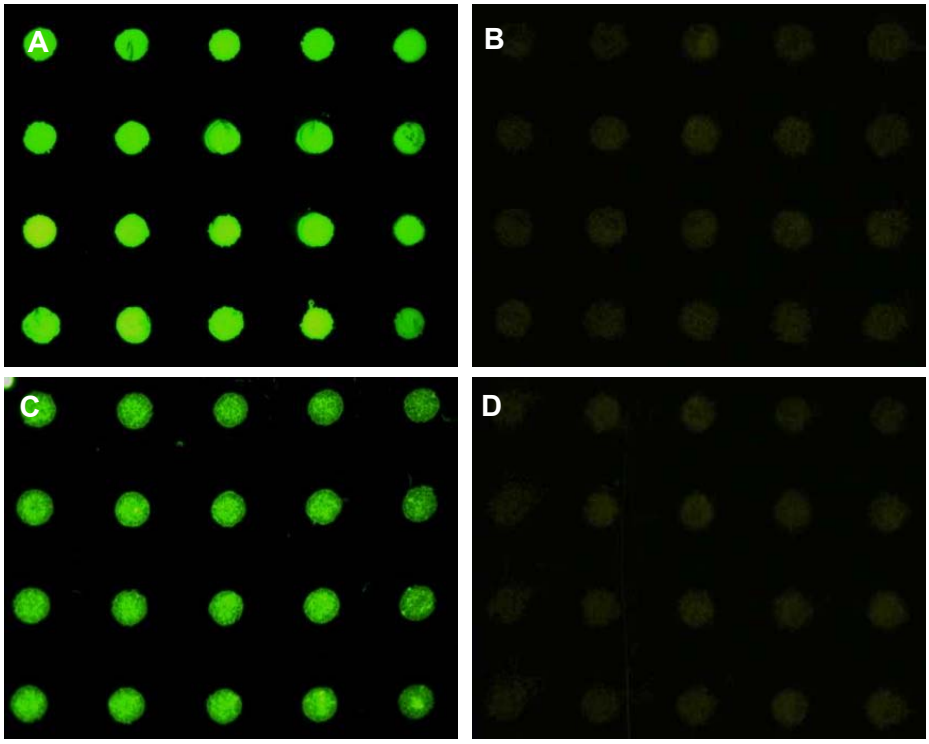

Figure 4.6. Bioactivity of micropatterned protein determined by immunoassay. Fluorescent images of (A) IFN and monoclonal FITC conjugated anti-IFN, (B) IFN control, (C) Fibronectin, polyclonal anti-fibronectin and FITC conjugated secondary antibody (D) Fibronectin control

4.3.3.3 Circular Dichroism of Proteins Conjugated on Nanoparticles

Circular dichroism (CD) spectroscopy measures differences in the absorption of left-handed polarized light versus right-handed polarized light which arise due to structural asymmetry. It can provide information on the type and amount of secondary structure present in the protein, in particular, the α helix content can be quantified by changes in ellipticity at 222 nm (Berova et al., 2000). This characterization has to be performed on protein immobilized on suspended particles instead of assembled on a substrate. However, valuable insights can be drawn from these studies due to similarity in terms of the surface properties and the topographical nature of the particles. As with other spectroscopy, the size of the colloids used must be small enough so as to minimize light

scattering in the far-UV range. Hence, gold nanoparticles of 20 and 50 nm were used in this study instead of PS-COOH microspheres. Moreover, it is also more appropriate to use nanoparticles instead of microspheres as only particles with sizes that are comparable to the size of the protein is expected to influence the conformation of the protein upon conjugation to the particle (Nygren and Karlsson, 1992).

Figure 4.7 A shows the CD spectra of BSA adsorbed on gold nanoparticles. The α helix content was calculated based on the ellipticity at 222 nm according to equation 4.1. The percentage of α helix content for BSA on various particle sizes is summarized in Figure 4.7 B. The α helix content is significantly lower for BSA adsorbed onto gold nanoparticles when compared to the free BSA. Moreover, the α helix content strongly decreases as the size of the nanoparticle increases. The α helix content decreases from 25% for freely soluble BSA to only 8.4% for BSA adsorbed on 50 nm gold particles. The result suggests that the conformation of a protein is affected by the size of the nanoparticles. This is in accordance with previous studies (Jiang et al., 2005; Lundqvist et al., 2004; Vertegel et al., 2004) that suggest particles of smaller sizes can preserve the conformation of protein better. The authors explained that this may be due to a greater surface curvature for smaller nanoparticles and hence a smaller area for interaction between the protein and particles. With a smaller area of interaction, the protein secondary structure will be affected to a smaller extent compared to those adsorbed on larger nanoparticles. There is no direct comparison of protein conformation adsorbed on particles and planar surface; however, a planar surface can be correlated to a large particle where the degree of curvature is small. Hence, it can be deduced from the above

results that proteins when immobilized on a nanoparticle can preserve its native structure and function better than when immobilized on a planar surface. The size of the nanoparticle should be comparable to the dimension of the protein in order for protein conformation to be retained.

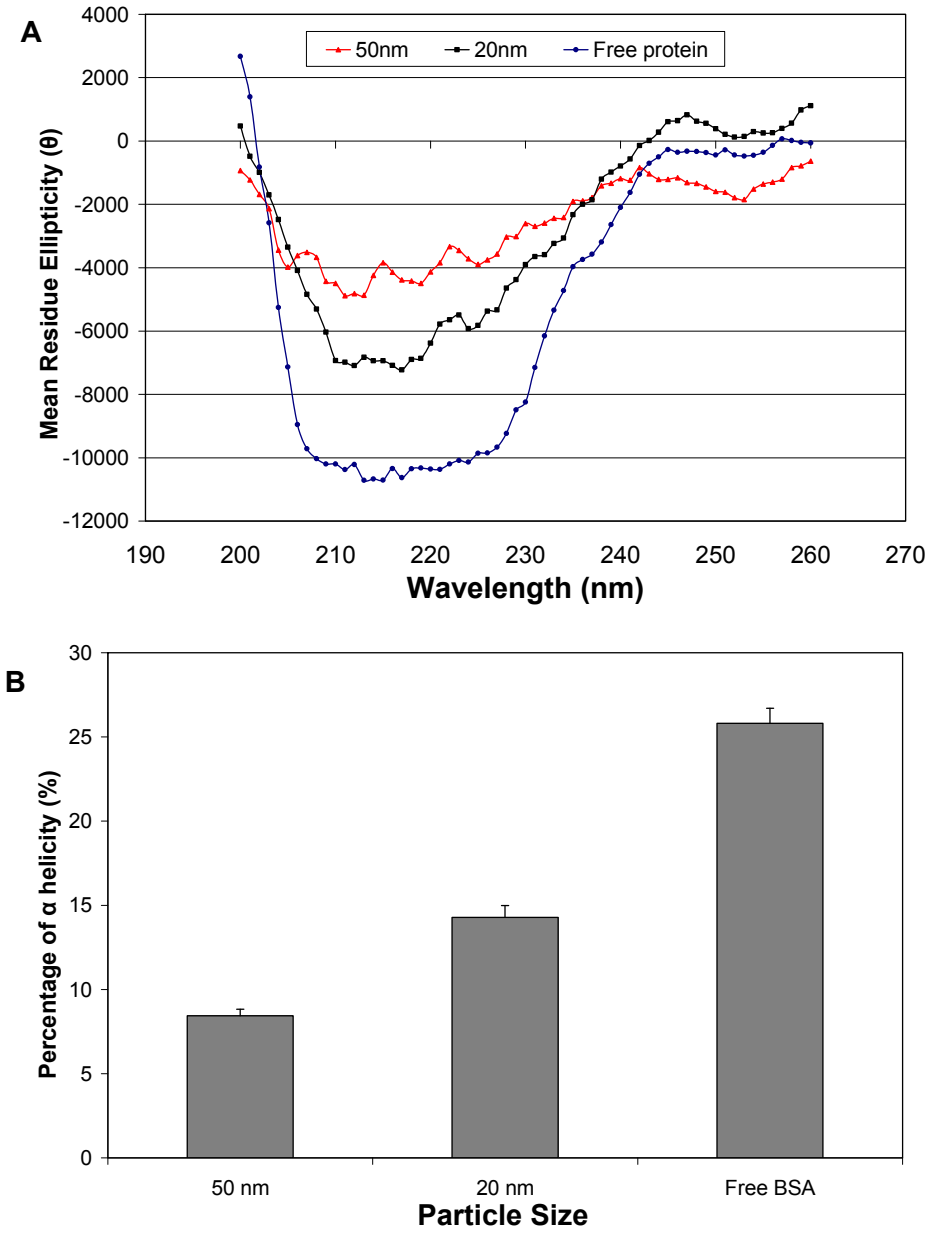

Figure 4.7. Conformation of BSA conjugated to gold nanoparticles. (A) CD spectra; (×) free BSA; BSA adsorbed onto gold nanoparticles of various sizes, (■) 20 nm; (▲) 50 nm. (B) Graph of percentage of alpha helicity for BSA adsorbed on gold nanoparticle and free BSA.

4.4 Conclusion

In summary, a new method of protein micropatterning on a non planar topography integrated on a planar substrate via assembly of particles is presented. The particles assembled substrate was highly selectively for protein adhesion, resulting in a precise protein micropattern. The protein density increased by approximately 2.5 times compared to a planar topography. The proteins remained functional as verified using an antibody-antigen immunoassay binding system. From the CD spectroscopy results, it can be inferred that proteins adsorbed on nanoparticles preserved its conformation better than on a planar substrate. Therefore, this protein micropatterning technique may be used in biosensors where both the density and bioactivity of proteins are important factors that will affect the device performance. The different parameters of the system, for example, the size, packing density and type of particles used for assembly can be varied according to the intended applications. This method is applicable for patterning a variety of biomolecules including antibodies, antigens, enzymes, receptors, peptides, oligonucleotides, DNA, and many more.

CHAPTER 5

CELL MICROPATTERNING ON TWO DIMENSIONAL ARRAYS OF MICROSPHERES

5.1 Introduction

The adhesion of cells within designated regions on solid surfaces while preventing non-specific attachment at other regions is the basis of cell micropatterning. Cell micropatterning plays an important role in the development of biosensors and lab-on-chip devices (Willner and Katz, 2000), tissue engineering (Bhatia et al., 1999) and fundamental studies of cell biology (Whitesides et al., 2001). The two main requirements of a good cell pattern are 1) high selectivity between the cell adhesive and resistant regions, and 2) cells remain functional after adhesion. Hence, it is critical that the regions for cell adhesion provide favourable cell-substrate interaction that can promote cell adhesion and functionality.

It is well known that the substrate topography has a profound effect on cell behaviour and this has been studied to understand fundamental cellular phenomena. Curtis (1964) pioneered the study on effects of topography on cells in 1964. Since then, much work has been carried out in this field and it is well documented that many type of cells respond to micro and nanotopography. For surface structures that are on a similar size scale as the extracellular matrix (ECM) proteins, the surface topography may alter the conformation or orientation of the ECM proteins, perhaps by revealing new binding sites or restricting access to previously available sites (Nygren and Karlsson, 1992). On the other hand, microtopography has structures that are larger than the size of proteins and they have negligible effect on protein behaviour. Therefore, the influence of microtopography on cellular response is due to its textured surface directly. The topographical properties of a

substrate affect the cellular behaviour of anchorage-dependent cells in terms of adhesion, spreading, proliferation, differentiation, apoptosis and gene expression (Curtis and Wilkinson, 1997; Dalby et al., 2003; Singhvi et al., 1994).

Micro or nanostructures that mimic the physiological interface are already implemented on surfaces of tissue engineering scaffolds and medical implants so as to better maintain cell morphology and functionality and also to enhance its biocompatibility (Desai, 2000). Similarly, topographical features can be integrated with cell micropatterning, the designated regions for cell attachment can boast topographical features that can enhance cell adhesion and preserve cell phenotype in an in-vitro environment. The following paragraphs will discuss the work done to investigate cell response on topography created by assembly of particles or other similar structures.

Miyaki et al.(1999) studied the topographical effect of surfaces covered with polystyrene microspheres on cell function. A monolayer of well ordered hexagonally packed microspheres with sizes ranging from 0.6 μm to 1.2 μm was prepared. The microtopographical effect of these surfaces was investigated with neutrophil-like cells by measuring the amount of active oxygen released. The release of reactive oxygen was dependent on the diameter of the assembled microspheres and attained a maximum for 1 μm particles. This study demonstrated that cells can recognize the surface roughness created by the closely packed microspheres. Cousins et al.(2004) created similar topography but in nano scale with 7 nm, 14 nm and 21 nm silica particles. The cellular response of L929 murine fibroblast was analyzed after one, three and seven days in

culture and compared with untreated glass surface. Generally, fewer cells attached to the silica modified surfaces and the cells that attached had a rounded morphology; after seven days, the fibroblast formed clusters of cells. This observation was distinctly different from fibroblast cultured on untreated glass surface whereby the cells proliferated with spread morphology and they were distributed evenly after seven days. This study shows that the nanotopography had initiated a cellular response that affects the morphology, adhesion and proliferation of fibroblast.

Instead of studying the topographical effect of a monolayer of closely packed particles, some researchers studied the cellular response on loosely deposited particles. Gleason et al.(2003) fabricated patterned arrays of adhesion protein by depositing fibronectin-coated 2 μm microspheres on the substrate. NIH 3T3 was cultured on these surfaces and the cells spread and attached on the fibronectin coated particles, it did not attach on the areas between the particles due to blocking with albumin. Surfaces with different densities of particles were produced so as to examine the effects of separation between adhesive islands on cell morphology. Cells attached on sparsely spaced particles exhibited a branched morphology while cells on closely packed particles had a compact morphology. The authors explained that with limited adhesive sites on a sparse array of particles, the cells had to adopt a branched morphology to maximize their surface contact. Another research group (Zheng et al., 2004) patterned NR6 fibroblast cells on an underlying layer of close or loosely packed particles. In their work, 1 μm carboxyl amine functionalized polystyrene particles were patterned on the substrate, the surface of the particles were then modified with cell adhesive peptide containing the RGD sequence. Their results

correlate well with Gleason's, which confirmed that cells attached and spread on surfaces with sparsely packed particles, while surface with closely packed particles are undesirable for cell adhesion and spreading.

Apart from using particles to create the underlying stratum for cell attachment, some researchers fabricated structurally similar topography using other techniques. Wan et al.(2005) produced hemispherical island structured on poly(L-lactide) surfaces by using polystyrene with hemispherical pits as template. The two sizes of island produced were 2.2 μm and 0.45 μm. They found that the attachment efficiency of osteoblast-like cells on the hemispherical structured surface was better than on smooth surface. The cells were able to attach to the convex surface of the islands and their tiny pseudopodial protrusions strode from one island to another. Dalby et al.(2002a) investigated cell response to nanostructured surfaces created with polymer demixing. They created shallow islands of 13, 35 and 95 nm. Of the three nantopographies, the 13 nm island gave the largest response to human endothelial cell, with highly spread morphologies containing well defined cytoskeleton. Human fibroblast cell responded in a similar manner to 13 nm island, it was observed that they were more spread with many filopodia as compared to the controlled surface (Dalby et al., 2002b). cDNA microarray was used to measure the response of genes due to the substrate and the results showed that broad gene up regulation was notable in cell signalling, proliferation, cytoskeleton and production of ECM proteins.

It is evident that a substrate with nano or microtopography plays a crucial role in affecting cellular response. The size of the particles or hemispherical island and its centre to centre spacing had resulted in varying response which is cell specific. Recognizing the types of topography that are favourable for preserving cell behaviour, and integrating it with micropatterning will lead to the development of functional cell patterns.

In this chapter, surfaces modified by assembly of PS-COOH microspheres were studied. The topographical parameters were controlled by using particles of different sizes and varying the density of the particles deposited. The ability of the microstructured surface to alter cellular adhesion, proliferation and morphology was investigated. The colloidal-based microstrutured surfaces were then incorporated into the patterned substrate to perform cell micropatterning.

5.2 Materials & Methods

Materials. 0.454 μm (2.59% w/w), 0.984 μm (2.62% w/w), 2.022 μm (2.65% w/w) carboxylated polystyrene microspheres (PS-COOH) and 0.913 μm (2.62 %) amino polystyrene microspheres (PS-NH_2) were purchased from Polysciences, Inc. Molecular Probes CellTracker Red CMTPX was purchased from Invitrogen (Singapore). Dulbecco's Modified Eagle's Medium (DMEM), phosphate buffer solution (PBS) and trypan blue were purchased from Sigma-Aldrich. Fetal bovine serum was bought from PAA Laboratories (Austria) and penicillin-streptomycin was purchased from Invitrogen

(Singapore). Cell Titer 96 ® Aqueous One Solution Cell Proliferation Assay was purchased from Promega (Singapore). HT-29 human adenocarcinoma cell line was obtained from American Type Culture Collection (Manassas, VA). All reagents and materials were used as received.

Cell culture. The HT-29 human adenocarcinoma cell line was obtained from American Type Culture Collection (Manassas, VA). It was cultured in a humidified atmosphere of 5% CO_2 in 25 cm^2 flask and fed with fresh medium every 2-3 days. The growth medium consisted of Dulbecco's Modified Eagle's Medium (DMEM, Sigma) supplemented with 10 % fetal bovine serum (PAA Laboratories, Austria), 100 units/mL penicillin, and 100 μg/mL streptomycin (GIBCO, USA). Subconfluent cells were passaged by trypsinization in 1 mL of Trypsin-EDTA (50 μg/mL trypsin, 20 μg/mL EDTA in PBS) for 30 s. After removal of trypsin, the cells were incubated at 37°C for 5 min. Fresh medium was then added to inhibit the effect of trypsin and the cells were dispersed by pipetting. The cells were washed by centrifugation and suspended in complete medium. The cell viability was determined by staining with Trypan Blue and the cell density was estimated by using a 0.9 mm^3 hemocytometer.

Cell seeding. The substrates were immersed in 70% ethanol in water for 30 min to minimize the risk of bacterial and fungal contamination. It was then rinsed with copious amount of PBS to remove ethanol remnants. Cells were seeded on the substrates placed in 24-well culture plate at a density of 5 x 10^4 cells per well. The cells were allowed to

adhere for 24 h under standard culture conditions. The substrates were rinsed vigorously with PBS to remove the non-adherent cells.

Viability assay. The viability of micropatterned cells was determined by using CellTracker Red CMTPX. Stock solution was prepared by dissolving CMTPX in DMSO to a concentration of 10 mM. The stock solution was then diluted to a working concentration of 2.5 μM in serum free DMEM. The working solution was warmed to 37°C. The medium from the well is removed and replaced with the probe and incubated for 45 min under growth conditions. The probe solution was replaced with fresh medium and incubated for another 30 min. The micropatterned cells were washed with PBS. The adhered cells were fixed with 4% paraformaldehyde in PBS for 20 min at room temperature. The samples were then dehydrated in a graded ethanol series.

Cell proliferation assay. HT-29 cells were seeded onto sterilized non-patterned substrate (1 cm x 1 cm) placed in a 24 well plate at a density of 3×10^4 cells per well. A lower cell density was used for proliferation studies so that there would be sufficient space for cells to proliferate for 7 days. On day 1, 3, 5 and 7, cell proliferation was determined utilizing the MTS assay. Triplicate substrates were used for each condition.

MTS assay. MTS assay was performed using Cell Titer 96 ® Aqueous One Solution. The MTS tetrazolium compound is bioreduced by metabolically active cells into a coloured formazan product that is soluble in culture medium. The substrate was rinsed with PBS twice and placed into a new 24 well plate. The substrate was incubated with

100 μL of MTS reagent diluted in 500 μL serum free DMEM for 3 h at 37°C in a humidified, 5% CO_2 environment. Thereafter, 5 x100 μL aliquot from each well were pipetted into 5 wells of a 96-well plate. The 96-well plate was then placed into a spectrophotometric plate reader (FLUOstar OPTIMA, BMG Lab Technologies, Germany) to record the absorbance of formazan at 492 nm. The amount of absorbance is directly proportional to the number of living cells in culture.

Microscopy. The cell pattern images were acquired using an upright microscope (Zeiss Axiostar Plus) equipped with a CCD camera (Media Cybernetics, Evolution^{TM} MP) with a pixel size of 3.4 x 3.4 μm. The filter (Chroma Technologies) used to excite the red CMTPX labelled cells was 546/12 nm. For SEM, the samples were sputter coated with gold (JEOL JFC-1600 Auto Fine Coater) for 50 s at 30 mA before examination with Hitachi field emission scanning electron microscopy, at an accelerating voltage of 10 keV.

5.3 Results and Discussion

5.3.1 Cell Proliferation on Non-patterned Substrates

Prior to performing cell micropatterning on the microspheres patterned substrate, preliminary studies were conducted to assess cell adhesion and proliferation on non-patterned substrate. The proliferation of HT29 on the structured substrates was studied from Day 1 to 7 with the MTS assay. The polystyrene microspheres modified substrates

with different surface chemistry, Packing Density and size were investigated. The results for the MTS assay are summarized in Figure 5.3.1 in terms of absorption values which is directly proportional to the number of viable cells. Generally, there was an increase in absorption from day 1 to 7, suggesting that cells are able to proliferate on the microspheres modified substrate.

5.3.1.1 Surface Chemistry

Firstly, polystyrene microspheres with different surface chemistry were studied. Two types of microspheres were used, namely the 1 μm PS-COOH and PS-NH_2. The Packing Density of the microspheres on the silicon substrate was approximately 95%. The absorption data from the MTS assay suggests approximately five fold increase in the cell population from Day 1 to Day 7. The proliferation results for both the substrate were similar and did not show pronounced difference over the 7 days (Figure 5.1 A). This may be attributed to their similar wettability as the contact angles for PS-COOH and PS-NH_2 are 33.0 ± 1.27° and 34.3 ± 1.50° respectively. Due to the similarity in cell proliferation results for these two types of microspheres, only PS-COOH microspheres was used for subsequent studies.

5.3.1.2 Particle Size

Cell proliferation on 0.5 μm, 1 μm, and 2 μm PS-COOH at 95% Packing Density and PS-COOH film were compared to study the effect of roughness. The most obvious observation is that the proliferation rate on the PS-COOH film is about 2 times lower than other microspheres assembled substrate up to Day 7, implying that the surface

roughness plays a critical role in promoting cell adhesion and proliferation. For Day 1 and 3, the proliferation on 0.5 μm PS-COOH assembled substrate was lower than 1 and 2 μm (Figure 5.1 B).

5.3.1.3 Packing Density

1 μm PS-COOH were assembled on the substrate with Packing Density of 0%, 25%, 45%, 75% and 95% on amine-terminated silicon surface. On Day 1 and 3, the number of cells increased as the Packing Density increased from 0% to 45%. The proliferation peaked on substrate with 45% Packing Density, suggesting that this is the optimal condition for cell adhesion and growth. With a further increase in Packing Density to 75% and 95%, the cell number decreased. After five and seven days of culture, there was no distinct trend as the cells had proliferated profusely and resulted in an overcrowding environment (Figure 5.3.1 C).

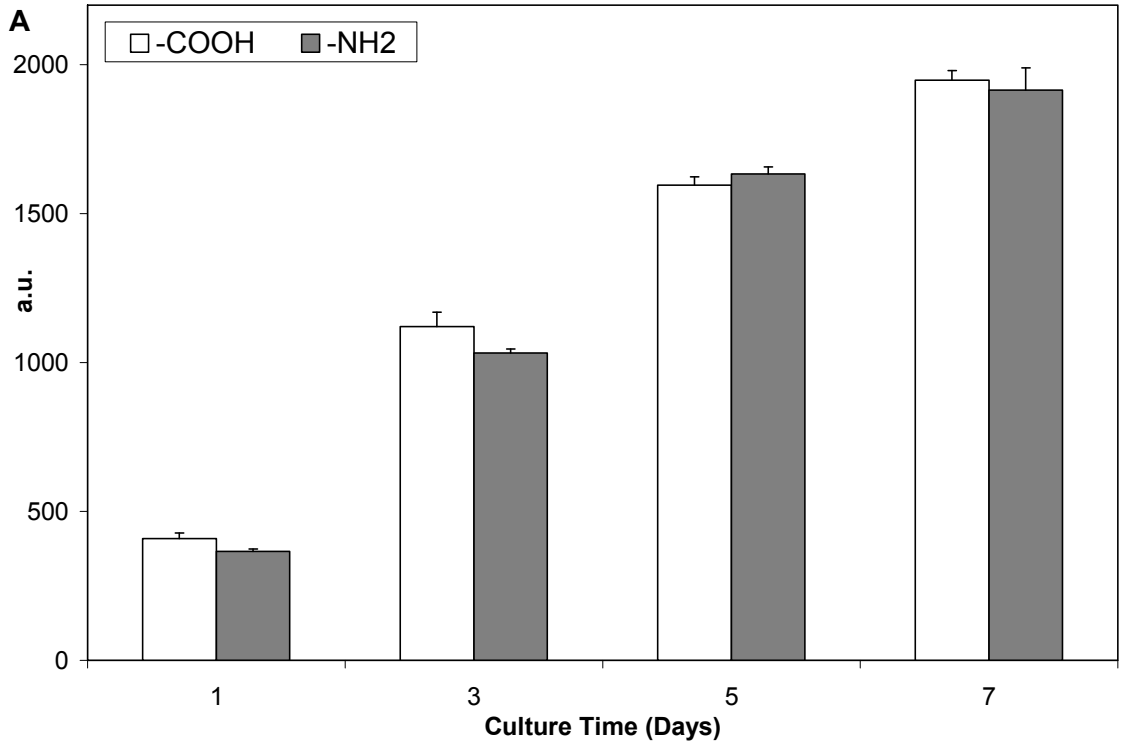

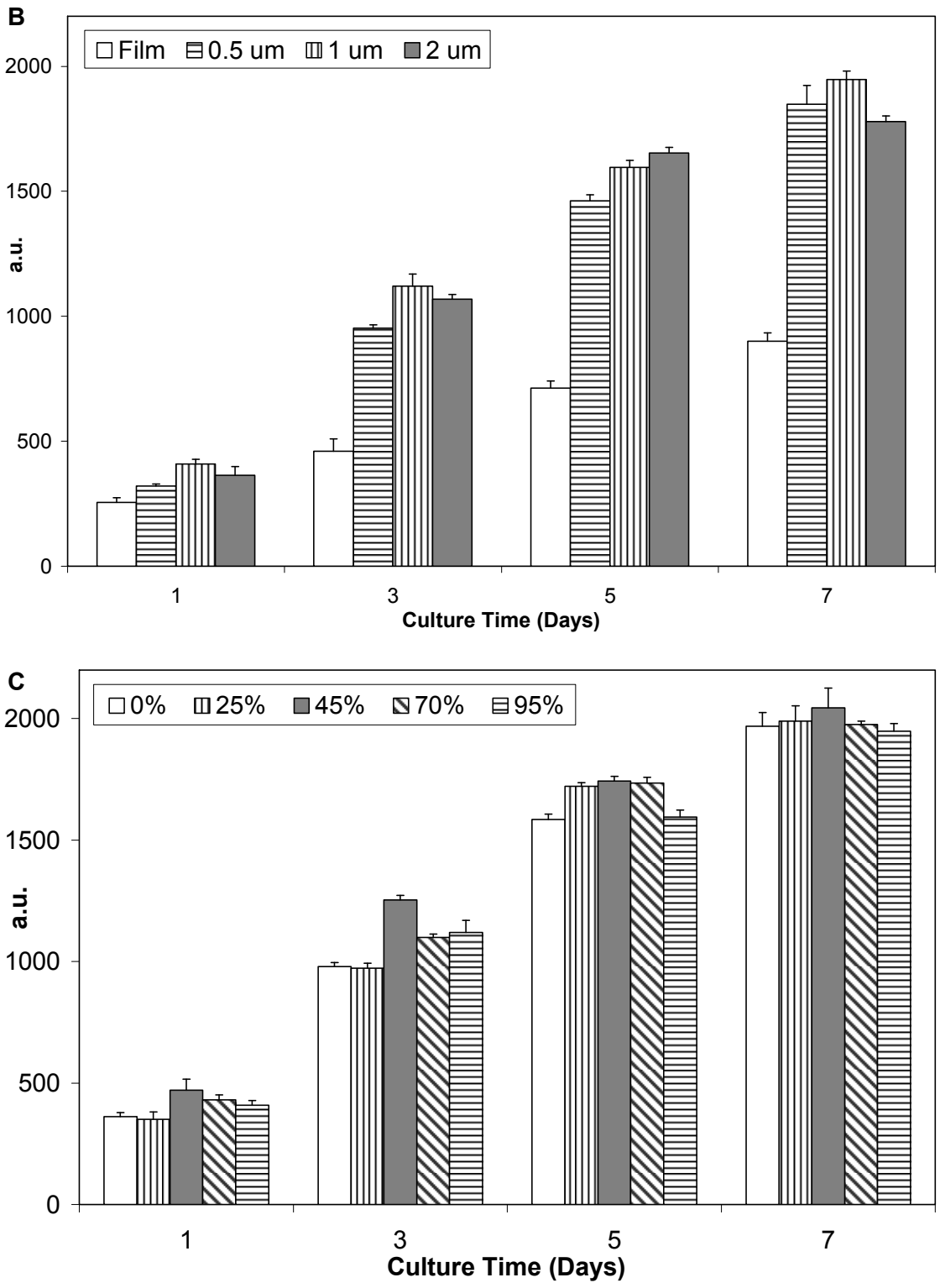

Figure 5.1. Proliferation of HT-29 on polystyrene microspheres up to 7 days. (A) 1 µm microspheres with different surface chemistry. (B) PS-COOH microspheres of various sizes. (C) 1 µm PS-COOH assembled with different Packing Density.

5.3.2 Cell Micropatterning on Surfaces Assembled with Microspheres

Here, a top down photolithography approach combined with bottom up self assembly of particles is used to guide cell adhesion. After assembly of microspheres, the parylene film was peeled off, revealing a non-fouling PEG background which is cell resistant while the microspheres patterned regions has carboxylic groups which have strong affinity for cells. Integrating colloidal assembly with cell micropatterning offers many advantages over the conventional micropatterning. In this technique, the topography can be fine-tuned according to the cell type to improve cellular adhesion and function. The optimal substrate when incorporated with cell micropatterning based assays such as biosensors and lab-on-a-chip devices can improve the efficiency and functionality of the devices considerably.

The cell micropatterning technique was demonstrated using HT-29 as the model cell line. HT-29 cells were seeded onto the micropatterned substrate and allowed to adhere for 24 h under standard culture conditions. Cell viability was assessed by staining with CellTracker Red CMTPX. The cells were fixed and observed. Figure 5.2 A shows the bright field image of an array of 1 μm PS-COOH microspheres and HT 29 cells attaching on the microspheres. There was no observable disturbance to the microspheres patterns after incubation in culture medium for one day. Figure 5.2 B shows the fluorescent image of the HT-29 cells stained with CMTPX, suggesting that the cell remained viable after attachment to the microspheres textured surface. The bright field and fluorescent image are overlay in Figure 5.2 C to show distinctly that the HT29 cells attached precisely to the

microspheres assembled surface while the background was effective in resisting cell adhesion. Figure 5.2 D is the SEM image of the patterned microspheres and cells.

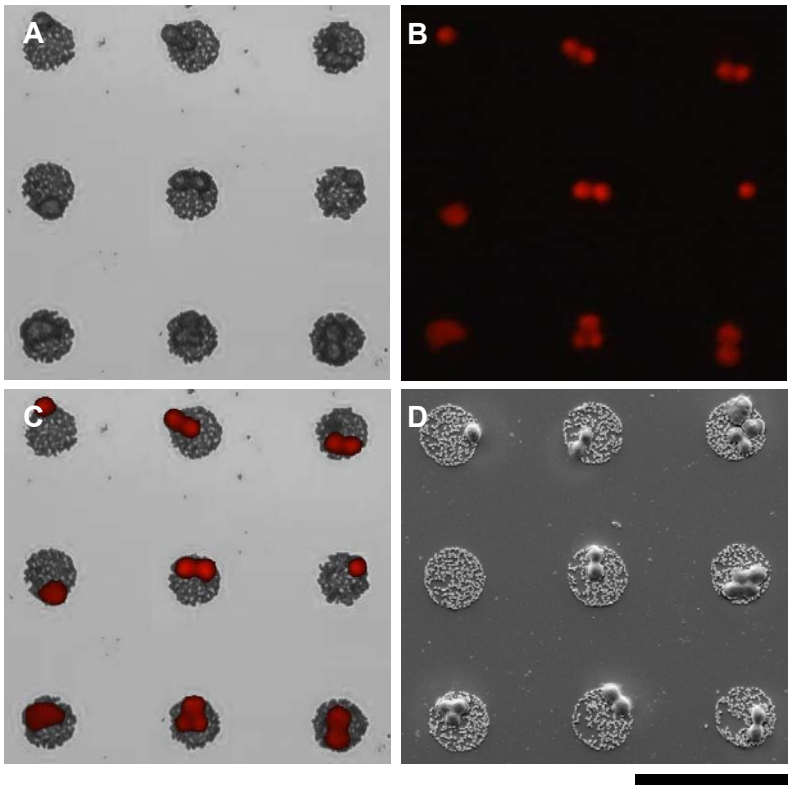

Figure 5.2. HT-29 cells micropatterned on surfaces assembled with 1 μm PS-COOH microspheres. (A) Bright field image, (B) Fluorescent image of cells stained with CMTPX, (C) Overlay of bright field and fluorescent image, (D) SEM image. The scale bar represents 100 μm.

5.3.3 Topographical Effects on Cells

In this section, the effects of topography on adhesion of HT-29 cells were investigated. The parameters that will shape the topography are Packing Density and size of the microspheres. Cell adhesion at randomly selected area on the array containing at least

300 microwells was quantified by counting the number of cells in each microwell under an optical microscope. Cell occupancy is defined as:

Cell Occupancy (%) = no. of wells occupied by cells x 100 / total no. of wells.

The Average number of cells per well was calculated as:

Average Cell no. = no. of cells / total no. of wells.

These two parameters are used to compare the adhesion of HT-29 cells on various topographies.

Firstly, the effect of particle size was studied using microwells closely packed (Packing Density of ~ 95%) with 0.5 μm, 1 μm and 2 μm PS-COOH microspheres or coated with PS-COOH film (Figure 5.3). The Cell Occupancy for microwells coated with PS-COOH film was 20% and the Average Cell no. was 0.43. There was significant improvement in cell adhesion on 0.5 μm microspheres; 54% of the microwells were occupied and the average number of cells per well was 1.3. Comparing these two substrates (characterized in Chapter 4), both are hydrophobic with a slightly higher contact angle for the 0.5 μm microsphere assembled surface. The improvement in cell adhesion may be attributed to the increase in surface area and surface roughness of the microsphere assembled microwells.

The cell adhesion efficiency for the 1 and 2 μm microspheres assembled microwells were similar; the Cell Occupancy and Average Cell no. was approximately 69% and 1.8 for both. The significant improvement in cell adhesion for the 1 μm and 2 μm, compared to 0.5 μm microspheres assembled surfaces may be due to the change in wettability; the 1

μm and 2 μm surfaces are hydrophilic while the 0.5 μm surfaces is hydrophobic. The similarity in cell adhesiveness for the 1 μm and 2 μm microspheres may be attributed to their similar hydrophilicity, while their differences in surface roughness did not influence the adhesion of HT-29 cells extensively. The results obtained indicate that adhesion of HT-29 cells is generally better on hydrophilic surface and a certain degree of roughness promotes adhesion; this finding is consistent with other cell types like osteoblast (Anselme, 2000), epithelial (Andersson et al., 2003) and fibroblast (Webb et al., 1998).

Next, the Packing Density of 1 μm PS-COOH microspheres was varied from 0% to 95% to study its influence on cell adhesion (Figure 5.4). The microspheres were deposited on an amino-silane modified surface in the microwells. The surface roughness increases proportionally with the Packing Density, whereas the contact angle is expected to be between that of amine-silane modified surface (empty microwell) and 1 um closely packed surface which is 30° - 40°. At 0% Packing Density, HT-29 adhered onto the amnio-terminated microwells with 40% Cell Occupancy and an average of 0.96 cell per well. At 25% Packing Density, the cells adhered on a composite surface consisting of microspheres and the amine modified background. The adhesion for HT-29 improved, suggesting that the cells prefer attachment to a microsphere decorated surface. As the density of particles increased to 45% or more, HT-29 cells are likely to be adhering solely on the microspheres and do not interact with the amine-terminated surface due to the small interparticle spacing. An increase in Packing Density in this range results in an increase in surface roughness and a decrease in the distance between adhesive sites. The number of cells adhered peaked at 45% Packing Density with 70% of the microwells

occupied and an average of 2.1 cells per microwell. This corresponds to 3.5 folds increase in Cell Occupancy when compared to microwells coated with PS-COOH film. A further increase in the Packing Density was accompanied by a slight decrease in cell attachment efficiency. This observation suggests that adhesion of HT-29 can be optimized by careful manipulation of surface roughness and distance between adhesive sites.

Figure 5.5 shows the typical fluorescent images of micropatterned cell labelled with CMPTX on three selected substrates, A) PS-COOH film; B) amine terminated silicon wafer, and C) 1μm PS-COOH microspheres at 45% Packing Density. There were obvious differences in cell coverage between the three substrates. On the PS-COOH film and amine modified patterned substrates; the Cell Occupancy was very low, with only a few microwells occupied by cells. The cell coverage improved significantly for surfaces deposited with polystyrene microspheres.

The topography presented to the cells influences its ability to adhere and spread. As the microspheres are not evenly distributed at low packing density, the number of micropheres underneath the cell was estimated so as to better describe the topography the cells are adhering to. The number of 1 um PS-COOH microspheres underneath each HT29 cells was estimated to be around 60, 85, 120, 135 and 300 for 25%, 45%, 65%, 75% and 95% packed microwells respectively. The morphology of the HT-29 cells was examined with SEM. It is observed that HT-29 cells are more spherical when they attached on PS-COOH film (Figure 5.6 A), and on microwells with 45% Packing Density

or lower (Figure 5.6 E-G). They become more spread and flatten when adhered over microwells with higher Packing Density (≥ 65%) (Figure 5.6 B-D, H,I). The morphology of cancer cells signifies the status of the cells, in terms of health and differentiation state (Cohen et al., 1999).

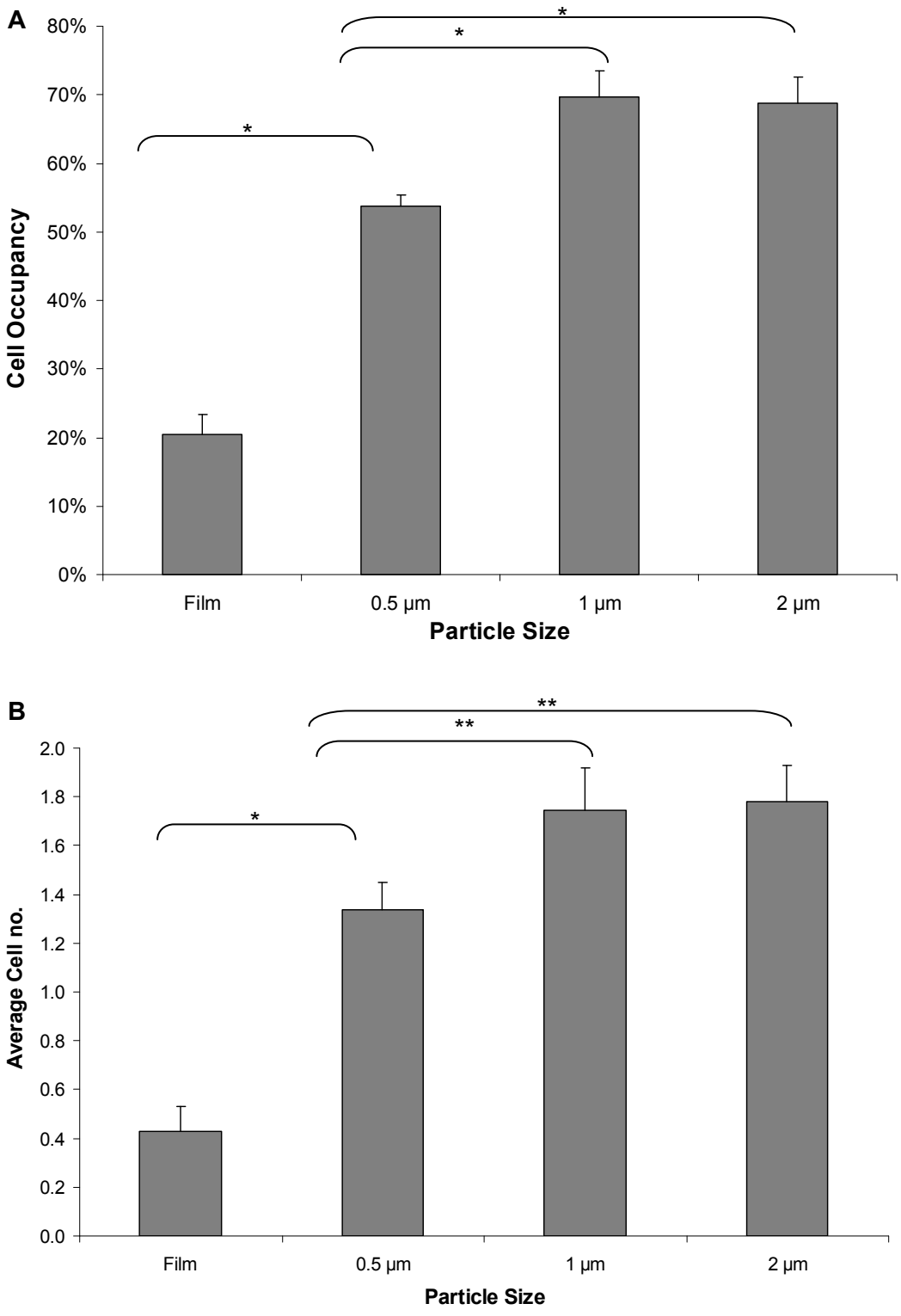

Figure 5.3. Effect of the size of particle on adhesion of HT-29 cells. Graph of (A) Cell Occupancy and (B) Average Cell no. against particle size. Results are mean values and standard deviations are indicated with error bar (n = 3). t-test * $p < 0.001$, ** $p < 0.005$.

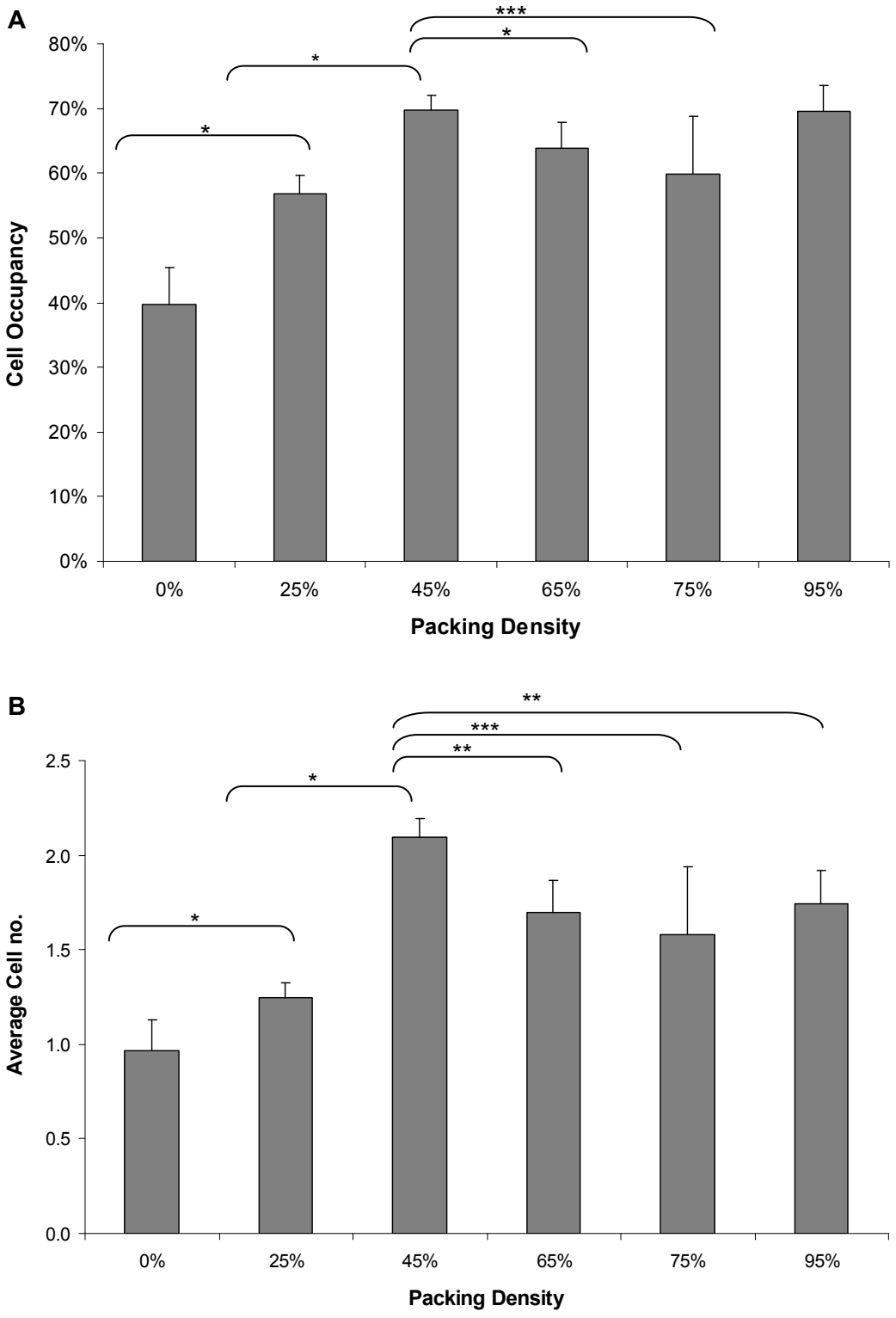

Figure 5.4. Effect of Packing Density of particles on adhesion of HT-29 cells. Graph of (A) Cell Occupancy and (B) Average Cell no. against Packing Density. Results are mean values and standard deviations are indicated with error bar (n = 3). t-test * $p < 0.001$, ** $p < 0.005$, *** $p < 0.01$.

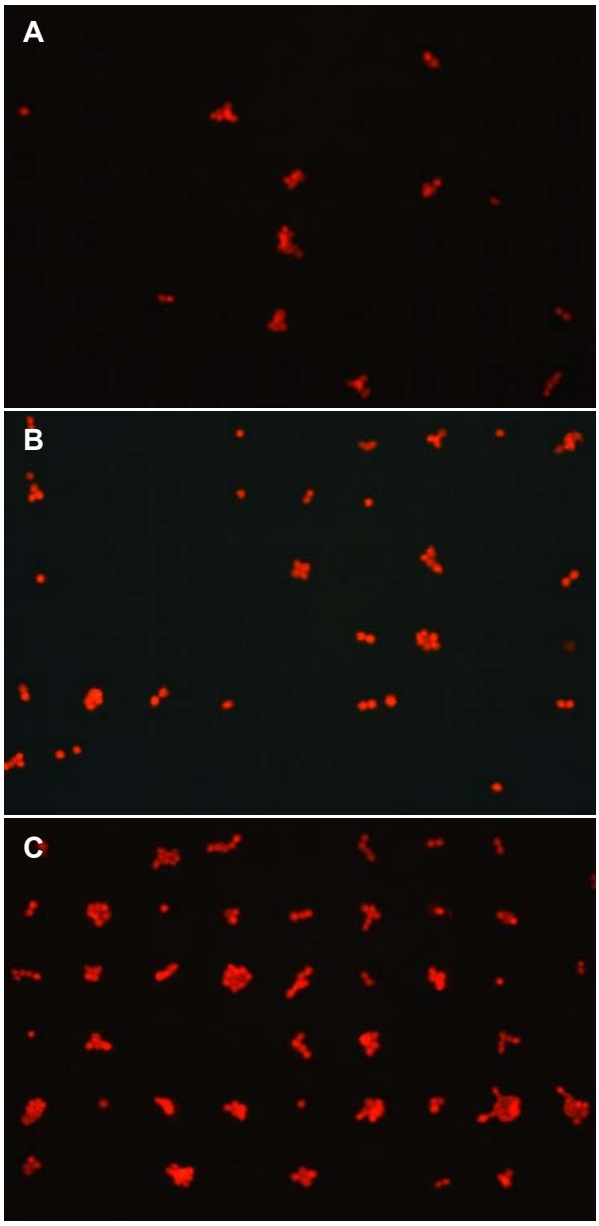

Figure 5.5. Comparison of HT-29 micropatterns obtained on microwells with different modifications. Fluorescent images of cells labelled with CMPTX on (A) PS-COOH film, (B) amine-terminated silicon surface, (C) 1 μm PS-COOH at 45% Packing Density.

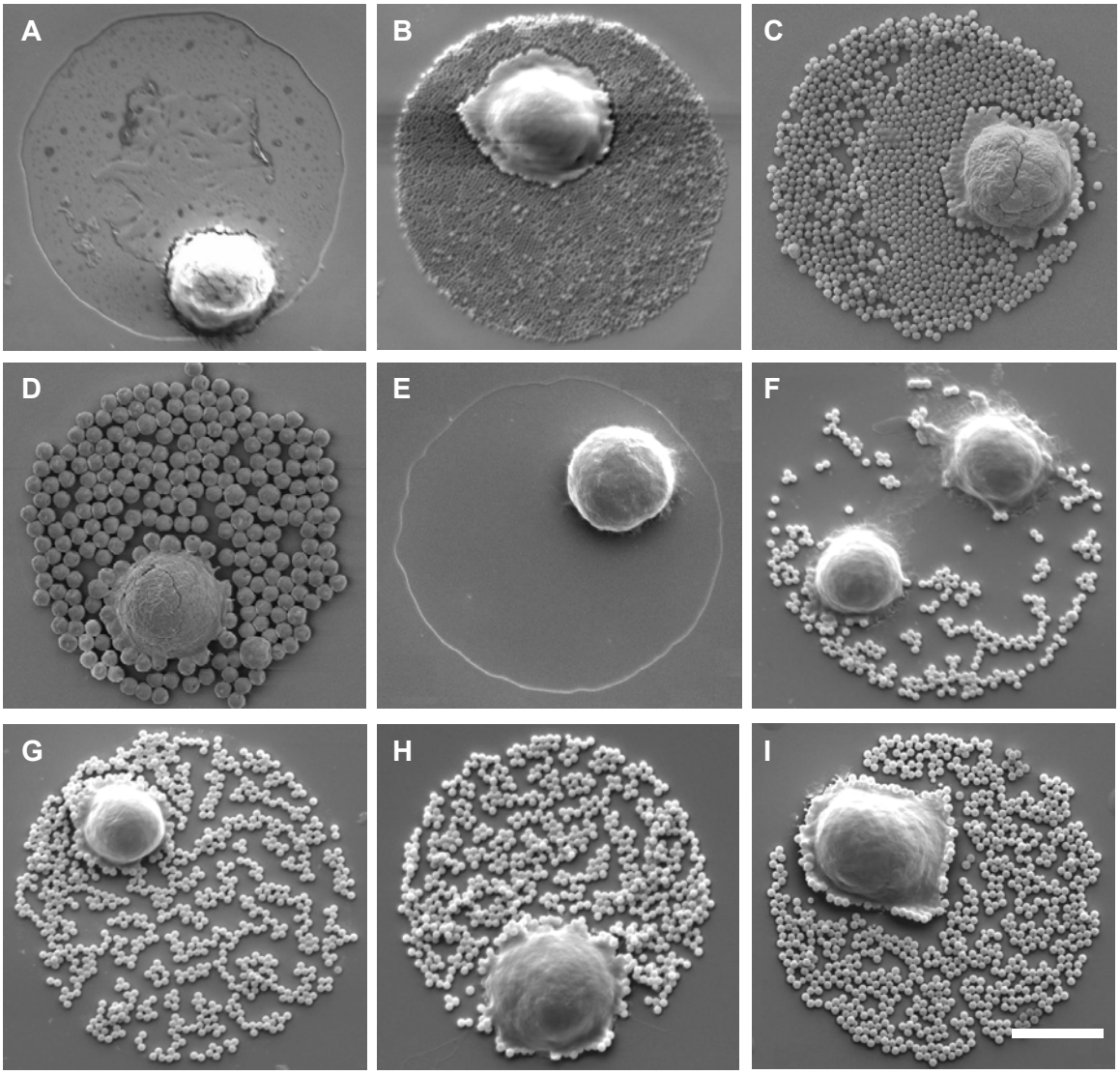

Figure 5.6. Morphology of HT-29 cells adhered to substrates with different topography. SEM images of HT-29 on (A) PS-COOH film, closely packed (Packing Density ~ 95%) PS-COOH microspheres of various sizes, (B) 0.5 µm, (C) 1 µm, (D) 2 µm. 1 µm PS-COOH microspheres with different Packing Density, (E) 0%, (F) 25%, (G) 45%, (H) 65%, (I) 75%. The scale bar represents 10 µm.

5.4 Conclusion

In this chapter, a technique of cell micropatterning on colloidal assembly was demonstrated. The cells adhered selectively over the regions assembled with PS-COOH microspheres, while the background regions grafted with PEG resisted cell adhesion. The microspheres present a micro topography which increases the roughness and affects the wettability of the substrate. The adhesion and proliferation of HT-29 on microspheres modified substrate improved significantly, as compared to the PS-COOH film. The adhesion and proliferation peaked on substrates with 45% Packing Density of 1 μm PS-COOH microspheres. The optimal substrate when incorporated with cell micropatterning based assays such as biosensors and lab-on-a-chip devices can improve the efficiency and functionality of the devices considerably

CHAPTER 6

CONCLUSION & FUTURE WORK

6.1 Conclusion

It is well known that the surface topography plays an important role in affecting protein and cell behaviour, however the benefits of using a structured surface has not been integrated with protein and cell micropatterning technique. Therefore, the objective in this thesis is to develop a novel protein and cell micropatterning technique that involves integration with colloidal assembly. The assembly of colloids introduces a micro / nanotopogarphy for protein and cell adhesion that can be controlled precisely. The following paragraphs will outline the findings obtained in each steps of the developmental process.

The first and foremost step is to design and fabricate a template that is compatible with both colloidal assembly and protein and cell mciropatterning. This was achieved with a bi-functional template which contains hydrophilic microwells surrounded by hydrophobic parylene film on the background. The hydrophilic template is suitable for assembly of colloidal particles by selective wetting and deposition of particles in the hydrophilic domains. After particle assembly, the parylene film can be peeled off to reveal a PEG grafted background, rendering the chip compatible with biopatterning.

The next step is the assembly of particles onto the template by selective wetting. A fluidic chamber is designed to control the flow of colloidal suspension over the template. By using this device, the concentration and rate of flow of the suspension can be kept constant and this facilitates uniform deposition of particles over a wide area. The

topography of the adhesive regions was manipulated by the assembly of PS-COOH microspheres of various sizes with packing density ranging from a sparsely deposited microwell to a microwell containing a monolayer of closely packed microspheres. The assembly of different types of particles like silica and gold nanoparticles was also demonstrated.

After colloidal assembly, the parylene film was removed; revealing a protein and cell resistant PEG grafted background. The templates with microwells assembled with a monolayer of closely packed PS-COOH microspheres were used for protein micropatterning so as to give uniform and high density protein spots. The protein density was 2.5 times higher than that obtained on a planar surface. The proteins remained functional as verified by antibody – antigen binding system. The CD spectra of proteins adsorbed onto nanoparticles suggested that the topography of the particles resulted in better preservation of the protein conformation than on a planar substrate. The advantages of this micropatterning technique are pertinent in biosensors where both protein density and functionality are critical.

Cell micropatterning was demonstrated successfully with HT-29; the cells positioned precisely on the microspheres assembled microwells. The effects of topography on cell adhesion were studied by using microwells assembled with PS-COOH microspheres of different sizes and packing density. The adhesion and proliferation of HT-29 on the micro structured surface improved significantly as compared to surfaces coated with PS-COOH film. The optimal topography for HT-29 adhesion is on surfaces modified with 1 μm PS-

COOH microspheres at 45% Packing Density; the increment in Cell Occupancy is 3.5 folds, comparing to the microwells coated with PS-COOH film. This study shows that the incorporation of topographical structures on the cell adhesive regions can improve the micropatterning efficiency significantly.

6.2 Future Work

Functionality of cells on microspheres assembled substrates

It was shown that the adhesion and proliferation of HT-29 cells improved on PS-COOH microspheres assembled surfaces; the effects of topography on the functionality of cells can also be characterized. As there are no definitive markers and tests to determine the differentiation and functionality of HT-29 cells, other cell lines should be used for this study. For example, the alkaline phosphatase activity can be measured for osteoblast cells to indicate its differentiation; or the functionality of hepatocytes can be determined by measuring the amount of urea and albumin production which are markers of liver metabolic and synthetic function respectively. Positive effects of topography on cell functionality will increase the merits of this cell micropatterning technique

Different types of structured topography

Apart from utilizing particles to modify the topography of the adhesive regions, other structures can be employed, for example, nanowires, nanotubes and micro / nanofibres. The challenge lies in achieving selective growth of structures on a patterned substrate

while maintaining a protein and cell resistant background. The growth conditions can be manipulated to synthesize structures of various sizes and packing density

References

Affrossman S, Henn G, Oneill SA, Pethrick RA, Stamm M. 1996. Surface topography and composition of deuterated polystyrene-poly(bromostyrene) blends. Macromolecules 29(14):5010-5016.

Aizenberg J, Braun PV, Wiltzius P. 2000. Patterned colloidal deposition controlled by electrostatic and capillary forces. Physical Review Letters 84(13):2997-3000.

Alarie JP, Sepaniak MJ, Vodinh T. 1990. Evaluation Of Antibody Immobilization Techniques For Fiber Optic-Based Fluoroimmunosensing. Analytica Chimica Acta 229(2):169-176.

Alcantar NA, Aydil ES, Israelachvili JN. 2000. Polyethylene glycol-coated biocompatible surfaces. Journal of Biomedical Materials Research 51(3):343-351.

Andersson AS, Brink J, Lidberg U, Sutherland DS. 2003. Influence of systematically varied nanoscale topography on the morphology of epithelial cells. Ieee Transactions On Nanobioscience 2(2):49-57.

Andruzzi L, Senaratne W, Hexemer A, Sheets ED, Ilic B, Kramer EJ, Baird B, Ober CK. 2005. Oligo(ethylene glycol) containing polymer brushes as bioselective surfaces. Langmuir 21(6):2495-2504.

Anselme K. 2000. Osteoblast adhesion on biomaterials. Biomaterials 21(7):667-681.
Bernard A, Delamarche E, Schmid H, Michel B, Bosshard HR, Biebuyck H. 1998. Printing patterns of proteins. Langmuir 14(9):2225-2229.

Berova N, Nakanishi K, Woody RW, editors. 2000. Circular dichroism : principles and applications New York Wiley-VCH.

Berry CC, Campbell G, Spadiccino A, Robertson M, Curtis ASG. 2004. The influence of microscale topography on fibroblast attachment and motility. Biomaterials 25(26):5781-5788.

Bhatia SN, Balis UJ, Yarmush ML, Toner M. 1999. Effect of cell-cell interactions in preservation of cellular phenotype: cocultivation of hepatocytes and nonparenchymal cells. Faseb Journal 13(14):1883-1900.

Bhatia SN, Yarmush ML, Toner M. 1997. Controlling cell interactions by micropatterning in co-cultures: Hepatocytes and 3T3 fibroblasts. Journal Of Biomedical Materials Research 34(2):189-199.

Biasco A, Pisignano D, Krebs B, Pompa PP, Persano L, Cingolani R, Rinaldi R. 2005. Conformation of microcontact-printed proteins by atomic force microscopy molecular sizing. Langmuir 21(11):5154-5158.

Brewer SH, Glomm WR, Johnson MC, Knag MK, Franzen S. 2005. Probing BSA binding to citrate-coated gold nanoparticles and surfaces. Langmuir 21(20):9303-9307.

Britland S, Clark P, Connolly P, Moores G. 1992a. Micropatterned Substratum Adhesiveness - A Model For Morphogenetic Cues Controlling Cell Behavior. Experimental Cell Research 198(1):124-129.

Britland S, Perezarnaud E, Clark P, McGinn B, Connolly P, Moores G. 1992b. Micropatterning Proteins And Synthetic Peptides On Solid Supports - A Novel Application For Microelectronics Fabrication Technology. Biotechnology Progress 8(2):155-160.

Chen CS, Mrksich M, Huang S, Whitesides GM, Ingber DE. 1997. Geometric control of cell life and death. Science 276(5317):1425-1428.

Chen KM, Jiang XP, Kimerling LC, Hammond PT. 2000. Selective self-organization of colloids on patterned polyelectrolyte templates. Langmuir 16(20):7825-7834.

Chen SF, Liu LY, Zhou J, Jiang SY. 2003. Controlling antibody orientation on charged self-assembled monolayers. Langmuir 19(7):2859-2864.

Chin VI, Taupin P, Sanga S, Scheel J, Gage FH, Bhatia SN. 2004. Microfabricated platform for studying stem cell fates. Biotechnology And Bioengineering 88(3):399-415.

Co CC, Wang YC, Ho CC. 2005. Biocompatible micropatterning of two different cell types. Journal Of The American Chemical Society 127(6):1598-1599.

Cohen E, Ophir I, Ben Shaul Y. 1999. Induced differentiation in HT29, a human colon adenocarcinoma cell line. Journal of Cell Science 112(16):2657-2666.

Connolly P, Clark P, Curtis ASG, Dow JAT, Wilkinson CDW. 1990. An Extracellular Microelectrode Array For Monitoring Electrogenic Cells In Culture. Biosensors & Bioelectronics 5(3):223-234.

Corey JM, Feldman EL. 2003. Substrate patterning: an emerging technology for the study of neuronal behavior. Experimental Neurology 184:S89-S96.

Cousins BG, Doherty PJ, Williams RL, Fink J, Garvey MJ. 2004. The effect of silica nanoparticulate coatings on cellular response. Journal Of Materials Science-Materials In Medicine 15(4):355-359.

Csucs G, Michel R, Lussi JW, Textor M, Danuser G. 2003. Microcontact printing of novel co-polymers in combination with proteins for cell-biological applications. Biomaterials 24(10):1713-1720.

Cui Y, Bjork MT, Liddle JA, Sonnichsen C, Boussert B, Alivisatos AP. 2004. Integration of colloidal nanocrystals into lithographically patterned devices. Nano Letters 4(6):1093-1098.

Curtis A, Wilkinson C. 1997. Topographical control of cells. Biomaterials 18(24):1573-1583.

Curtis ASG, Varde M. 1964. Control of cell behaviour: topographical factors. Cancer. Res. Inst. 33:15-26.

Dalby MJ, Riehle MO, Johnstone H, Affrossman S, Curtis ASG. 2002a. In vitro reaction of endothelial cells to polymer demixed nanotopography. Biomaterials 23(14):2945-2954.

Dalby MJ, Riehle MO, Sutherland DS, Agheli H, Curtis ASG. 2004. Fibroblast response to a controlled nanoenvironment produced by colloidal lithography. Journal Of Biomedical Materials Research Part A 69A(2):314-322.

Dalby MJ, Riehle MO, Yarwood SJ, Wilkinson CDW, Curtis ASG. 2003. Nucleus alignment and cell signaling in fibroblasts: response to a micro-grooved topography. Experimental Cell Research 284(2):274-282.

Dalby MJ, Yarwood SJ, Riehle MO, Johnstone HJH, Affrossman S, Curtsi ASG. 2002b. Increasing fibroblast response to materials using nanotopography: morphological and genetic measurements of cell response to 13-nm-high polymer demixed islands. Experimental Cell Research 276(1):1-9.

Deegan RD, Bakajin O, Dupont TF, Huber G, Nagel SR, Witten TA. 1997. Capillary flow as the cause of ring stains from dried liquid drops. Nature 389(6653):827-829.

Denis FA, Hanarp P, Sutherland DS, Gold J, Mustin C, Rouxhet PG, Dufrene YF. 2002. Protein adsorption on model surfaces with controlled nanotopography and chemistry. Langmuir 18(3):819-828.

Desai TA. 2000. Micro- and nanoscale structures for tissue engineering constructs. Medical Engineering & Physics 22(9):595-606.

Ding XM, Kawaguchi Y, Sato T, Narazaki A, Niino H. 2004. Fabrication of microarrays on fused silica plates using the laser-induced backside wet etching method. Langmuir 20(22):9769-9774.

Docoslis A, Alexandridis P. 2002. One-, two-, and three-dimensional organization of colloidal particles using nonuniform alternating current electric fields. Electrophoresis 23(14):2174-2183.

Duffy DC, McDonald JC, Schueller OJA, Whitesides GM. 1998. Rapid prototyping of microfluidic systems in poly(dimethylsiloxane). Analytical Chemistry 70(23):4974-4984.

Eck W, Stadler V, Geyer W, Zharnikov M, Golzhauser A, Grunze M. 2000. Generation of surface amino groups on aromatic self-assembled monolayers by low energy electron beams - A first step towards chemical lithography. Advanced Materials 12(11):805-808.

Fan FQ, Stebe KJ. 2004. Assembly of colloidal particles by evaporation on surfaces with patterned hydrophobicity. Langmuir 20(8):3062-3067.

Folch A, Ayon A, Hurtado O, Schmidt MA, Toner M. 1999. Molding of deep polydimethylsiloxane microstructures for microfluidics and biological applications. Journal Of Biomechanical Engineering-Transactions Of The Asme 121(1):28-34.

Folch A, Jo BH, Hurtado O, Beebe DJ, Toner M. 2000. Microfabricated elastomeric stencils for micropatterning cell cultures. Journal Of Biomedical Materials Research 52(2):346-353.

Folch A, Toner M. 1998. Cellular micropatterns on biocompatible materials. Biotechnology Progress 14(3):388-392.

Folch A, Toner M. 2000. Microengineering of cellular interactions. Annual Review of Biomedical Engineering 2:227-256.

Foresta dB, Tortech L, Vincent M, Gallay J. 2002. Location and dynamics of tryptophan in transmembrane alpha-helix peptides: a fluorescence and circular dichroism study. European Biophysics Journal With Biophysics Letters 31(3):185-197.

Fustin CA, Glasser G, Spiess HW, Jonas U. 2004. Parameters influencing the templated growth of colloidal crystals on chemically patterned surfaces. Langmuir 20(21):9114-9123.

Galli C, Coen MC, Hauert R, Katanaev VL, Wymann MP, Groning P, Schlapbach L. 2001. Protein adsorption on topographically nanostructured titanium. Surface Science 474(1-3):L180-L184.

Gleason NJ, Nodes CJ, Higham EM, Guckert N, Aksay IA, Schwarzbauer JE, Carbeck JD. 2003. Patterning proteins and cells using two-dimensional arrays of colloids. Langmuir 19(3):513-518.

Gross GW, Harsch A, Rhoades BK, Gopel W. 1997. Odor, drug and toxin analysis with neuronal networks in vitro: Extracellular array recording of network responses. Biosensors & Bioelectronics 12(5):373-393.

Haab BB. 2001. Advances in protein microarray technology for protein expression and interaction profiling. Current Opinion in Drug Disovery & Development 4:116-123.

Hammond PT, editor. 2004. Surface-directed colloid patterning: Selective Deposition via Electrostatic and Secondary Interactions. Weihem: Wiley-VCH.

Han M, Sethuraman A, Kane RS, Belfort G. 2003. Nanometer-scale roughness having little effect on the amount or structure of adsorbed protein. Langmuir 19(23):9868-9872.

Healy KE, Thomas CH, Rezania A, Kim JE, McKeown PJ, Lom B, Hockberger PE. 1996. Kinetics of bone cell organization and mineralization on materials with patterned surface chemistry. Biomaterials 17(2):195-208.

Huang WF, Liu QS, Li Y. 2006. Capillary filling flows inside patterned-surface microchannels. Chemical Engineering & Technology 29(6):716-723.

Ilic B, Craighead HG. 2000. Topographical Patterning of Chemically Sensitive Biological Materials Using a Polymer-Based Dry Lift Off. Biomedical Microdevices 2(4):317-322.

Jackman RJ, Duffy DC, Cherniavskaya O, Whitesides GM. 1999. Using elastomeric membranes as dry resists and for dry lift-off. Langmuir 15(8):2973-2984.

Jackson BL, Groves JT. 2007. Hybrid protein-lipid patterns from aluminum templates. Langmuir 23(4):2052-2057.

James CD, Spence AJH, Dowell-Mesfin NM, Hussain RJ, Smith KL, Craighead HG, Isaacson MS, Shain W, Turner JN. 2004. Extracellular recordings from patterned neuronal networks using planar microelectrode arrays. Ieee Transactions On Biomedical Engineering 51(9):1640-1648.

Jiang X, Jiang UG, Jin YD, Wang EK, Dong SJ. 2005. Effect of colloidal gold size on the conformational changes of adsorbed cytochrome c: Probing by circular dichroism, UV-visible, and infrared spectroscopy. Biomacromolecules 6(1):46-53.

Jun S, Jang EJ, Park J, Kim J. 2006. Photopatterned semiconductor nanocrystals and their electroluminescence from hybrid light-emitting devices. Langmuir 22(6):2407-2410.

Kane RS, Takayama S, Ostuni E, Ingber DE, Whitesides GM. 1999. Patterning proteins and cells using soft lithography. Biomaterials 20(23-24):2363-2376.

Kim E, Xia YN, Whitesides GM. 1995. Polymer Microstructures Formed By Molding In Capillaries. Nature 376(6541):581-584.

Kim E, Xia YN, Whitesides GM. 1996. Micromolding in capillaries: Applications in materials science. Journal Of The American Chemical Society 118(24):5722-5731.

Kleinfeld D, Kahler KH, Hockberger PE. 1988. Controlled Outgrowth Of Dissociated Neurons On Patterned Substrates. Journal Of Neuroscience 8(11):4098-4120.

Kralchevsky PA, Nagayama K. 1994. Capillary Forces Between Colloidal Particles. Langmuir 10(1):23-36.

Landolt D, Chauvy PF, Zinger O. 2003. Electrochemical micromachining, polishing and surface structuring of metals: fundamental aspects and new developments. Electrochimica Acta 48(20-22):3185-3201.

Lemieux B, Aharoni A, Schena M. 1998. Overview of DNA chip technology. Molecular Breeding 4(4):277-289.

Lom B, Healy KE, Hockberger PE. 1993. A Versatile Technique For Patterning Biomolecules Onto Glass Coverslips. Journal Of Neuroscience Methods 50(3):385-397.

Lu N, Chen XD, Molenda D, Naber A, Fuchs H, Talapin DV, Weller H, Muller J, Lupton JM, Feldmann J and others. 2004. Lateral patterning of luminescent CdSe nanocrystals by selective dewetting from self-assembled organic templates. Nano Letters 4(5):885-888.

Lundqvist M, Sethson I, Jonsson BH. 2004. Protein adsorption onto silica nanoparticles: Conformational changes depend on the particles' curvature and the protein stability. Langmuir 20(24):10639-10647.

Lyles BF, Terrot MS, Hammond PT, Gast AP. 2004. Directed patterned adsorption of magnetic beads on polyelectrolyte multilayers on glass. Langmuir 20(8):3028-3031.

MacBeath G, Schreiber SL. 2000. Printing proteins as microarrays for high-throughput function determination. Science 289(5485):1760-1763.

Massia SP, Stark J. 2001. Immobilized RGD peptides on surface-grafted dextran promote biospecific cell attachment. Journal of Biomedical Materials Research 56(3):390-399.

Massia SP, Stark J, Letbetter DS. 2000. Surface-immobilized dextran limits cell adhesion and spreading. Biomaterials 21(22):2253-2261.

Masuda Y, Itoh T, Koumoto K. 2005. Self-assembly patterning of silica colloidal crystals. Langmuir 21(10):4478-4481.

Maury P, Escalante M, Reinhoudt DN, Huskens J. 2005. Directed assembly of nanoparticles onto polymer-imprinted or chemically patterned templates fabricated by nanoimprint lithography. Advanced Materials 17(22):2718-2723.

Mehrvar M, Abdi M. 2004. Recent developments, characteristics, and potential applications of electrochemical biosensors. Analytical Sciences 20(8):1113-1126.

Mendelsohn JD, Yang SY, Hiller J, Hochbaum AI, Rubner MF. 2003. Rational design of cytophilic and cytophobic polyelectrolyte multilayer thin films. Biomacromolecules 4(1):96-106.

Miura Y, Sato H, Ikeda T, Sugimura H, Takai O, Kobayashi K. 2004. Micropatterned carbohydrate displays by self-assembly of glycoconjugate polymers on hydrophobic templates on silicon. Biomacromolecules 5(5):1708-1713.

Miyaki M, Fujimoto K, Kawaguchi H. 1999. Cell response to micropatterned surfaces produced with polymeric microspheres. Colloids And Surfaces A-Physicochemical And Engineering Aspects 153(1-3):603-608.

Mohammed JS, DeCoster MA, McShane MJ. 2004. Micropatterning of nanoengineered surfaces to study neuronal cell attachment in vitro. Biomacromolecules 5(5):1745-1755.

Mrksich M, Dike LE, Tien J, Ingber DE, Whitesides GM. 1997. Using microcontact printing to pattern the attachment of mammalian cells to self-assembled monolayers of alkanethiolates on transparent films of gold and silver. Experimental Cell Research 235(2):305-313.

Nakanishi K, Sakiyama T, Imamura K. 2001. On the adsorption of proteins on solid surfaces, a common but very complicated phenomenon. Journal Of Bioscience And Bioengineering 91(3):233-244.

Nelson CM, Jean RP, Tan JL, Liu WF, Sniadecki NJ, Spector AA, Chen CS. 2005. Emergent patterns of growth controlled by multicellular form and mechanics.

Proceedings Of The National Academy Of Sciences Of The United States Of America 102(33):11594-11599.

Ng JMK, Gitlin I, Stroock AD, Whitesides GM. 2002. Components for integrated poly(dimethylsiloxane) microfluidic systems. Electrophoresis 23(20):3461-3473.

Nygren H, Karlsson C. 1992. Intermolecular interaction and ordering of fibrinogen at a liquid-solid interface. Progress in Colloid and Polymer Science 88:96-99.

Ostuni E, Kane R, Chen CS, Ingber DE, Whitesides GM. 2000. Patterning mammalian cells using elastomeric membranes. Langmuir 16(20):7811-7819.

Pancrazio JJ, Whelan JP, Borkholder DA, Ma W, Stenger DA. 1999. Development and application of cell-based biosensors. Annals Of Biomedical Engineering 27(6):697-711.

Papra A, Gadegaard N, Larsen NB. 2001. Characterization of ultrathin poly(ethylene glycol) monolayers on silicon substrates. Langmuir 17(5):1457-1460.

Pardo L, Wilson WC, Boland TJ. 2003. Characterization of patterned self-assembled monolayers and protein arrays generated by the ink-jet method. Langmuir 19(5):1462-1466.

Park J, Moon J. 2006. Control of colloidal particle deposit patterns within picoliter droplets ejected by ink-jet printing. Langmuir 22(8):3506-3513.

Petri DFS, Wenz G, Schunk P, Schimmel T. 1999. An improved method for the assembly of amino-terminated monolayers on SiO2 and the vapor deposition of gold layers. Langmuir 15(13):4520-4523.

Piner RD, Zhu J, Xu F, Hong SH, Mirkin CA. 1999. "Dip-pen" nanolithography. Science 283(5402):661-663.

Pohl HA. 1978. Dielectrophoresis. U.K.: Cambridge University Press.
Pregibon DC, Toner M, Doyle PS. 2006. Magnetically and biologically active bead-patterned hydrogels. Langmuir 22(11):5122-5128.

Qian WP, Yao DF, Yu F, Xu B, Zhou R, Bao X, Lu ZH. 2000. Immobilization of antibodies on ultraflat polystyrene surfaces. Clinical Chemistry 46(9):1456-1463.

Quere D. 2002. Rough ideas on wetting. Physica a-Statistical Mechanics and Its Applications 313(1-2):32-46.

Revzin A, Tompkins RG, Toner M. 2003. Surface engineering with poly(ethylene glycol) photolithography to create high-density cell arrays on glass. Langmuir 19(23):9855-9862.

Roth EA, Xu T, Das M, Gregory C, Hickman JJ, Boland T. 2004. Inkjet printing for high-throughput cell patterning. Biomaterials 25(17):3707-3715.

Saito N, Maeda N, Sugimura H, Takai O. 2004. Generation of amino-terminated surfaces by chemical lithography using atomic force microscopy. Langmuir 20(13):5182-5184.

Singhvi R, Stephanopoulos G, Wang DIC. 1994. Effects Of Substratum Morphology On Cell Physiology - Review. Biotechnology And Bioengineering 43(8):764-771.

Smith RK, Lewis PA, Weiss PS. 2004. Patterning self-assembled monolayers. Progress In Surface Science 75(1-2):1-68.

Stevens PW, Wang CHJ, Kelso DM. 2003. Immobilized particle arrays: Coalescence of planar- and suspension-array technologies. Analytical Chemistry 75(5):1141-1146.

Stoll D, Bachmann J, Templin MF. 2004. Microarray technology: an increasing variety of screening tools for proteomics research. Drug Discovery Today 3(1):24-31.

Sutherland DS, Broberg M, Nygren H, Kasemo B. 2001. Influence of nanoscale surface topography and chemistry on the functional behaviour of an adsorbed model macromolecule. Macromolecular Bioscience 1(6):270-273.

Suzuki M, Yasukawa T, Mase Y, Oyamatsu D, Shiku H, Matsue T. 2004. Dielectrophoretic micropatterning with microparticle monolayers covalently linked to glass surfaces. Langmuir 20(25):11005-11011.

Sydor JR, Nock S. 2003. Protein expression profiling arrays: tools for the multiplexed high-throughput analysis of proteins. Proteome Science 1(1):3.

Tegoulia VA, Rao WS, Kalambur AT, Rabolt JR, Cooper SL. 2001. Surface properties, fibrinogen adsorption, and cellular interactions of a novel phosphorylcholine-containing self-assembled monolayer on gold. Langmuir 17(14):4396-4404.

Teixeira AI, Abrams GA, Bertics PJ, Murphy CJ, Nealey PF. 2003. Epithelial contact guidance on well-defined micro- and nanostructured substrates. Journal Of Cell Science 116(10):1881-1892.

Tziampazis E, Kohn J, Moghe PV. 2000. PEG-variant biomaterials as selectively adhesive protein templates: model surfaces for controlled cell adhesion and migration. Biomaterials 21(5):511-520.

Veinot JGC, Yan H, Smith SM, Cui J, Huang QL, Marks TJ. 2002. Fabrication and properties of organic light-emitting "nanodiode" arrays. Nano Letters 2(4):333-335.

Veiseh M, Zareie MH, Zhang MQ. 2002. Highly selective protein patterning on gold-silicon substrates for biosensor applications. Langmuir 18(17):6671-6678.

Velev OD, Kaler EW. 2000. Structured porous materials via colloidal crystal templating: From inorganic oxides to metals. Advanced Materials 12(7):531-534.

Vertegel AA, Siegel RW, Dordick JS. 2004. Silica nanoparticle size influences the structure and enzymatic activity of adsorbed lysozyme. Langmuir 20(16):6800-6807.

Wagner P, Kim R. 2002. Protein biochips: an emerging tool for proteomics research. Current Drug Discovery(May):23-28.

Wan YQ, Wang Y, Liu ZM, Qu X, Han BX, Bei JZ, Wang SG. 2005. Adhesion and proliferation of OCT-1 osteoblast-like cells on micro- and nano-scale topography structured pply(L-lactide). Biomaterials 26(21):4453-4459.

Wang YC, Ho CC. 2004. Micropatterning of proteins and mammalian cells on biomaterials. Faseb Journal 18(1).

Webb K, Hlady V, Tresco PA. 1998. Relative importance of surface wettability and charged functional groups on NIH 3T3 fibroblast attachment, spreading, and cytoskeletal organization. Journal of Biomedical Materials Research 41(3):422-430.

Whitehead KA, Colligon J, Verran J. 2005. Retention of microbial cells in substratum surface features of micrometer and sub-micrometer dimensions. Colloids And Surfaces B-Biointerfaces 41(2-3):129-138.

Whitesides GM, Ostuni E, Takayama S, Jiang XY, Ingber DE. 2001. Soft lithography in biology and biochemistry. Annual Review of Biomedical Engineering 3:335-373.

Wijnhoven J, Vos WL. 1998. Preparation of photonic crystals made of air spheres in titania. Science 281(5378):802-804.

Willner I, Katz E. 2000. Integration of layered redox proteins and conductive supports for bioelectronic applications. Angewandte Chemie-International Edition 39(7):1180-1218.

Xia DY, Biswas A, Li D, Brueck SRJ. 2004. Directed self-assembly of silica nanoparticles into nanometer-scale patterned surfaces using spin-coating. Advanced Materials 16(16):1427-1432.

Xia YN, Mrksich M, Kim E, Whitesides GM. 1995. Microcontact Printing Of Octadecylsiloxane On The Surface Of Silicon Dioxide And Its Application In Microfabrication. Journal Of The American Chemical Society 117(37):9576-9577.

Xia YN, Whitesides GM. 1998. Soft lithography. Annual Review Of Materials Science 28:153-184.

Xia YN, Yin YD, Lu Y, McLellan J. 2003. Template-assisted self-assembly of spherical colloids into complex and controllable structures. Advanced Functional Materials 13(12):907-918.

Xu T, Petridou S, Lee EH, Roth EA, Vyavahare NR, Hickman JJ, Boland T. 2004. Construction of high-density bacterial colony arrays and patterns by the ink-jet method. Biotechnology And Bioengineering 85(1):29-33.

Yabu H, Shimomura M. 2006. Mesoscale pincushions, microrings, and microdots prepared by heating and peeling of self-organized honeycomb-patterned films deposited on a solid substrate. Langmuir 22(11):4992-4997.

Yamasaki T, Tsutsui T. 1998. Spontaneous emission from fluorescent molecules embedded in photonic crystals consisting of polystyrene microspheres. Applied Physics Letters 72(16):1957-1959.

Yan X, Yao JM, Lu GA, Chen X, Zhang K, Yang B. 2004. Microcontact printing of colloidal crystals. Journal Of The American Chemical Society 126(34):10510-10511.

Yang SM, Miguez H, Ozin GA. 2002. Opal circuits of light - Planarized microphotonic crystal chips. Advanced Functional Materials 12(6-7):425-431.

Yao JM, Yan X, Lu G, Zhang K, Chen X, Jiang L, Yang B. 2004. Patterning colloidal crystals by lift-up soft lithography. Advanced Materials 16(1):81-84.

Yin YD, Lu Y, Gates B, Xia YN. 2001. Template-assisted self-assembly: A practical route to complex aggregates of monodispersed colloids with well-defined sizes, shapes, and structures. Journal Of The American Chemical Society 123(36):8718-8729.

Zhang H, He HX, Wang J, Mu T, Liu ZF. 1998a. Force titration of amino group-terminated self-assembled monolayers using chemical force microscopy. Applied Physics a-Materials Science & Processing 66:S269-S271.

Zhang MQ, Desai T, Ferrari M. 1998b. Proteins and cells on PEG immobilized silicon surfaces. Biomaterials 19(10):953-960.

Zheng HP, Berg MC, Rubner MF, Hammond PT. 2004. Controlling cell attachment selectively onto biological polymer-colloid templates using polymer-on-polymer stamping. Langmuir 20(17):7215-7222.

Zheng HP, Lee I, Rubner MF, Hammond PT. 2002. Two component particle arrays on patterned polyelectrolyte multilayer templates. Advanced Materials 14(8):569-572.